POTENTIAL OF NANOSENSORS: DESIGNING OF HEXAGONAL BORON NITRIDE-BASED NANOSENSOR FOR METHANE-SENSING

THESIS SUBMITTED IN PARTIAL FULFILMENT OF THE REQUIREMENT FOR THE AWARD OF THE DEGREE OF

MASTER OF TECHNOLOGY IN VLSI DESIGN & MICROELECTRONICS TECHNOLOGY

THESIS SUBMITTED BY

SUSHAMA DHAR

University Roll No.: **002010703009**

Registration No.: **154111** of **2020-2021**

Examination Roll No.: **M6VLS23006**

UNDER THE SUPERVISION OF

DR. SAYAN CHATTERJEE

DEPARTMENT OF ELECTRONICS & TELECOMMUNICATION ENGINEERING

JADAVPUR UNIVERSITY, KOLKATA-700032

WEST BENGAL, INDIA

AUGUST 2023

FACULTY OF ENGINEERING & TECHNOLOGY
ELECTRONICS AND TELECOMMUNICATION ENGINEERING
JADAVPUR UNIVERSITY

CERTIFICATE OF EXAMINATION

This is to certify that the thesis entitled **"Potential of Nanosensors: Designing of Boron Nitride based Nanosensor for Methane Sensing"** has been carried out by **SUSHAMA DHAR (Roll No.: 002010703009, Examination Roll No.: M6VLS23006 and Registration No.: 154111 of 2020-2021)** under my guidance of and supervision and can be accepted in partial fulfillment for the degree of Master of Technology in VLSI Design & Microelectronics Technology. In my opinion, the work fulfills the requirement for which it is submitted. To the best of my knowledge, the matter embodied in the thesis has not been submitted to any other organization.

_____

DR. SAYAN CHATTERJEE

THESIS SUPERVISOR

DEPARTMENT OF ELECTRONICS AND TELE-COMMUNICATION ENGINEERING
JADAVPUR UNIVERSITY
KOLKATA – 700032

_____ _____

PROF. MANOTOSH BISWAS

HEAD OF THE DEPARTMENT
DEPARTMENT OF ELECTRONICS AND TELECOMMUNICATION ENGINEERING
JADAVPUR UNIVERSITY
KOLKATA – 700032

PROF. ARDHENDU GHOSHAL

DEAN
FACULTY COUNCIL OF ENGINEERING AND TECHNOLOGY(FET)
JADAVPUR UNIVERSITY
KOLKATA- 700032

FACULTY OF ENGINEERING & TECHNOLOGY
ELECTRONICS AND TELECOMMUNICATION ENGINEERING
JADAVPUR UNIVERSITY

CERTIFICATE OF EXAMINATION

This is to certify that the thesis entitled **"Potential of Nanosensors: Designing of Boron Nitride based Nanosensor for Methane Sensing"** has been carried out by **SUSHAMA DHAR (Roll No.: 002010703009, Examination Roll No.: M6VLS23006 and Registration No.: 154111 of 2020-2021)** under my guidance of and supervision and can be accepted in partial fulfillment for the degree of Master of Technology in VLSI Design & Microelectronics Technology. In my opinion, the work fulfills the requirement for which it is submitted. To the best of my knowledge, the matter embodied in the thesis has not been submitted to any other organization.

Sayan Chatterjee 24/8/23

DR. SAYAN CHATTERJEE

THESIS SUPERVISOR

Dr. Sayan Chatterjee
Professor
Electronics & Telecomm. Engg. Dept.,
Jadavpur University, Kolkata - 700032.

DEPARTMENT OF ELECTRONICS AND TELE-COMMUNICATION ENGINEERING
JADAVPUR UNIVERSITY
KOLKATA – 700032

Manotosh Biswas 24/08/23

PROF. MANOTOSH BISWAS

HEAD OF THE DEPARTMENT
DEPARTMENT OF ELECTRONICS AND
TELECOMMUNICATION ENGINEERING
JADAVPUR UNIVERSITY
KOLKATA – 700032

MANOTOSH BISWAS
Professor and Head
Electronics and Telecommunication Engineering
Jadavpur University, Kolkata - 32

Ardhendu Ghoshal 24/08/23

PROF. ARDHENDU GHOSHAL

DEAN
FACULTY COUNCIL OF
ENGINEERING AND TECHNOLOGY(FET)
JADAVPUR UNIVERSITY
KOLKATA- 700032

DEAN
Faculty of Engineering & Technology
JADAVPUR UNIVERSITY
KOLKATA-700 032

FACULTY OF ENGINEERING & TECHNOLOGY
ELECTRONICS AND TELECOMMUNICATION ENGINEERING
JADAVPUR UNIVERSITY

CERTIFICATE OF APPROVAL*

The foregoing thesis is hereby approved as a credible study of an Engineering subject and presented in a manner satisfactory to warrant acceptance as a pre-requisite to the degree for which it has been submitted. It is understood that by this approval the undersigned do not necessarily endorse or approve any statement made, opinion expressed or conclusion drawn therein but approve the thesis only for which it is submitted.

Committee on the final examination for the evaluation of the Thesis

of **Sushama Dhar**

_____

(Signature of the Supervisor)

_____

(Signature of the Examiner1)

_____

(Signature of the Examiner2)

***Only in case the thesis is approved.**

FACULTY OF ENGINEERING & TECHNOLOGY
ELECTRONICS AND TELECOMMUNICATION ENGINEERING
JADAVPUR UNIVERSITY

DECLARATION OF ORIGINALITY AND COMPLIANCE OF ACADEMIC ETHICS

It is hereby declared that this thesis entitled **"Potential of Nanosensors: Designing of Boron Nitride based Nanosensor for Methane Sensing"** contains a literature survey and original research work done by the undersigned candidate, as a part of her degree of **Master of Technology in VLSI Design & Microelectronics Technology**. All information has been obtained and presented in accordance with academic rules and ethical conduct. It is also asserted that, as required by these rules and conduct, the undersigned has fully cited and referenced all materials and results that are not original to this work.

Thesis Title:

POTENTIAL OF NANOSENSORS: DESIGNING OF BORON NITRIDE-BASED NANOSENSOR FOR METHANE SENSING

SUSHAMA DHAR

University Roll No.: **002010703009**
Registration No.: **154111 of 2020-2021**
Examination Roll No.: **M6VLS23006**

DEPARTMENT OF ELECTRONICS AND TELECOMMUNICATION ENGINEERING
JADAVPUR UNIVERSITY
KOLKATA – 700032
INDIA

_____ _____

Date **Signature of the candidate**

ACKNOWLEDGEMENT

The success and final outcome of my thesis required a lot of guidance and assistance from many people and I am extremely fortunate to have got this all along the completion of my thesis work. Whatever I have done is only due to such guidance and assistance and I would not forget to thank them.

First and foremost, I owe my profound gratitude to my project supervisor, **Dr. Sayan Chatterjee** who guided me till the completion of my project work by providing his precious advice and constant support. I would like to express my special appreciation and thanks to him for giving his full effort in guiding me to maintain my progress. He has been a tremendous mentor for me because, without his invaluable suggestions and his continued motivation, my project work would not have taken a worthwhile shape.

I am also grateful to Prof. Chandan Ghosh of the Nanotechnology Department for his health and guidance.

I would like to express my gratitude to the head of the department Dr. Manotosh Biswas for providing me with all the facilities for carrying out the entire project work. I would like to express my sincere appreciation to all the teaching and non-teaching staff of the department for providing the necessary support and aid.

Last but not least, a special heartfelt thanks to my beloved family. Words cannot express how grateful I am to my parents for all of the sacrifices that they have made on my behalf. Their prayer for me was what sustained me thus far.

_____

SUSHAMA DHAR

Date:

Place: Kolkata

TABLE OF CONTENTS:

LIST OF FIGURES:

LIST OF TABLES

ABSTRACT

Methane, as one of the greenhouse gases, has a significant impact on global warming, roughly 21 times that of carbon dioxide. Hazardous gases like methane must be regularly monitored for leakage or concentration measurement in daily life and industrial operations. Methane is also combustible, explosive, and poisonous. Explosions produced by methane leaks are a regular hazard to people's lives and property safety. As a result, it is crucial to develop a method for precisely monitoring methane gas. To accomplish this, a sensing device with high selectivity, sensitivity, and responsiveness to changes in their environment is needed that can provide rapid and accurate information about a variety of substances and conditions in real time. A nanosensor can detect even trace amounts of a target material due to its high surface-to-volume ratio and unique features at the nanoscale, making it important for tracking dynamic processes such as chemical reactions, biological interactions, and environmental variations.

In this work, a 2D nanomaterial-based gas-sensor has been designed to sense methane gas. Boron-nitride Quantum dots have been synthesized by liquid exfoliation technique. Characterization of the quantum dots were done using SEM and XRD techniques. Electrical measurements were taken in different ambience and temperature for the performance evaluation of the designed gas sensor. The purpose of this nanosensor design is to harness the unique properties of the nanomaterial and nanotechnology to create a highly sensitive, selective and versatile sensor that can be further integrated into various systems and structures, including wearable devices, lab-on-a-chip platforms, and even within living organisms.

Chapter I

INTRODUCTION

1.1. OVERVIEW

In 1974, the "Nanotechnology" term was coined by Prof. Norio Taniguchi at the Tokyo University of Science [1]. The study of tiny structures is known as nanotechnology (nano-small). One billionth of a meter, or roughly 1,000 times smaller than the diameter of a human hair, is a nanometer. Everyday items like lightweight components and innovative, high-performance battery storage systems are made possible by nanotechnology. Engineers, biologists, chemists, doctors, and nanotechnologists all contribute to the growth of our society through their skills and knowledge. Every sector of the economy, from the diagnosis and treatment of disease to environmental cleaning, has the potential to benefit from nanotechnology.

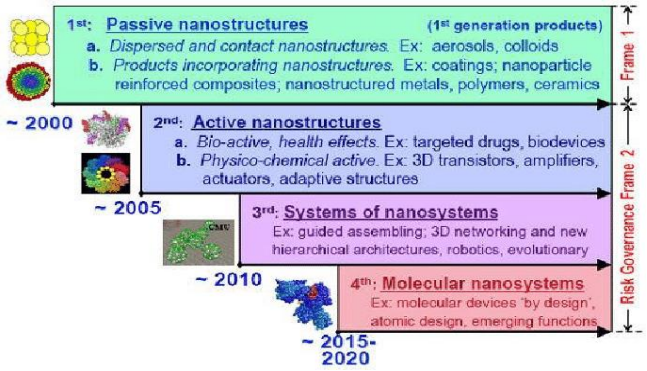

Fig. 1.1 Nanotechnology Generations: Proposed by US NNI's Mike Roco. [2]

Nanotechnology has the potential to change science and technology in a number of fields, including medicine and physiology [3, 4], as well as the delivery of medications and medical diagnostics. Nanotechnologists are also increasingly involved in chip production. It enables the creation of a careful regulatory framework by the government for a new class of chemicals and substances. Today, we are dealing with severe health issues such as diabetes, cancer [5], Parkinson's disease, and so on. It is used to restore injured tissue. Nanotechnology can aid in the development of green technologies that reduce pollution.

1.2. SENSORS AND THEIR REALTIME APPLICATIONS

In today's rapidly evolving technological landscape, the integration of sensors in real-time applications has revolutionized numerous industries and opened up new possibilities for data-driven decision making. Sensors, often referred to as the "eyes" and "ears" of modern systems, are devices capable of detecting and measuring physical phenomena, such as temperature, pressure, motion, and more. These devices convert the captured physical parameters into electrical signals that can be processed and analyzed in real time.

Real-time applications are systems that require immediate response and continuous monitoring of data to ensure timely actions and accurate decision making. By incorporating sensors into these applications, businesses and industries can gather valuable insights, enable automation, enhance safety measures, and optimize operational efficiency.

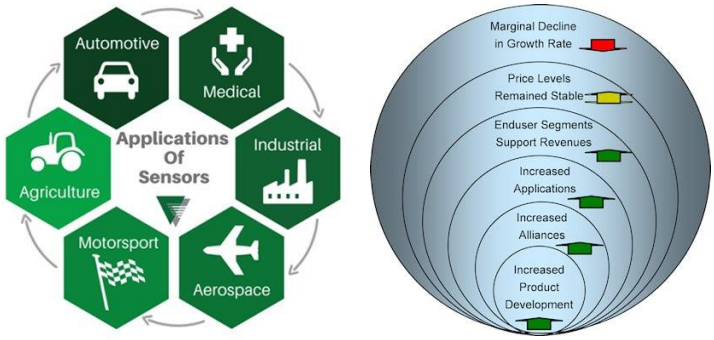

Fig. 1.2 Realtime application of Sensors [6]

- In industrial automation, sensors are deployed to monitor various parameters, including temperature, pressure, flow rate, and vibration [6,7]. Real-time data collected from these sensors enables precise control of manufacturing processes, detection of anomalies, and timely response to ensure optimal performance and prevent costly downtime.

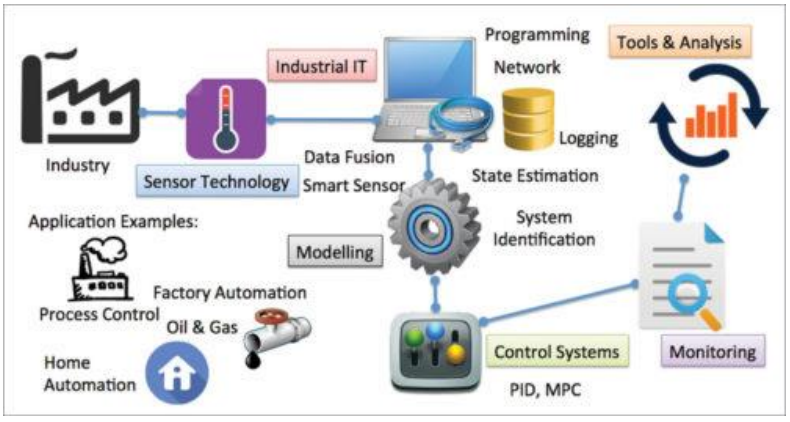

Fig. 1.3 Sensors Application in Industrial Automation. [6]

- Environmental monitoring systems rely on sensors to measure air quality, water quality, noise levels, and weather conditions [8]. Real-time data from these sensors allows us to assess pollution levels, predict natural disasters, and make informed decisions to mitigate environmental risks.
- In the realm of smart cities [9] sensors are a fundamental component, facilitating intelligent management of resources and infrastructure. Traffic management systems employ sensors to detect vehicle presence, optimize traffic flow, and minimize congestion. Waste management systems employ sensors to monitor fill levels in bins, optimize collection routes, and reduce operational costs.

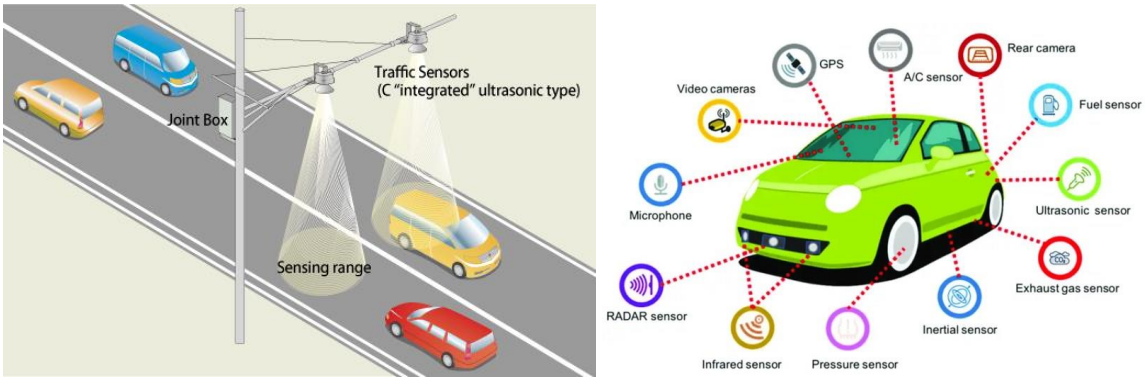

(a) (b)

Fig. 1.4 (a) Traffic Sensors (b) Diagram of Automobile Sensors. [10]

- In healthcare [11] sensors play a vital role in patient monitoring, enabling healthcare professionals for tracking vital signs including heart rate, blood pressure, and oxygen levels. Real-time monitoring empowers medical staff to detect critical situations promptly, provide timely interventions, and improve patient outcomes.

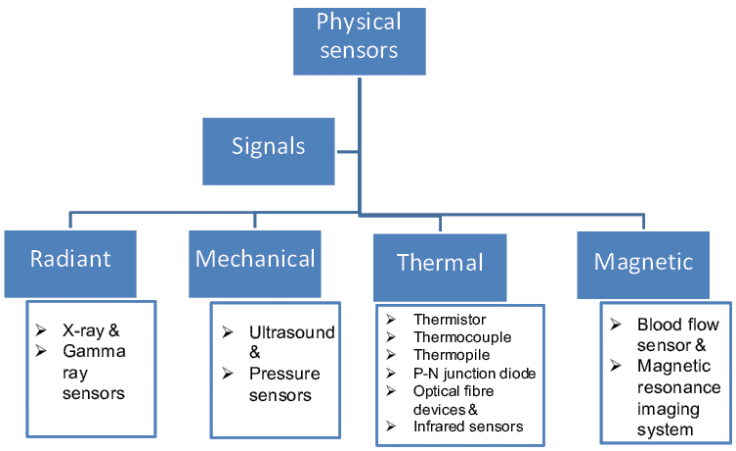

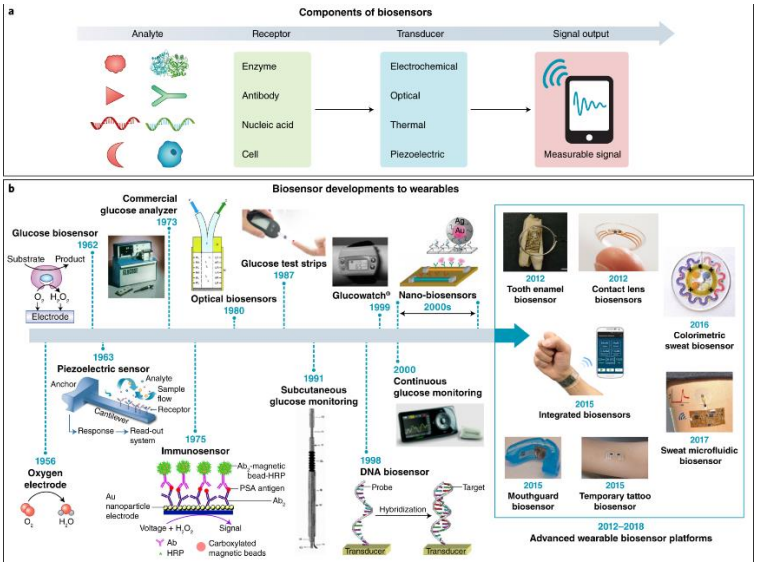

Fig. 1.5 Application of Sensors in Medical Devices. [12]

- Furthermore, the Internet of Things (IoT) has seen an exponential growth, with sensors acting as the backbone of interconnected devices [13]- [16]. By incorporating sensors into IoT applications, we can gather real-time data from various sources and leverage it for improved decision making, automation, and personalized user experiences.

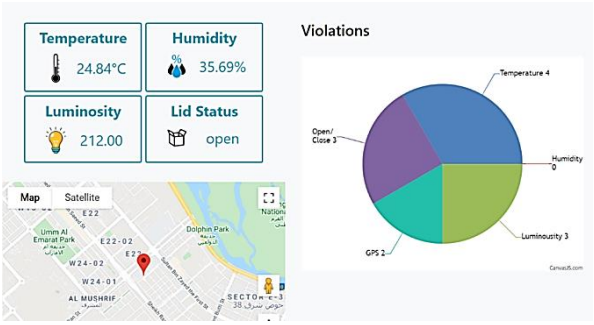

Fig. 1.6 Live status page on how sensor readings can be displayed in real-time using IoT. [9]

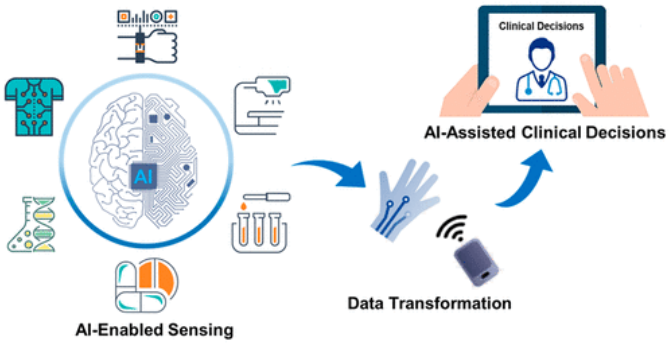

Fig. 1.7 AI in Medical Sensors for Clinical Decisions. [12]

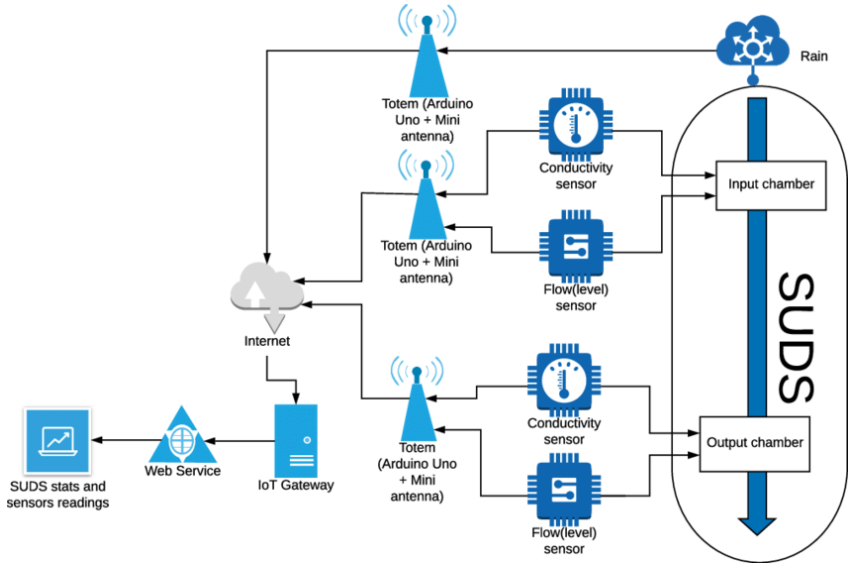

Fig. 1.8 SUDS case study : IoT solution. [13]

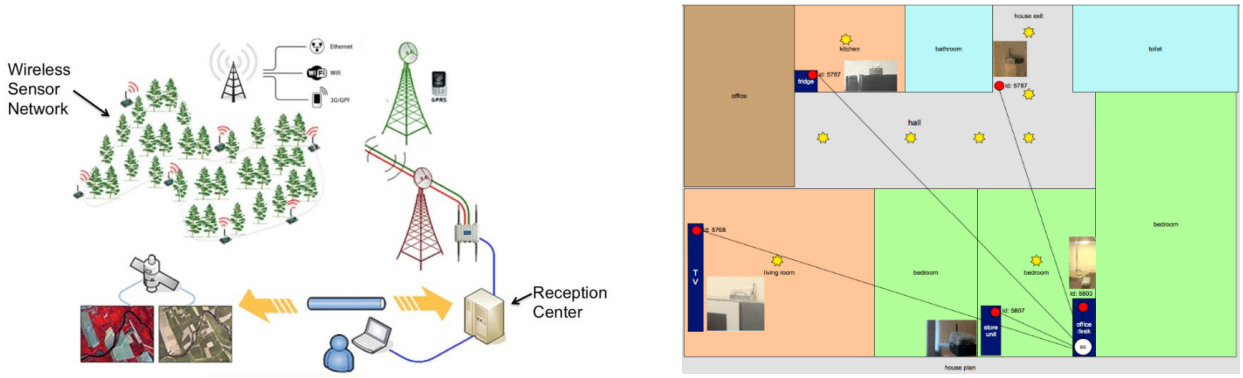

Fig. 1.9 IoT Using Wireless Sensor Networks and Smartphones. [14]

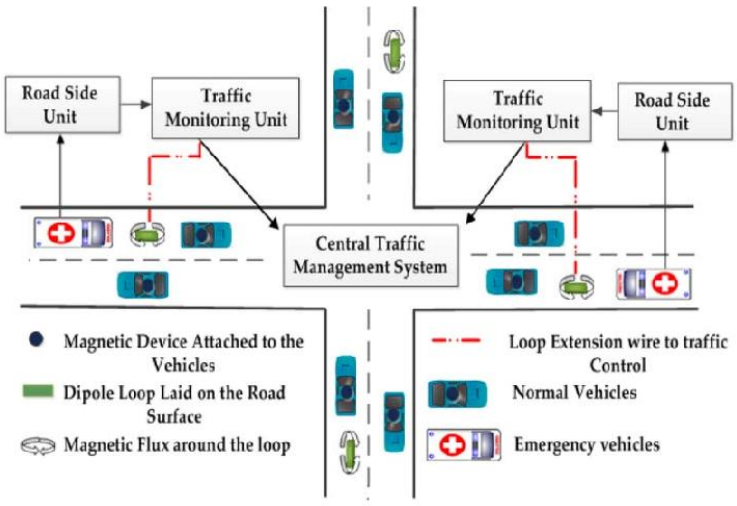

Fig. 1.10 Smart Traffic management system in real-time using IoT and Big Data. [15]

In conclusion, sensors in real-time applications have transformed the way we interact with and understand the world around us. From industrial automation to healthcare, environmental monitoring to smart cities, sensors provide real-time data that empowers organizations and individuals to make informed decisions, optimize processes, and create a more efficient and connected future.

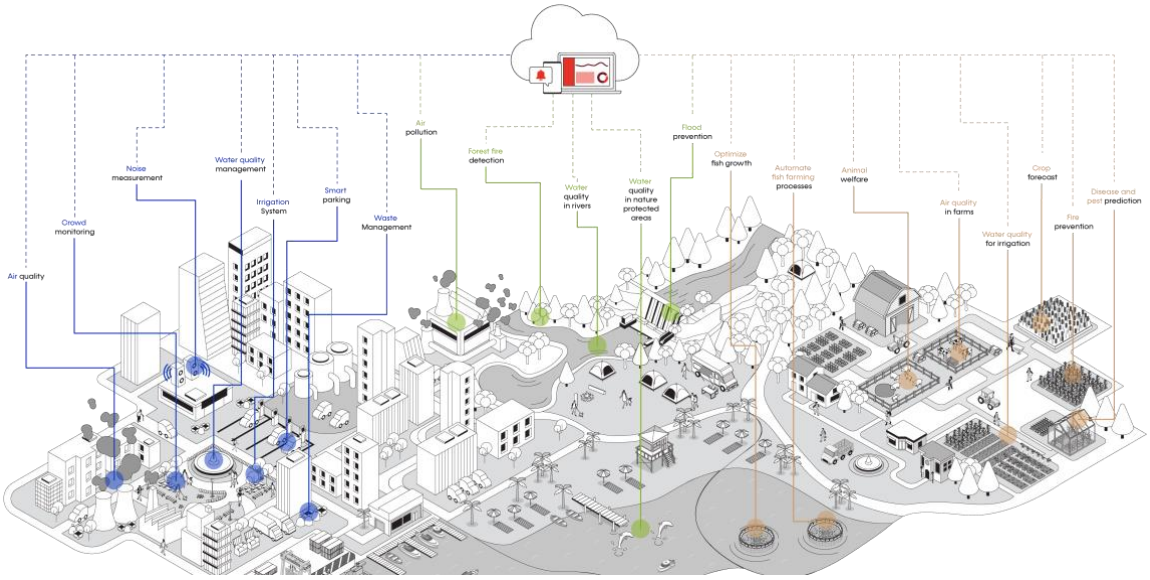

Fig. 1.11 Sensor Application for Smarter World. [16]

1.2.1 SENSORS

A sensor is a device that measures a physical characteristic, such as temperature, mass, or electrical or photonic properties, consecutively generates a signal for monitoring or further analysis. [17]. The development history of a sensor is broad. The first thermostat was developed in the 18th century probably in 1880, and the first infrared sensor appeared in 19th century [18].

The current focus of research is on building high-performance gas sensors [19] with low operating temperatures and cheap manufacturing costs. Since it uses incredibly little electricity and doesn't need a heater for high temperature operation, a gas sensor that operates at ambient temperature is quite alluring. Because of the advancement of nanoscience and nanotechnology, technology has a huge influence on many facets of our society and has made significant improvement.

1.2.2 NANOSENSORS

With its recent rapid advancement, nanotechnology offers immense potential across nearly all industries. These developments have been advantageous for the development of the nanosensor industry. To accommodate their need for miniaturization, several electronics businesses have backed these advancements. Over the last 20 years [18], a significant amount of research has been done in the field of nanomaterials for a variety of applications, including nanosensors. The sample amounts required are relatively tiny, and detection is carried out extremely quickly due to nanosensors' ability to handle signals generated at the nanoscale. All of these characteristics have aided the use of diverse nanosensor types in a variety of applications, particularly in the domains of medicine and homeland security [19].

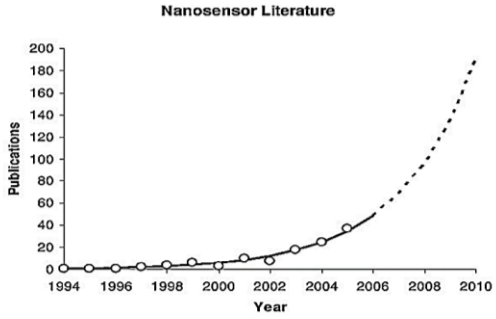

Fig. 1.12 Count of precise searches for the term "nanosensor" in journal paper titles during a 12-year period (1994–2005, inclusive), with an estimate for 2010. [27]

1.2.2.1 TYPES OF NANOSENSORS

Nanomaterials are now being investigated more and more. Nanomaterials have captured consumers' interest in a range of applications, including biomedical, agricultural, gas sensors, batteries, and optoelectronic machinery, thanks to their electrical, magnetic, and mechanical properties [20]. Since there are many different nanosensors accessible today, categorization can be challenging given the short history of nanosensors [21].

However, there are three broad categories into which nanosensors may be divided: Reception modules, Structure, and Application.

I. **Based on energy source***,* nanosensors can be categorized into two types [22]: Energy-free passive nanosensors like thermocouples and piezoelectric nanomaterials, as well as active nanosensors like thermistors.

- **Affinity-based nanosensors**: Include hormones [18,22], antibodies, and receptors for nucleic acids that bind target molecules catalytically and permanently.
- **Catalytic-based Sensors**: These include enzyme- or cell-based receptors that bind relevant chemicals and catalytically transform them into identifiable products.

II. **Based on their structural characteristics**, nanosensors may be further divided into two types:
- **Optical nanosensors [22-27]:** These devices exploit fluorescence's sensitivity to monitor amplitude, energy, polarization, delay time, and decay phase qualitatively and quantitatively.
- **Electrochemical nanosensors**: This type of nanosensors primarily recognizes the chemical or electrical characteristics of a particular material and transduces a signal.

III. **Depending on their applications**, Nanosensors can be categorized as chemical nanosensors, nanoscale electrometers, nanobiosensors, deployable sensors, and other types of sensors [22,24-25].
- **Chemical Nano-Sensors:** These sensors can detect single chemical and biological molecules since they are made of capacitive cantilevers and electronics.
- **Nanoscale electrometers:** Use polymers to detect DNA, cancer, and other substances, and **nano-biosensors**, which use polymers to do the same.
- **Deployable sensors: U**sed in military and other applications relating to national security.

1.2.2.2 APPLICATIONS OF NANOSENSORS

Researchers at the Georgia Institute of Technology created one of the earliest functional instances of a nanosensor in 1999 [22-24]. A single particle was linked to the extremity of a carbon nanotube, and the nanotube's vibrational frequency was determined with and without the particle. The researchers were able to determine the linked particle's mass using the difference in frequency. Since then, more and more research has been conducted on nanosensors, leading to the development of contemporary nanosensors for a variety of uses. Currently healthcare [25], defence and military, and others such as food, environment, and agriculture are the part of nanosensors application in market place. Nanosensors are becoming

more important in practically every facet of modern life. The presence of potentially harmful substances or microbes in food, water, or the air may be found using a variety of sensors.

- Throughout the globe, these sensors are preserving lives. Nanosensors are having a significant influence in the medical industry [27-29].

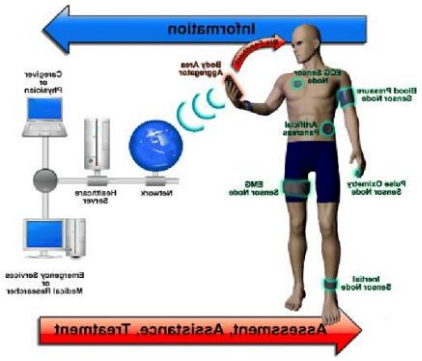

Fig. 1.13 Real-time health monitoring with nanosensors as a part of the Internet of Nano Things (IoNT). [2]

- For instance, several nanosensors are employed in cancer diagnosis, DNA and protein detection, and targeted medication delivery.

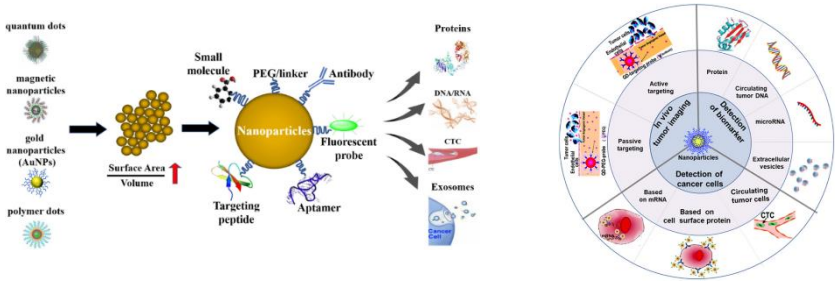

Fig. 1.14 Nanotechnology in cancer diagnosis. [28]

- Homeland security has developed uses for deployable sensors.
- Unmanned aerial vehicles are now equipped with a variety of chemical sensors to help them identify hazardous gas on the battlefield and save the lives of troops [29].
- RFID chips, another use for nanosensors, are used in a number of tagging systems.

Table 1.1 Significant potentials of nanosensors. [18,30]

SL No.	Potential	Description
1.	Tracking environmental changes, water and soil.	Real-time monitoring of changes in the environment, soil, and water is made simple with nanosensors. Additionally, it aims to broaden its application base to include dispersed networks and lab-on-a-chip technologies. Nanoscale concentrations of solids, liquids, and gases can be detected using nanotechnology sensors to identify possible dangers. In this approach, nanowire arrays are combined on a tiny semiconductor chip to produce a powerful field-effect transistor.
2.	To prevent contaminating food, find infections.	To prevent food contamination, nanosensors are employed to detect pathogens. This technique is an effective tool for applications involving sensing. Given that it provides vital information that advances our understanding of basic biological processes, it is also a crucial instrument for tracking dynamic biomolecular changes and biological functions. This method has been enhanced to identify a large number of samples for soil and water fertilisers as well as food pathogens. It may be used to monitor pesticides and fertilizers on a whole farm, enabling farmers to manage their usage as necessary.
3.	Examine the water and macronutrient contents.	During poor agricultural seasons, any lack of proper fertilisers and nutrients typically leads in significant declines in crops. The right macronutrient and water levels may be checked using precision farming nanotechnology sensors. This makes crop ripening, fertilization, and yield possible at their best. Many nanotubes are produced by the sensor industry and are used to instantly determine the ion content of agricultural samples.
4.	Health data	Nanosensors can readily collect sensitive health data. The preservation of these data assures that they are only utilized for the purpose of collection, making them one of the most significant barriers to wider use. Monitoring is becoming more common, and the Internet of Nano Things makes it easier to watch individuals.
5.	Detect specific gases	Today, air pollution is an increasing problem, and contaminating gases often affect human health. With advances in nanotechnology, nanosensors can now detect

	in the surroundings.	trace amounts of particular gases in the environment. This can help to promote healthy living and working environments while also preventing negative health impacts. These metal oxide nanostructures can be integrated with existing gases and gadgets. The gas composition is identified for home, industrial, and environmental uses.
6.	Detect human physiological data	Biomedical sensor systems (systems based on microelectromechanical, biological, and chemical sensing, as well as electrocardiograms and electromyograms.) have the ability to continually monitor human physiological data in real-time and without intrusion by utilizing semiconductivity and flexible electronics packaging technologies. When the conditions for sensitiuvity and selectivity are fulfilled, biological and chemical sensors can compete with costly analytical instruments.
7.	Keep an eye on bio-cells.	Nanosensors have demonstrated their exceptional ability to watch single bio-cells and organisms with precise spatial and temporal precision down to the molecule level. These leverage the unique features of nanomaterials and nanoparticles to detect and quantify the presence of a wide range of infectious diseases, including viruses and dangerous bacteria.
8.	Intelligent tracking and tracing.	Nanosensors can be used on Active transport tracking systems for smart tracking and tracing for logistics management. Nanosensors are often used in agricultural food items to monitor soil conditions and farm ambient conditions. Chemical nanosensors are used to determine the chemical and material composition of food, water, environmental, and medicinal samples. These sensors use very sensitive chemical receptors and transducers, as well as poisons and chemical compounds. They are capable of detecting concentrations as low as a million parts per billion.

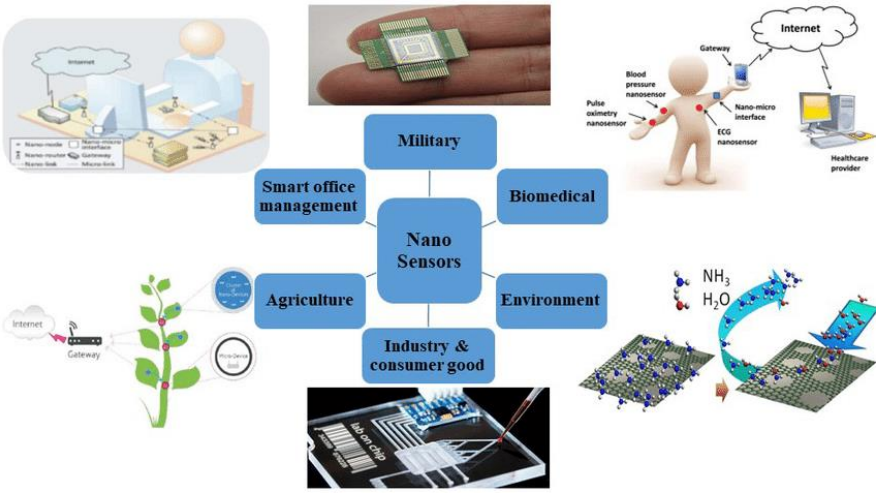

Fig. 1.15 Application fields of nano-sensor networks. [29]

1.2.3 NANOMATERIALS

Nanostructured materials with precise dimensions and tiny sizes have shown significant promise for usage as sensing layers. The advantages of using nanostructured materials for gas sensing include the enormous surface-to-volume ratio [17], high specific surface area, enhanced surface-active site, as well as the recently recognized influence of crystal facets with high surface reactivity. The performance of a sensor is greatly influenced by the quantity of atoms present at a material's surface since most interactions between gas molecules and materials occur there. Nanostructured materials contain a substantially higher proportion of surface atoms than bulk atoms compared to non-nanostructured materials because of the high surface-to-volume ratio. As a result, gas sensors made of nanostructured materials may function better [18].

Nanoparticles (NPs) with at least one dimension in the nanometer range and specific properties that aren't present in the material's bulk are referred to as nanomaterials [31]. Although unknowingly present in some ancient artifacts, the development of nanoparticles as we know them today dates back to 1857, the year when Michael Faraday [32] published his report on the production of what was then known as "activated gold," a colloidal solution. Due to their nanoscale dimension and very high surface-to-volume ratio, nanomaterials exhibit exceptional characteristics that are distinct from those of their bulk size in a variety of ways, including magnetic [31], mechanical, optical, and chemical [31].

1. **Nanoparticles:** These are small particles with dimensions in the nanoscale. Hollow spheres, quantum dots, and particles all have 0 or 3 dimensions with a diameter of 100 nm. They can be metallic, such as gold or silver nanoparticles, or non-metallic, such as carbon nanotubes or quantum dots. Nanoparticles find applications in various fields like medicine, electronics, and environmental science [33]-[35].

2. Nanotubes: Carbon nanotubes are cylindrical carbon structures with diameters on the nanoscale [33,36]. Tubes, fibers, platelets have dimensions less than 100 nm. They possess exceptional mechanical, electrical, and thermal properties, making them useful in industries like aerospace, electronics, and energy storage.

3. **Nanocomposites:** These materials are composed of a matrix material with nanoscale fillers dispersed throughout. These are composite materials in which nanoparticles or nanofillers are dispersed in a bulk matrix. The presence of nanoparticles enhances the properties of the composite, such as strength, stiffness, and electrical conductivity. Nanocomposites have applications in aerospace, automotive, and sports industries. Nanocomposites [37] exhibit improved mechanical, electrical, and thermal properties compared to traditional composites. They are employed in industries ranging from automotive to construction.

4. **Nanowires:** Nanowires are ultra-thin wires with diameters in the nanoscale range. Nano rods, nano wires [38] have dimension less than 100 nm.They can be made from various materials, including metals, semiconductors, and oxides. Nanowires find applications in nanoelectronics, sensors, and energy conversion devices.

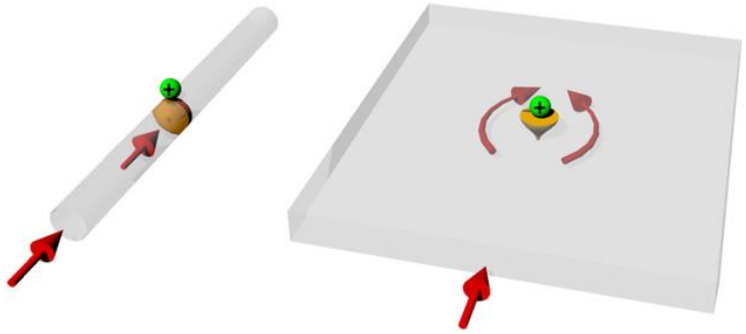

Fig. 1.16 (a) 1-D Nanowire (b) 2-D Nanofilm [38]

5. Nanofilms: Nanofilms [37] or thin films are coatings or layers with thicknesses on the nanoscale. They can be deposited on various substrates and offer benefits like improved corrosion resistance, optical properties, and surface functionalities. Nanofilms are used in electronics, optics, and solar cells.

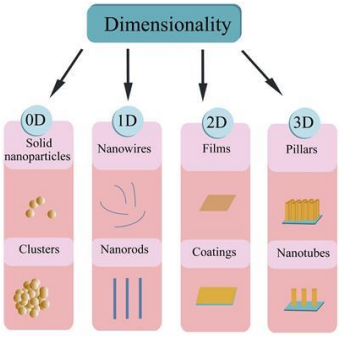

Fig. 1.17 Nanomaterial's classification based on dimensionality. [34]

The history of nanomaterials dates back to ancient times, with early practices involving the manipulation of materials at the nanoscale. However, the term "nanotechnology" was coined by physicist **Richard Feynman in 1959** during a lecture titled "There's Plenty of Room at the Bottom," [2] where he discussed the possibilities of manipulating and controlling matter at the atomic and molecular scale. Significant advancements in nanomaterials occurred in the 1980s and 1990s with the development of techniques like scanning tunneling microscopy (STM) and atomic force microscopy (AFM), which allowed scientists to observe and manipulate materials at the nanoscale. In 1985, [35] the discovery of fullerenes, a type of nanoscale carbon structure, marked a significant milestone in the field. sIn the late 1990s and early 2000s, the field of nanotechnology gained substantial attention and investment, leading to rapid progress in the synthesis, characterization, and application of various nanomaterials. This period saw the emergence of carbon nanotubes, quantum dots [37], and other nanoscale structures with unique properties.

According to their chemical composition, nanomaterials [39] are divided into four categories: (1) carbon-based, (2) organic-based, (3) inorganic-based, and (4) composite-based nanomaterials.

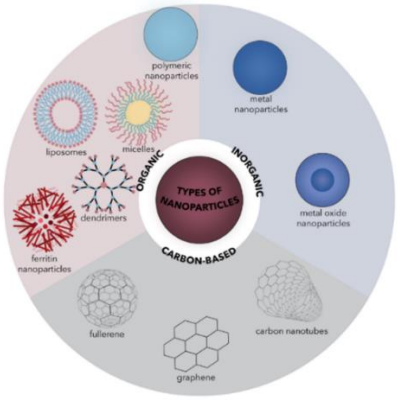

Fig. 1.18 Types of Nanoparticles. [39]

1.2.3.1 DIFFERENT NANOMATERIALS FOR NANOSENSORS

1.2.3.1.1 Carbon based Nanosensors:

- **Carbon Nanotubes (CNTs):** Carbon nanotubes [31,36] are cylindrical structures consisting of rolled-up sheets of graphene, which is a single layer of carbon atoms arranged in a hexagonal lattice. Single-walled (SWNT) and multi-walled (MWNT) CNT are the two varieties available. Each concentric ring of MWNT is separated by around 0.34 nm, whereas the diameter of SWNT ranges from 0.4 to 2 nm. CNTs possess [38] exceptional strength, high electrical conductivity, and excellent thermal conductivity. They are used in electronics, energy storage, composite materials, and biomedical applications.
- **Graphene:** Graphene is a two-dimensional sheet of carbon [30,40,41] atoms arranged in a hexagonal lattice. It is the thinnest and strongest material known, with excellent electrical and thermal conductivity. Graphene has applications in electronics, sensors [46], energy storage, and composite materials, among others.
- **Fullerenes:** Fullerenes are spherical or cage-like carbon structures comprising interconnected hexagonal and pentagonal rings [42]. The most famous fullerene is C60, also known as buckminsterfullerene or Buckyball. Fullerenes have unique electronic and photovoltaic properties, and they find applications in nanotechnology, medicine, and electronics.
- **Carbon Dots:** Small carbon nanoparticles that are generally less than 10 nanometers in size are known as carbon dots, carbon quantum dots, or C-dots. They exhibit excellent optical properties, such as strong fluorescence, which make them valuable in fields like bioimaging, sensing, and optoelectronics.
- **Carbon Nanofibers:** Carbon nanofibers are elongated structures composed of stacked graphene sheets. They possess high tensile strength and are used in composites, energy storage devices, and as catalyst supports.
- **Diamondoids:** Diamondoids are tiny diamond-like structures made up of carbon atoms. They have unique electronic and quantum properties and hold promise for applications in nanoelectronics, quantum computing, and nanomedicine.

For a better understanding of the variety of nanomaterials, Fig. 1.19 provides a schematic depiction of carbon-based nanomaterials.

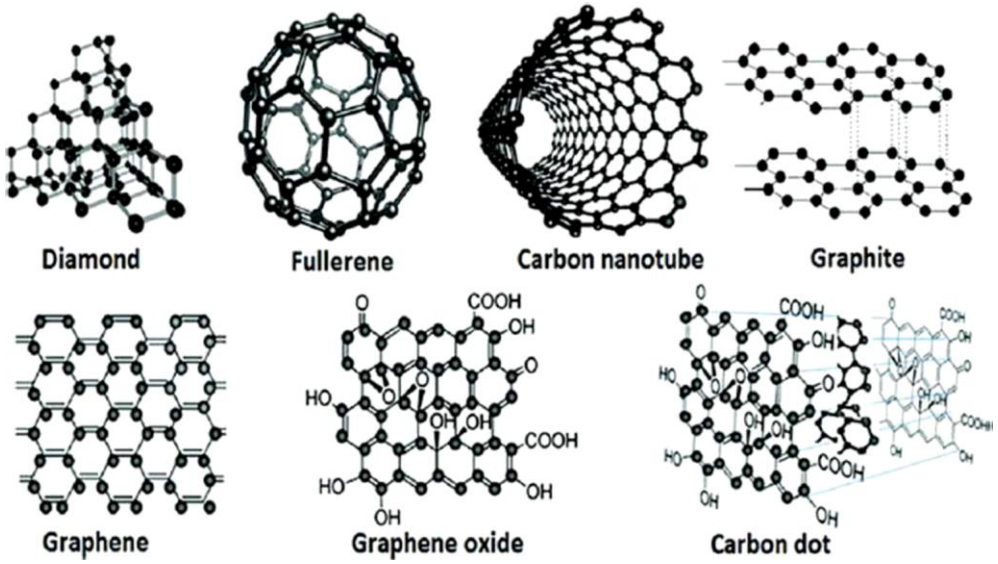

Fig. 1.19 Carbon based Nanomaterials. [41]

1.2.3.1.2 Inorganic based Nanosensors

Inorganic-based nanomaterials are nanoscale structures primarily composed of inorganic elements, such as metals, metal oxides, semiconductors, or ceramics.

- **Metal Nanoparticles**: Metal nanoparticles [41], such as gold, silver, and platinum nanoparticles, have been studied for centuries. However, their nanoscale properties and applications gained significant attention in the late 20th century. The synthesis of metal nanoparticles with controlled size and shape became possible with advancements in nanoscience and nanotechnology.

Fig. 1.20 Inorganic nanoparticles and its application. [43]

- **Semiconductor Nanoparticles**: Semiconductor nanoparticles [44], also known as quantum dots, gained prominence in the 1980s. Quantum dots are nanoscale crystals of semiconductor materials, such as cadmium selenide (CdSe) or lead sulfide (PbS) [45]. They possess unique optical and electronic properties, making them valuable in applications like optoelectronics, displays, and biological imaging.

- **Metal Oxide Nanoparticles**: Metal oxide nanoparticles [46,47], including titanium dioxide (TiO_2), zinc oxide (ZnO), and iron oxide (Fe_2O_3), have been extensively researched. They exhibit diverse properties such as high surface area, photocatalytic activity, and magnetic properties. Metal oxide nanoparticles find applications in photocatalysis, sensors, energy storage, and medicine.

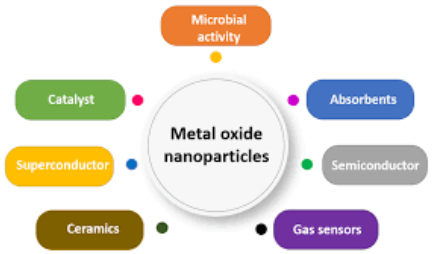

Fig. 1.21 Metal Oxide Nanoparticles application. [48]

- **Nanowires and Nanotubes:** Inorganic nanowires and nanotubes, such as silicon nanowires and titanium dioxide nanotubes [49], have been studied since the early 2000s. These one-dimensional structures possess unique electrical, thermal, and mechanical properties. They are used in nanoelectronics, energy storage, and sensing applications.

- **Layered Materials:** Layered inorganic materials [50], such as graphene oxide, molybdenum disulfide (MoS_2)[51], and hexagonal boron nitride (hBN), have gained significant attention in recent years. These materials have atomically thin layers and exhibit interesting properties for applications in electronics, energy storage, and optoelectronics.

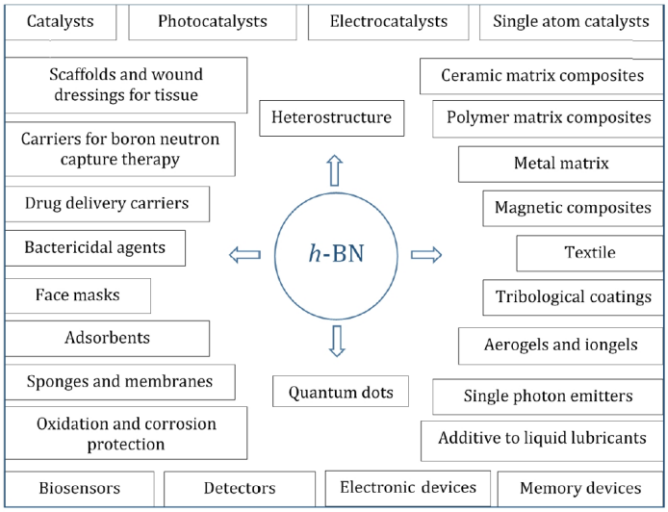

Fig. 1.22 Application of Layered inorganic material: hBN.[33]

The history of inorganic-based nanomaterials is closely linked to the development of nanoscience and nanotechnology. The ability to synthesize, characterize, and manipulate inorganic materials at the nanoscale has grown significantly with advancements in microscopy, nanofabrication techniques, and materials synthesis methods.

1.2.4 NANOMANUFACTURING PROCESS

Manufacturing nanomaterials or diverse nanoscale structures for a variety of purposes is known as nanomanufacturing. Nanomanufacturing involves both the creation of nanoscale materials and the fabrication of items "top down" or "bottom up" in the tiniest phases for maximum precision [36]. This may be seen as an improved kind of micromanufacturing or microfabrication in which the manufacturing is done at a dimension that is many orders smaller. Although the terms "nanofabrication" is used as analogous to "nanomanufacturing".

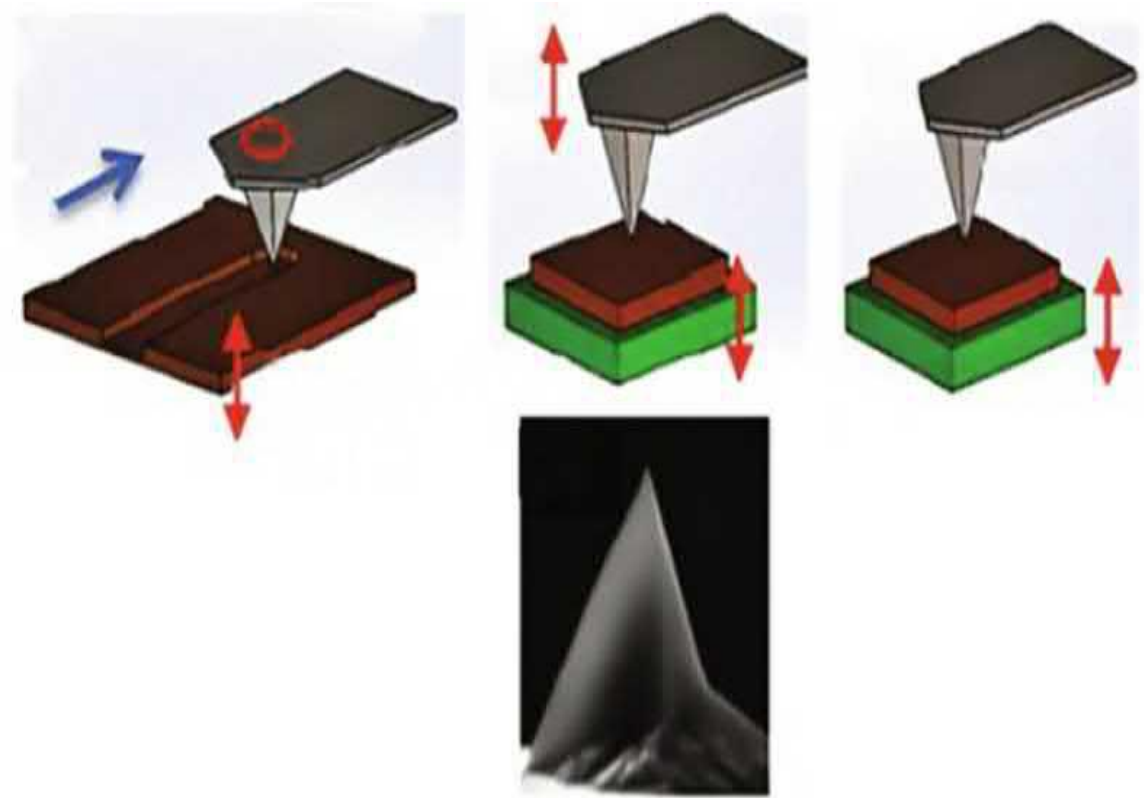

FIG 1.23 Ultrasonic assisted AFM-based nanomanufacturing process. [52]

Figure 1.23 depicts a schematic design of an ultrasonic-assisted nanomanufacturing procedure. The illustration depicts multiple potential vibration configurations for the machining process, including low-frequency tip-sample contact and ultrasonic tip-sample interaction. According to the study team, this technique may be used to create 3D nanoobjects with distinct height levels as well as continually variable heights.

Three major techniques may be used to categorize the many types of nanomanufacturing processes that have been created: top-down approach, bottom-up approach, and molecular assembly. The following sections provide a brief description of these three methods:

1.2.4.1 Top-Down Approach

Top-down approach: A large stone or wood block is progressively shaped into its ultimate form. This technique is used in nanomanufacturing when a sizable block of material is taken and gradually machined away until the desired shape is achieved. The top-down approach [33] consists of the two phases of **nanolithography** and **pattern transfer.**

In nanolithography, the desired design is created on a specific sort of sacrificial layer called a resist. Numerous nanolithography methods exist, including photolithography, electron beam lithography, X-ray lithography, soft lithography, and others. Every situation has a same fundamental concept. A layer of resist is initially applied to the substrate. As in photolithography, which employs ultraviolet light, electron beam lithography, which employs an electron beam, and X-ray lithography, which employs an X-ray, the photoresist is then exposed to an energy source while being treated to a pattern.

The resist goes through a chemical reaction as a result of this patterned exposure, and the chemical and mechanical characteristics change all across the coating. Later, depending on whether the resist is positive or negative, a portion of it is removed (either the exposed portion or the unexposed portion), creating a pattern. The metal layer is now prepared for etching. Following etching, the resist pattern is eliminated mechanically or chemically. Fig. depicts the shortened procedure visually.

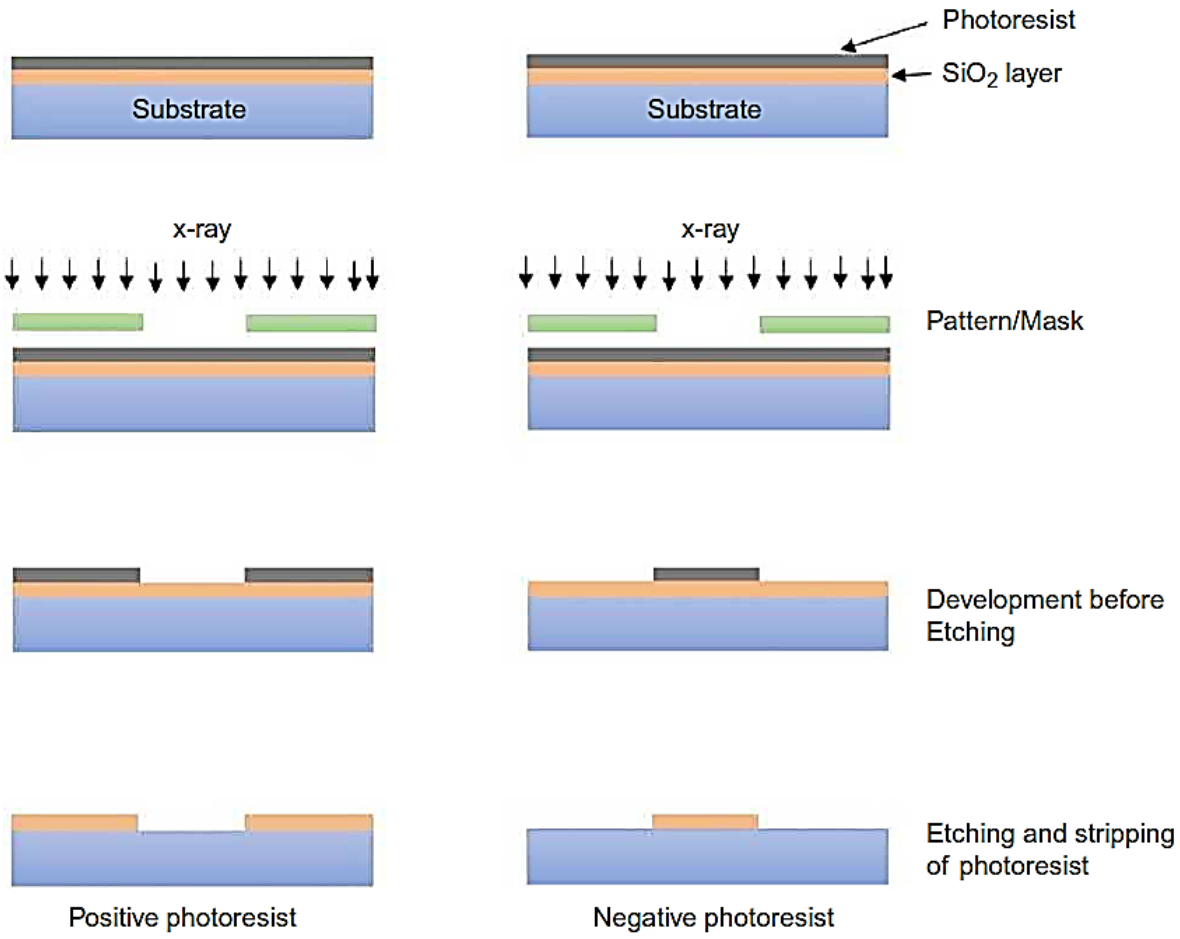

Fig. 1.24 Image of Positive and Negative resist in X-ray lithography [52]

1.2.4.2 Bottom-up approach

Building a house brick by brick from the ground up is an analogy for the bottom-up approach Fig 1.25. To produce the final structure using this process, minuscule components—even molecules—are assembled or combined. Common bottom-up processes [33] include joining and assembling, coating, contact printing, imprinting, physical or chemical vapour deposition, and vapour deposition. The medical and healthcare industries have a lot of potential applications for the bottom-up paradigm. A device that can function on a single cell may be nanofabricated utilising a bottom-up strategy with carbon nanomaterials and carbon nanotubes.

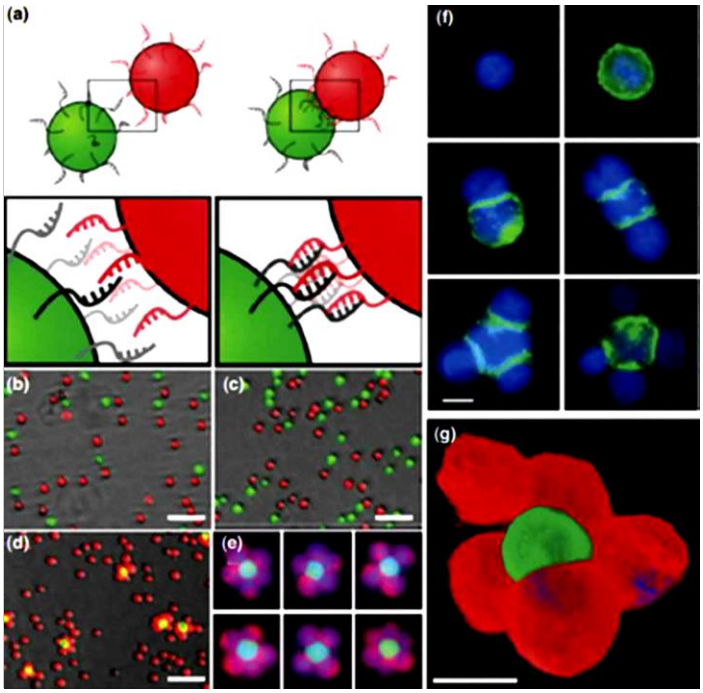

Fig. 1.25 Bottom-up approach used in Tissue engineering. [52]

1.2.4.3 Molecular Self-assembly

The most current technique is known as molecular self-assembly [36], in which the individual components, notably molecules, assemble themselves in the proper configuration to make a nanoobject without the aid of an outside force. When molecules come together to form a structure, a variety of molecular properties, including shape, surface properties, charge, polarizability, and magnetic dipole, play a role. Before this method is used in industry, further advances are needed in this still-evolving subject.

1.3 DISCUSSION

It is widely believed that Nobel laureate Richard Feynman's renowned 1959 speech, "**There's Plenty of Room at the Bottom,"** in the year 1959 marked the birth of nanotechnology [2]. But towards the start of 1980, the applications of this technology became clear. Since then, nanotechnology has exploded in popularity and is now used in a variety of areas of our lives. The field of nanotechnology gained momentum in the 1980s and 1990s with the development of tools like scanning probe microscopy (SPM) and advances in semiconductor manufacturing. These breakthroughs allowed scientists to observe, manipulate, and engineer materials at the nanoscale.

The performance of a sensor is greatly influenced by the quantity of atoms present at a material's surface since most interactions between gas molecules and materials occur there. Nanostructured materials contain a substantially higher proportion of surface atoms than bulk atoms compared to non-nanostructured materials because of the high surface-to-volume ratio. As a result, gas sensors made of nanostructured materials may function better. Reviews have spoken about the benefits of employing nanoparticles for gas sensing.

At the nanoscale, materials can exhibit unique properties not seen at larger scales. For example, nanoparticles might have improved mechanical, electrical, thermal, or optical properties, making them useful for various applications. Nanotechnology can lead to more efficient processes and devices due to its ability to optimize and tailor materials at the atomic and molecular levels. Nanoscale components can enable the miniaturization of devices and systems, which is particularly valuable in fields like electronics, medicine, and environmental monitoring.

Nowadays, chemical species and nanoparticles are detected and monitored using nanosensors together with physical properties like temperature at the nanoscale. Nanoscale devices track and convert physical quantities into signals that can be seen and analysed. Nanosensors are employed in the monitoring of industrial and transportation systems, disease detection, pollution management, and medical procedures. By measuring physical properties like volume, concentration, movement and speed, gravitational, electric, magnetic forces, pressure, temperature, etc. In order to provide medication and track the growth of particular regions of the body, this technology can identify individual cells at the molecular level.

Chapter II

LITERATURE REVIEW

2.1 METHANE GAS-SENSORS OF DIFFERENT TECHNOLOGIES AND MATERIALS

Li et al. introduced a simple method [53] to produce a composite palladium and multi- walled carbon nanotubes by reducing their aqueous mixtures with $NaBH_4$. The morphology of the composite was examined using AFM and TEM. Electrical reactions between this composite and methane were investigated at ambient temperature. It reacted with 4.5% to 2% of methane. Furthermore, these reactions were extremely reversible as well as repeatable, indicating its promise as a room temperature contender as methane detector. Later Zhang et al. [54] examined the innovation of several types of nanosensors (Carbon nanotubes based). The aim was to rationally functionalize CNTs utilizing various techniques (covalent and non-covalent) and materials (polymers and metals), in order to improve sensing performance (sensitivity, selectivity, and response time). Due to its promise for quick and selective detection of numerous gaseous species using new nanostructures integrated in small and power-efficient electronics, carbon nanotube (CNT)-based gas sensors and sensor arrays have attracted a great deal of scientific attention in recent years.

P. Bhattacharya [46] demonstrated the comparative performance of MIM sensors using sol-gel and UV-assisted electrochemical anodization to create nanocrystalline-nanoporous ZnO as the active sensing layer is presented in this work. In the presence of different methane concentrations and in temperature ranges from 150 °C to 300 °C, the sensor structures based on Pd-Ag (26%)/ZnO/Zn were examined. In terms of operating temperature, response magnitude, response time, and recovery time, the electrochemically produced ZnO demonstrated improved performance. Additionally, it demonstrated responsiveness to methane at considerably lower concentrations (such 0.01% and 0.05%) than the solgel-derived sensors did. The electrochemically generated ZnO was shown to perform better than sol-gel derived ZnO due to its considerably higher porosity and much smaller particle size. However, despite its promising performance, the electrochemically created MIM sensor is incompatible with the ordinary IC technology since it cannot choose the substrate. Therefore, there aren't many uses for developing stand-alone sensor devices. The MIM device created from sol-gel, on the other

hand, is built on Si substrate, making it IC compatible and appropriate for the integrated sensor platform.

In 2012, Biaggi-Labiosa et al. summarized a room temperature methane sensor [47] designing technique for the first time which was fabricated using SnO_2 nanorods as the sensing material. Multiwall carbon nanotubes (MWCNTs) were used as templates to create the porous SnO_2 nanorods. When subjected to 0.25% CH_4 in air, current versus time curves were produced, validating the sensor system's room temperature detecting capabilities. The sensor also has a wide temperature range for varying CH_4 concentrations (25-500 ℃), making it effective in tough situations.

In this paper, H Roshan [45], describes the effective synthesis of lead sulphide nanocrystals (PbS NCs)/reduced graphene oxide (rGO) with various weight ratios for methane sensing applications. TEM, XRD and FESEM were used to characterise the crystal structure and morphology of the synthesised material. Characterization findings show that rGO nanosheets provide a good surface for the nucleation of PbS NCs. The electrical conductivity, sensor response, and reaction time of the sensors are all impacted by rGO because of its high mobility. We looked examined how electrical conductivity and methane sensing properties changed with reduced Graphene Oxide concentrations in ambient temperature, synthetic 3.5 wt% reduced Graphene Oxide sample performed the best in detection of CH_4. At lower explosive limit of methane, the suggested sensor has shown a satisfactory response (greater than 40%). Later Nagih M. Shaalan [55] stepped ahead by creating $Cu_xSn_{1-x}O_2$ nanocomposite which incorporates Cu^{2+} into the SnO_2 matrix utilising a cost-effective technique and precursor, discovering the identification of SnO_2 phase only at X-ray diffraction (XRD) when copper precursor concentration is low of copper. X-ray fluorescence (XRF) and elemental analysis of energy-dispersive X-ray (EDX) mapping were used to quantify the distribution of Cu in the SnO_2 matrix. A distinct monoclinic phase of CuO (designated here as CuO/SnO2) develops at high copper concentrations. Aside from photoluminescent spectra, Cu-SnO_2 or CuO phases were shown to develop at low and high concentrations. At low concentrations, only the SnO_2 emission peak with a minor blueshift was seen, but at high concentrations, only the CuO emission peak was observed. Investigations were done on how Cu concentration affected SnO_2's ability to detect methane (CH_4) gas. The sensor implanted with 2.00% Cu was found to have an excellent sensitivity and a quick response-recovery time when observed with other sensors listed above. Thus, a Cu incorporation-based sensing mechanism for $Cu_xSn_{1-x}O_2$ and

CuO/SnO_2 is suggested. Later in the same year, [56] the detection of hydrocarbons - methane and propane - in urban air for industrial safety properties has been accomplished using a single metal oxide semiconductor gas sensor. Nanocrystalline SnO2 and alumina micro-hotplates were used to create sensors. The sensor is operational. During the raw sensor data gathering, temperature modulation was used. Preparation of Scaling, baseline extraction, and elimination of non-valid data points have been performed on the acquired data. These techniques have been proved to be important prior to the implementation of machine learning algorithms. In the 40-200 ppm range, an accuracy of 86% for proper gas identification has been observed.

Several methane sensors, such as optical, calorimetric, pyroelectric, semiconducting oxide, and electrochemical sensors, have been summarized thoroughly by Tahani Aldhafeeri [57] in this review. The definitions, methods, and most recent advancements of these sensors are covered in the discussion material. Natural gas's main component, methane, has a major role in climate change and global warming. Reliable and cost-effective sensors must be studied and developed in order to detect and fix methane leaks. To aid with future research requirements, a comparison of several approaches is offered, emphasising their benefits and drawbacks. Later same year, Máté J. Bezdek [58] presented a chemi-resistive sensor for the detection of CH_4, that poses an explosive risk in atmosphere. Chemi-resistor employs low-power,cost and distributed detection of CH_4 in air to find gas leaks in homes, factories, and pipelines. Particularly, the single-walled carbon nanotubes (SWCNTs) that have been noncovalently functionalized with poly(4-vinylpyridine) (P4VP) serve as the basis for the chemi-resistors. P4VP coordination allows a platinum-polyoxometalate (Pt-POM) CH_4 oxidation precatalyst to be included into the sensor. The resultant SWCNT-P4VP-Pt-POM composite shown strong stability to air and time as well as ppm-level sensitivity to CH_4.

With the hypothesised origin of the observed chemiresistive response being the formation of a high-valent platinum intermediate during CH_4 oxidation. The chemiresistor was shown to have a preference for CH_4 over gases like carbon dioxide and hydrogen as well as heavier hydrocarbons like n-hexane, benzene, toluene, and o-xylene. It was also shown how useful the sensor was for detecting CH_4 using a basic portable multimeter. Moshayedi et al. [59] also fabricated a multinanosensor for simultaneous detection of CO_2, CH_4, CH_2OH, NH_3 and its electrochemical response to various concentration in the same year. The Graphene-Oxide/Polyaniline (GO/PANI) nano-composite was produced in the first phase to be used in the fabrication of this multi nano sensor. The chemical make-up, shape, and structure of nano-

composite were examined using FT-IR spectroscopy, FE-SEM, HR-TEM and XRD. Outcomes demonstrate that the Graphene Oxide was successfully fabricated, and the polyaniline particles are firmly affixed to surfaces of the Graphene Oxide sheets. The generated nano-composite was then put on silver-coated electrodes. In order to evaluate the responsiveness, and sensitivity of the multi-nano sensor to each of the gases, amperometric experiments were utilized, and the findings revealed that the sensitivity of the multi-nano sensor manufactured to detect the aforementioned gases is acceptable. According to the electrochemical tests, each multi-nano sensor component's response to a mixture of the aforementioned four gases is defined as a four-unknown equation. By taking into account the responses of four multi-nano sensor components at once to the four-gas mixture, four four-unknown equations are obtained, and by solving the equation, the precise concentration of each of the four measured gases can be ascertained.

Leonardo Furst [60] created a low-cost platform for monitoring methane in this study, and it was utilized in two different contexts to continually evaluate and enhance its performance. Most of the sources of methane, a significant greenhouse gas and precursor to tropospheric ozone, are associated with human activity. Methane has well-known sources, and it is frequently measured with expensive gas analyzers with high operating expenses. Numerous studies have looked at the use of inexpensive gas sensors as a substitute for monitoring methane concentrations, but more research is still needed in this area to assure accurate results. The Figaro TGS2600, a metal oxide semiconductor (MOS) based on tin dioxide (SnO_2), served as the methane sensor. After completing a multi-point calibration, the monitoring platform was initially used in a small ruminant barn. The system was employed in a wastewater treatment facility at a later stage, together with a multi-gas analyzer called the Gasera One Pulse. The relationship between the readings from the two devices served as the basis for the calibration of a cheap sensor. An active ventilation system was employed to enhance the sensor's performance, and temperature and relative humidity were also assessed in order to make changes to minimise their influence on the sensor data. The system demonstrated its ability to monitor low methane concentrations in both locations using consistent temporal and geographical patterns. At the WWTP, a striking similarity in behaviour between the two measurement systems was also seen. A good alternative, at least as a screening monitoring system, was generally shown by the low-cost system under various environmental circumstances. In the same year an automated gas sampling unit was created for a continuous methane monitoring system employing inexpensive gas sensors, the TGS 2611 and MQ-4, and a simple cloud-based data gathering platform. Systems that combine automated gas sampling with a number of inexpensive gas sensors may

have the ability to function as trustworthy, quick methane analyzers. However, there aren't many reports of these kinds of technologies that have been tested in real-world settings. By evaluating samples of high- and low-concentration methane, the author Isura Sumeda [61] confirmed the consistency, repeatability, and reproducibility of the data produced were confirmed by the inexpensive gas sensors TGS 2611 and MQ-4. A gas chromatograph was used as a reference analyzer to check the normalized root-mean-square errors (NRMSEs) of the TGS 2611 sensor for the samples with CH_4 concentration of 3%, 4%, 6%, and 7%. These were, in order, 0.0788, 0.0696, 0.1198, and 0.0719. Anaerobic digesters of laboratory size were tested using the created technology. The two months of continuous operation of the anaerobic digesters showed the possible usage of sensors for methane detection and monitoring in the field level application. This work combined the advantages of affordable sensors with a unique strategy to lessen their drawbacks and provide a reliable monitoring system.

The most often studied gas is methane, which may be found in quantities ranging from a single ppm or ppb to 100%. Gas sensors have a broad variety of uses, including those in cities, industries, rural measures, and environmental monitoring. The monitoring of human greenhouse gases in the atmosphere and the detection of methane leaks are two of the most significant applications. Hence, Miroslaw Kwasny reviewed [62], popular optical techniques for methane detection have been discussed, including lidar methods, cavity ringdown spectroscopy (CRDS), cavity-enhanced absorption spectroscopy (CEAS), direct tunable diode spectroscopy (TDLS), and non-dispersive infrared (NIR) technology. Additionally, their laser methane analyzer designs have been proposed for a variety of applications (DIAL, TDLS, NIR).

2.2 OTHER GAS SENSORS

In order to build high performance gas sensors, it has become more vital to design and prepare oxides with innovative architectural patterns. In recent years, interest in porous nanostructures oxide semiconductor sensing materials has grown due to their large specific surface area, low density, and superior surface permeability. Numerous porous nanostructured oxides and their composites have been successfully synthesised for the development of high-performance gas sensors with improved sensitivity, selectivity, and decreased detection limits. These oxides and composites had improved sensing behaviours (such considerably greater sensitivity and

quicker reaction speed), which may be attributed to the porous structures and the synergistic effects, as shown by the following gas sensing experiments.

A mathematical model of the MOSFET gas sensor was presented in 2002, together with its operational specifications for various hydrogen pressures. Ong et al. [63] demonstrated that the simulation is performed under steady-state circumstances. Chemical processes begin when the MOSFET sensor is exposed to hydrogen gas and finally reach equilibrium. In these circumstances, it is possible to predict how the sensor will respond to different hydrogen pressures by using the linear connection between the shift in the threshold voltage and the various hydrogen pressures that is discovered. The experimental data and simulation results show great agreement, demonstrating the model's evidence.
The MOSFET gas sensor's mathematical model and operating requirements for a range of hydrogen pressures were described by Safari [64]. The simulation is done in steady-state conditions. As hydrogen gas came to the contact with MOSFET sensor, chemical activities start and eventually achieve equilibrium. In these conditions, it is possible to predict how the sensor will respond to different hydrogen pressures by using the linear connection between the shift in the threshold voltage and the various hydrogen pressures that is discovered. The findings of the simulation and experimental data are very congruent, supporting the model's claims.

In 2013, Moshayedi [65] presented the mathematical modeling for the SnO_2 gas sensor. This author’s goal was to build the transfer function of SnO_2 type gas sensor. It was done for transient response and steady-state zones based on sensor data. The mathematical equation for the response, which depends on different concentrations, temperature, and humidity, may be derived using the model. The data were analyzed with Matlab software, and the transfer function parameters were improved using a genetic algorithm. Additionally, it has been researched how concentration variation affects the transfer function coefficients. The findings imply that the modeling can be helpful for researching physical and chemical interactions as well as replicating sensor response behavior.

A graphene field-effect transistor (GFET) gas sensor powered by a low voltage and gated electrochemically by an ionic liquid (IL) is presented by Inaba et al. The graphene is given a gate voltage via an electric double layer of the IL. When compared to solid-gate materials such as silicon dioxide (SiO_2), the nanometer-thick double layer allows for low-voltage operation.

The ILGFET was created using graphene generated by chemical vapor deposition (CVD). The ammonia (NH_3) gas response of the constructed ILGFET was examined to assess its gas sensing property.The IL-gate GFET is made up of a graphene channel between the source and drain electrodes, as well as an IL that covers the channel.

Sensor technology has a significant impact on many elements of our society and has made significant progress as a result of the advancement of nanoscience and nanotechnology. The current focus of research is on producing high-performance gas sensors with low operating temperatures and inexpensive manufacturing costs. Since it uses very little power and doesn't need a heater for high-temperature operation, a gas sensor that functions at room temperature is especially desired since it makes the manufacturing of sensor devices easier and reduces operating expenses. Nanostructured materials are at the heart of each room-temperature sensor platform's development. This article [66] discusses the most important developments in basic science, sensing methods, and the use of nanostructured materials for room-temperature conductometric sensor systems.

Fatma Sarf [67] invented MO nanostructures, which was made of C-based materials are preferable over doped MO films because they function even at ambient temperature. Numerous strategies to increase gas sensitivity have been put forward up to this point. Sensitivity, the primary determinant of sensor performance, may be made stable and capable of future growth with the use of surface modification techniques such various doping types and MO-C composite. Semiconducting metal oxide (SMO) gas sensors were created, manufactured, and evaluated in terms of their capacity for sensing and the micro-hotplate's thermo-mechanical behavior. The sensors operate at a low 10.5 mW power consumption while exhibiting high sensitivity at low volatile organic compound (VOC) concentrations. Additionally, with reaction and recovery durations of 20 s and 2.3 min, respectively, the sensors offer rapid performance.

$Cu_xSn_{1-X}O_2$ nanocomposite was synthesized by Shaalan et al. [55] using a low-cost precursor and technique, and only modest concentrations of Sn02 were used to detect the phase of the metal. The effect of Cu content on SnO_2 sensing characteristics toward methane (CH_4) gas was also studied. Later, it has been shown by Lahlalia et al. [68], that the chemisorption/physisorption process is significantly impacted by nanoparticle forms on the film surfaces, grain sizes, gas types, and operating temperatures. On long-life sensitivity and long-term stability aspects, low concentration detection, determining grain size, and lowering

operating to ambient temperature are existing challenges. Due to the configuration of the atomic surfaces and the active gas adsorption sites that are produced by the doping atoms, doping is a successful method for increasing gas sensitivity. Y. Nishuine [69] demonstrated a very unique hot wire type semiconductor type sensor, with integrated detection element and the heater. The sensitivity of the device is very high, hence large output change. Due to the high-power consumption, MEMS technology has been used to design Ultra-low power MEMS CH sensor, enabling utility companies to install the devices in urban area.

A SnO_2/ZnO heterostructure-based, very sensitive and selective NO2 gas sensor was developed by B. Sharma [71] using sputtering. The characterization of SnO_2/ZnO heterostructure thin film samples were done by FESEM, XRD, EDS and XPS. In comparison to sensors based on their mono-counterparts, heterostructure-based sensors successfully developed larger gas response (S = 66.9) and quicker response-recovery (20 s, 45 s) nature at 100°C toward 100 ppm Nitrogen DiOxide gas. SnO_2/ZnO heterostructures' stability and selectivity were investigated. A detailed description of the more desired sensing mechanism of SnO_2/ZnO heterostructures for NO_2 was provided. Nanosensor development and enhancement have been significant research fields in recent decades. Many different materials and chemicals have been studied for their sensing characteristics. The goal of a research conducted in the same year [72] was to create a novel detecting layer for gas sensors based on chitosan as a polymer augmented with graphene as a nanofiller. The concentrations of graphene used by the author, Fahim, to make the chitosan solution were 0.1, 0.5, and 1 wt%. To fully comprehend the nanocomposite, a variety of characterizations (such as pore size variation, gas permeability, mechanical properties, and electrical resistance) were looked at. Oxygen was used as a sample gas in characterizing investigations. It was revealed that the composite exhibited unusual behavior, having a bigger gas concentration gradient as graphene concentration declined and a stronger electrical conductivity as graphene concentration grew. Gases can be detected mechanically or electrically using these two criteria. Future research should be conducted to establish the circumstances (such as air pressure, room temperature, UV light, and so on) for gas sensing.

This literature has documented the continuous evolution of SMOx sensor materials, along with an expansion of their gas-sensitive capabilities for gas detection [73]. Morphology/nanostructuring and dopants to change MOx's crystallographic structure are the key material-specific factors that may be adjusted throughout the synthesis process and have a

significant impact on the gas sensing characteristics. Gas sensors often employ semiconductor metal oxides (SMOxs) because of its excellent sensing capabilities, availability, and simplicity of production. SnO_2 and TiO_2, which have broad band gaps and give a distinctive set of functional qualities, are the greatest examples of these sensing materials. The most significant of these functional features are electrical conductivity and strong surface reactivity substance detection. Pratik V. Shinde [74] demonstrated the operation of magnetic gas sensors, their basics, current advancements, and their potential for the future in the same year. The basic idea behind how gas sensor's function is to convert the effects of gas adsorption on an active material's surface into a detectable signal in terms of the material's altered electrical, optical, thermal, mechanical, magnetic (magnetization and spin), and piezoelectric characteristics. The magnetic properties of the active materials in magnetic gas sensors are monitored using a variety of techniques, including the Hall-effect, magnetization, ferromagnetic resonance, magneto-optical Kerr effect, and magnetostatic wave oscillation effect etc. The chemical selectivity and sensitivity to dampness and high-temperature functioning of several kinds of gas sensors are drawbacks. For instance, in the case of chemiresistive-type gas sensors, the total electrical effect is highly complicated owing to concurrent surface processes, and the change in sensor resistance might substantially vary in the actual environment due to the existence of other gas species. Additionally, reliable connections for powdered samples for the traditional electrical property-based gas sensors are difficult to manufacture. Due to their flammable characteristics at higher working temperatures, electrical property-based hydrogen gas sensors can pose a fire threat. Magnetic properties of the materials in magnetic gas sensors are affected when exposed to gas molecules.

In the recent year 2022, Sharma et al. [75] demonstrated progress on group III nitride nanostructure-based gas sensors. This paper summarizes the present state of group III nitride-based gas sensors. The metal-semiconductor interface's Schottky barriers react to gas adsorption on the metal surface. Several dangerous gases have been detected using metal Schottky contact-based group III nitrides. This evaluation focuses on three important themes. To begin, recent gas-sensing findings on the uses of binary and ternary nitride layers and group III nitride nanomaterials for detecting many dangerous gases are presented. Second, several heterostructures of functional materials group and III nitrides that are responsible for gas sensing are reviewed in depth, along with the sensing methods that they employ. Finally, the paper discusses the future prospects and forecast for group III nitride-based gas sensors.

2.3 BORON NITRIDE BASED GAS SENSORS

Li et al. [76] researched about the gas sensing properties of BNNT and C-doped BNNT for a few tiny gas molecules, such as methane, carbon dioxide, hydrogen, water, nitrogen, ammonia, oxygen molecules and so on. This has been done using the density functional theory calculations, showing the low sensitivity property of BNNT and a high sensitivity to the gaseous Oxygen, nitrogen and F_2 molecules. After the absorption of O_2, NO_2, and F_2 molecules, the electronic structures of BNNT and C-doped BNNT undergo remarkable modifications. From the point of view of interaction energy, CH_4, CO_2, H_2, H_2O, N_2 and NH_3gas molecules and BNNT and C-BNNT, the interaction between them is relatively weak. The interaction between them O_2, NO_2 and BNNT and C-BNNT is relatively strong. Although the contact between gas molecules and BNNT may be increased by C-doped BNNT, its sensitivity cannot be increased as compared to pure BNNT.

A work [77] has reported synthesis of a large-area h-BN film using APCVD on a Cu foil, followed by Cu etching and transfer to a target substrate. The concentration of the precursor borazine and the ambient gas conditions, such as the hydrogen to nitrogen ratio, have a significant impact on the growth rate of the h-BN film at a constant temperature. The growth time or growth conditions may be adjusted to produce b-BN films of various thicknesses. These h-BN films are polycrystalline, and the c-axis of the crystallites has varied axes, according to the results of transmission electron microscopy analysis. By using electron energy loss spectroscopy, it was discovered that the stoichiometry ratio of boron and nitrogen is almost 1:1. The parallel capacitance experiments on h-BN film yielded a dielectric constant of 24. Before and after device integration, the CVD graphene device's mobility (in the few thousand cm(V-s) range) remained constant. In top-gated CVD graphene devices, these CVD-grown h BN sheets were integrated as a dielectric layer.

Most recent developments in hBN-based devices are analytically summarised in this study. where Neeraj Goel [78] focused on gas sensors in particular. Additionally, a thorough explanation of the physics of hBN-based gas sensors has been provided here. Additionally, a complete compilation of current technical developments to overcome ingrained characteristics like weak surface reactivity and low conductivity has been made. We have now covered some

of the major difficulties that hBN technology must overcome in order to create useful gas sensors. In the same year Acharya et al. [79] reviewed an article on BNQDS based sensors. This article provides an outline of the early-stage research development of BNQDs. The author provided an unbiased appraisal of various synthesis methods, property analyses, and applications of BNQDs, and he outlined his outlook on the evolution of these new nanomaterials in the coming years. Boron nitride quantum dots (BNQDs) are gaining popularity due to their many fluorescent, optoelectronic, chemical, and biological features. Excitation-dependent emission (and, in certain circumstances, non-excitation dependent) has been documented, as have chemical functionalization, bioimaging, phototherapy, photocatalysis, chemical and biological sensing.

2.4 2D MATERIAL BASED GAS SENSORS

P. K. Kannan et al. presented an article [80] on recent development of 2D layered inorganic material, where the author provides an in-depth look at recent advancements in the use of 2D layered inorganic nanomaterials for sensors. For diverse sensing applications, including gas sensing, electrochemical, SERS and biosensing, SERS sensors, and photodetection, some of the essential properties of 2D materials are explored. Additionally, examples are used to explain the core principles of how the sensors work.

High-boiling-point solvents are avoided because they leave a residue and cause aggregation. Chemical sensor performance has been significantly enhanced by gas sensors built from 2D-MoO3 nanosheets. The 2D-MoO3 sensor's [50] response rises from 7 to 33, its reaction time falls from 27 to 21 seconds, and its recovery time drops from 26 to 10 seconds when compared to bulk MoO3 sensors. The 2D-structure's improved performance is ascribed to its reactive spots and significantly increased surface area. In the same year, Morgan [81] discussed current advances in 2D materials, heterostructure production, and sensing applications, concluding with present issues and proposals for future advancements in this merging field.

Shin et al. [82] recently presented recent ReaxFF force field developments. The author also discussed applications in modeling the 2D materials (Nonlayered and Layered): graphene, transition metal dichalcogenides, MXenes, h-BN, groups three, four and five-elemental materials, and mixed dimensional van der Waals heterostructures. The work has also addressed the difficulties and plans for the development of ReaxFF and potential large-scale simulations.

2.5 SUMMARY IN TABULAR FORM:

Table 2.1 Evaluation of previously designed Methane Sensors of different technologies

Method	Year	Researchers	Key Techniques/ Instruments	Advantages
Vapor phase polymerization, Ultrasonification, Dip coating.	2008	Li et al. [53]	Facile method; Vapor phase polymerization; Ultrasonification; Transmission electron microscopy; atomic force microscopy, data-acquisition card	Extremely Reversible and Repeatable reaction. Indicates at room temperature.
Covalent and non-covalent method, CVD, Drop casting method	2008	Zhang et al. [54]	Functionalizing CNTs using Covalent and non-covalent methods. CNT chemiresistor and chemical field effect transistor (ChemFET).	Increase in sensing performance due to functionalized CNT sensors: sensitivity, selectivity, and reaction time. Development of analyte-specific, quick, and reliable sensors and sensor arrays, together with adequate numerical algorithms to interpret sensor array data, and creation of high throughput nanomanufacturing technologies.
Sol-gel, Vertical Electron Transport mechanism,	2010	P. Bhattacharya [46]	Vertical Electron Transport mechanism. Sol-gel method.	Compared to traditional devices, the devices have a high reaction rate

UV-assisted electrochemical Anodization			Nanocrystalline-nano-porous ZnO thin films. FESEM, XRD.	with quick response and recovery for lowering gases like H2 and methane. MIM device created from sol-gel, built on Si substrate, makes it IC compatible and appropriate for the integrated sensor platform.
Sacrificial template, thermal evaporation–condensation (TEC) approach, Microfabrication techniques, dielectrophoresis. Photolithography, sputtering processing.	2012	Biaggi-Labiosa et al. [47]	SnO_2–MWCNT hybrid nanostructures, SnO_2 based nanorods as sensing material, Gas sensors based on polycrystalline tin oxide/ semiconducting metal oxide. HRTEM. ED pattern.	Superior over high temperature methane sensors in power consumption. Considering the sensitivity of the sensing layer improves with grain size, nanocrystalline SnO_2 is projected to be very sensitive. Miniature size, low weight and cost, and convenience of use.
Modified hummer's method, Facile room temperature synthesis, hydrothermal method XRD, FTIR, TEM.	2019	Roshan et al. [45]	PbS, Reduced Graphene Oxide nanocomposite	At the lower explosive limit of methane, the sensor has a satisfactory response (greater than 40%). At low concentrations, only SnO_2 can only emit peak with a minor blueshift.
Flame spray pyrolysis technique, Baseline cut-off, data scaling, extraction of data points	2019	Krivetskiy et al. [56]	Metal oxide semiconductor; artificial neural networks; gas sensor; temperature modulation; signal pre-processing.	Accuracy of 86% for proper gas detection. Effects of metal oxide gas sensor drift in real-world urban air. MOX sensors are made suitable for the

				use in industrial safety duties involving the leaking of flammable and explosive gases.
IR absorption spectroscopy. electromagnetic radiation detection. Infrared heating. Sol-gel process. TDM Technique. Oxidation-Reduction reaction.	2020	Aldhafeeri et al. [57]	Methane detection; optical sensors; electrochemical sensors; calorimetric sensors; pyroelectric sensors; semiconducting oxide sensors	More precise, reliable sensors, improved natural gas pipeline safety.
Analyte detection using SWCNTs, Spray Coating	2020	Bezdek [58]	Chemiresistors catalysis, SWCNT-P4VP composites, Platinum-polyoxometalate (Pt-POM) aerobic CH4 oxidation precatalyst	The chemiresistor operates in air at room temperature, with ppm-level sensitivity for CH4, and selectivity over heavier hydrocarbons as well as gases like CO2 and H2.Can be combined with a portable multimeter.
Modified hummers method, Chemical synthesis Method, FT-IR, FE-SEM, HRTEM, XRD. Four-channel amperometric analysis	2020	Moshayedi et al. [59]	Graphene-Oxide/Polyaniline (GO/PANI) nano-composite. Multinanosensor, Carbon-based nanomaterial.	Well-bonded polyanile particles on the surface of GO Sheets. This multi-nano sensor can be used to create devices to distinguish between live and dead bodies trapped beneath collapsed structures.
Multi-point calibration	2021	Leonardo Furst et al. [60]	Figaro TGS 2600 sensor,	Portable and cost effective system for

			10-bit Arduino Analog-to-Digital Converter (ADC), multi-gas analyzer (Gasera One Pulse).	methane detection- Cost effective; Improve in the resolution of the sensor for lower concentrations
Automated Gas sampling, Gas chromatography	2021	Nagahage et al. [61]	TGS 2611 MQ-4, Cloud based data gathering platform.	Consistency, repeatability, and reproducibility of the data produced were confirmed by the inexpensive gas sensors TGS 2611 and MQ-4.
Lidar methods, (TDLS), cavity ringdown spectroscopy (CRDS), cavity-enhanced absorption spectroscopy (CEAS), NIR tech.	2023	Kwasny et al. [62]	Methane detection, gas sensor, optical methods, concentration.	Variety of applications (DIAL, TDLS, NIR).

Table 2.2 Evaluation of previously designed Other Gas-sensors

Method	Year	Researchers	Key Techniques/ Instruments	Advantages
Mathematical, Modeling, Simulation. Photolithography patterning.	2002	Ong et al. [63]	Multiwall Carbon Nanotube. Gas adsorption; Hydrogen pressure MOSFET gas sensor; Platinum gate	Wireless monitoring applications. Experimental data and simulation results show great Agreement.
Mathematical Modeling, simulation	2009	Safari et al. [64]	Hydrogen pressure MOSFET gas sensor Platinum gate	Variations in the MOSFET gas sensor's threshold voltage when

				subjected to various hydrogen gas pressures. The linear relationship between ΔVT/(ΔVT-ΔVTmax) and the root of the hydrogen gas pressure is clearly seen in the excellent agreement between the analytical and experimental results.
Mathematical Modeling. Multi-exponential method	2013	Moshayedi et al. [65]	Gas sensor; TGS 813; second-order response; transient estimate; genetic algorithm (GA); and second-order transfer function model. MATLAB, LabVIEW VI and DAQ card.	Possibility of an entire modeling system, comprising sensor response, the impact of all chemical and physical interactions, and a mathematical model.Model as the initial gate for the sensor characterization.
CVD EB Lithography.	2014	Inaba et al. [66]	IL GFET Raman spectrography	Response Time 33s. IL- gate structure, capable of decreasing operating gate voltage.
Electronic Sensitization. Chemical Sensitization.	2015	Zhang et al.	Nanostructured materials: Single element materials. Si-based materials, Tellurium-based	Pt-SnO 2 /RGO sensor, sensitive to 0.3% H 2 at ambient temperature. Stability can be preserved without

Atomic Force Microscopy (AFM)			materials. Carbon nanostructures.	signifi cant degradation for several months.
Doping	2019	F. sarf [67]	MO Nanostructures	Great sensitivity at low volatile organic compound (VOC) concentrations at a modest 10.5 mW power consumption; Quick responses and recoveries with times of 20 s and 2.3 min
Doping	2019	Lahlalia et al. [68]	Gas absorption	Long-life sensitivity and long-term stability aspects, low concentration detection.
SDC Sputtering; Screen-printing method.	2019	Shaalan et al. [55]	X-ray(EDX) Mapping; TEM; X-ray Fluorescence (XRF)	Sensitivity of 69.0 at 350 °C and response–recovery time is very less compared with the other sensors.
MEMS Technology	2019	Nishiue [69]	Hot-wire type Semiconductor sensor.	Battery powered methane detection; Integrated detection element, simple structure;Mass production; Very low resistance; Very high sensitivity.
Gas Sensors Based on Oxide Semiconductors with Porous Nanostructures	2019	P. Sun [70]	Porous nanostructures oxides and their composites	High performances gas sensors with enhanced sensitivity, selectivity, Faster response speed.
Sputtering.	2020	Bh. Sharma et al. [71]	Gas Sensing, FESEM	Greater response= 66.9 , faster

			XRD EDS XPS	response-recovery (20 s, 45 s) at 100◦C working temperature towards 100 ppm NO_2.
Characterization.	2020	Fahim [72]	Gas-sensor on chitosan, Graphene as Fiber.	Greater gas concentration gradient and a higher electrical conductivity
Electyrochemical Anodization, hydrothermal method Matrix-assisted pulsed laser evaporation. Sonochemical method etc	2021	Saruhan et al. [73]	MOx's crystallographic structure. Semiconductor Metal Oxide Nanostructure	Excellent sensing capabilities, availability, and simplicity of production, Broad band gaps give a distinctive set of functional qualities, functional features are electrical conductivity and strong surface reactivity substance detection
Hall effect, magnetization, magneto-optical Kerr effect, spin orientation, ferromagnetic resonance, and magnetostatic wave oscillation effect.	2021	Shinde [74]	Magnetic Gas Sensor	Chemical selectivity and sensitivity are better respect to other gas sensors.

Table 2.3 Evaluation of previously designed Boron Nitride based Gas Sensors

Method	Year	Researchers	Key Techniques/ Instruments	Advantages
DFT,Adsorption. Generalized gradient approximation structure optimization and electronic structure calculations	2007	Li et al. [76]	Boron nitrogen nanotube; gas molecule; Carbon doping; gas sensor;	interaction between them O2, NO2 and BNNT and C-BNNT is relatively strong.
APCVD	2012	Kim et al. [77]	Electron energy loss spectroscopy. APCVD	CVD-grown h-BN films, integrated as a dielectric layer in top-gated CVD graphene devices. Thickness of the h-BN films can be controlled by different growth conditions and growth times.
DFT, chemisorption; Solvothermal process	2021	Goel et al. [78]	DFT, Coulomb scattering	Operates at lower operating temperature. Higher performance, flexible and wearable gas senor.
Edge functionalization, Light absorption	2021	Acharya et al. [79]	BNQDS. Van der Walls nanostructures, Solar energy harvesting	Simple and cost-efficient; Response and recovery time of 20 s and good stability.

Table 2.4 Evaluation of previously designed 2D Material based Gas sensors

Method	Year	Researchers	Key Techniques/ Instruments	Advantages
Micromechanical exfoliation; micro-mechanical cleavage, pulsed laser deposition (PLD)	2015	P. K. Kannan et al. [80]	Gas sensing, electrochemical, SERS; biosensing,optical microscopy, AFM, FESEM and HRTEM	Comparison between recent 2D layered gas sensors
Liquid exfoliation	2019	Ji et al. [50]	UV-Vis-NIR spectroscopy; X-ray diffraction; Raman spectroscopy; TEM; AFM	Increased sensors response: 7-33; Reduced response time from 27 to 21 seconds, and shortened recovery time from 26 to 10 seconds.
	2019	Morgan et al. [81]	Raman spectra, Scanning tunneling microscopy, transmission electron microscopy, and electron energy loss spectroscopy (EELS)	2D material properties and sensor device applications; Sensors operating at room temperature
Modeling, Simulation of vapor-phase and colloidal synthesis of 2D materials	2023	Nayir et al. [82]	Synthesis techniques; Multiscaled modeling	Different modeling techniques, synthesis techniques, Gas sensing techniques have been discussed.

2.6 OBJECTIVES OF THIS WORK

2D material-based nano gas sensors hold great promise for gas detection and monitoring applications due to their unique properties and high sensitivity and the integration of 2D materials (Graphene, TMDs: MoS_2, WS_2, Phosphorene, black phosphorus, silicene, germanene) with innovative device architectures and fabrication techniques has the potential to revolutionize the field of gas sensing, It has been recognized that hexagonal BN provides a clean and stable surface for gas adsorption and reduces interference from other environmental factors due to its insulating property with wide band gap, high thermal stability and excellent chemical inertness. On the other hand, Silicon is a widely used semiconductor material that allows for the integration of electronic components, such as transistors or microelectromechanical systems (MEMS), to enhance the sensing capabilities and enable signal processing.

- ✓ Hence two composite structures of h-BN/Si and h-BN/SiO_2 have been proposed here for methane Gas sensing.
  - It is expected that the h-BN layer deposited on silicon can enable the detection of gases through various sensing mechanisms, such as surface adsorption or charge transfer. The interaction between the gas molecules and the h-BN surface can induce changes in the electrical, optical, or mechanical properties of the h-BN layer, which can be measured and correlated to the gas concentration or presence. In this case, the h-BN layer acts as the sensing material while the silicon substrate provides a platform for device integration and electrical connections.
  - On the hand, Silica, also known as silicon dioxide (SiO_2), is an insulating material commonly used in the fabrication of substrates and optical devices. While silica itself is not typically used as a gas sensing material, it provides a stable and inert platform for the deposition of h-BN. Silica can withstand high temperatures, has good thermal stability, and offers excellent optical transparency, which can be advantageous for certain gas sensing applications. Also, this composite structure can be used for sensitive and selective gas detection in various applications. Overall, the h-BN/SiO_2 hybrid gas sensor combines the gas-sensing capabilities of h-BN with the desirable properties of silica as a substrate

Chapter III

CHEMISTRY AND CHARACTERIZATION

3.1 CHEMISTRY BEHIND METHANE DETECTION

The principle of methane detection typically involves the interaction between methane molecules and the sensing material, which leads to a measurable signal indicative of the presence and concentration of methane.

Here's a general overview of the chemistry involved:

Sensing Material: The sensing material of the methane sensor plays a crucial role in detecting methane. It is designed to have an affinity for methane molecules, allowing them to interact with the material's surface.

Adsorption: When methane gas comes into contact with the sensing material, it undergoes adsorption. Adsorption is the process by which gas molecules adhere to the surface of a solid material. In the case of methane sensors, the sensing material's surface properties facilitate the adsorption of methane molecules. Methane exhibits several absorption lines in the 1.63-1.69 μm range [61]. With a total absorption (cross-section) of 5.13×10^{-20} cm^2, these lines are suitably powerful.

Surface Reactions: Upon adsorption [72], methane molecules may undergo various surface reactions on the sensing material's surface. These reactions can modify the electronic or chemical state of the sensing material, leading to a measurable response.

Electron Transfer: In some cases, methane sensors utilize materials capable of electron transfer reactions. When methane molecules interact with the sensing material [71], they may donate or accept electrons, resulting in changes in the material's electrical conductivity or charge distribution [72].

Catalysis: Certain methane sensors employ catalytic materials [57] that facilitate the chemical reaction between methane and another species present on the sensor's surface. For example, methane can react with oxygen in the presence of a catalyst to produce carbon dioxide and water. This reaction can be detected as a change in the sensor's output.

Transduction: The changes occurring at the sensing material's surface are transduced into a measurable signal. This can be accomplished through various means, including changes in electrical resistance, capacitance, conductance, optical properties, or changes in the surface potential.

Signal Processing: The output signal from the methane sensor is typically processed using suitable electronics and algorithms to interpret the concentration of methane gas. Calibration curves or calibration methods are used to relate the sensor's response to the actual methane concentration.

It's important to note that different types of methane sensors employ diverse sensing principles and materials. Therefore, the specific chemistry involved can vary depending on the sensor technology, such as catalytic sensors, semiconductor-based sensors, or optical sensors.

3.1.1 METHANE SENSOR

In order to monitor and detect methane [83] levels in air in percent LEL (Lower Explosive Limit) levels or in percent by volume levels, a methane gas sensor has been designed. It is a device that is employed as an integral part of a fixed gas detection system.

3.1.2 METHANE MOLECULE FROM THE PERIODIC TABLE

According to the periodic table, it belongs to group 14. It is nonmetallic and tetravalent, which means that four of its electrons may be used to create chemical connections. The gas hydrogen is combustible, colorless, odorless, and non-toxic. It has atomic number 1, making it the lightest element. A diatomic, hydrogen has the chemical formula H_2.

The simplest saturated hydrocarbon, methane in the paraffin family, contains four equivalent C-H bonds, making it a tetrahedral molecule, is highly stable and at normal temperature due to the structure also it is inert to acid, base, Oxidising and reducing agent. But methane participates in substitute reaction due to sp3 hybridization and regular tetrahedral structure of C atom at the Centre of CH_4. It has the chemical formula CH_4. With just one carbon atom and four hydrogen atoms, it was the most basic alkane. Alessandro Volta made the first scientific discovery of methane in 1776 [83]. It is created by anaerobes in the colon.

3.1.3 STRUCTURE OF METHANE MOLECULE

Methane consists of four hydrogen atoms and one carbon atom. With an atomic number of 6, carbon is a non-metallic chemical element that is denoted by the letter C.

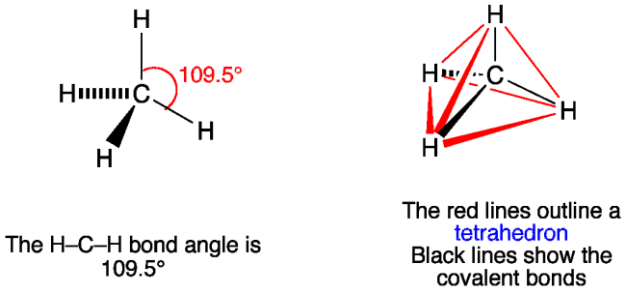

Fig. 3.1 (a) Methane molecule structure. [83]

The structure, consists of a central carbon atom bonded to four hydrogen atoms, the carbon atom is located at the center, and the four hydrogen atoms are attached to it. The arrangement of the atoms can be visualized as a tetrahedron. Here the carbon atom is at the center of the structure, and four atoms of hydrogen occupy the four corners.

Each hydrogen atom forms a single covalent bond with one carbon atom, sharing an electron pair, meaning they have the same bond length. Covalent bonds are formed through the overlapping of the valence orbitals of the participating atoms. In the case of methane, the carbon atom forms four such covalent bonds, one with each hydrogen atom. There is just one form of derivative CH_3Z that may be produced when any one of the methane's H-atoms is swapped out for a monovalent atom or group (Z). This demonstrates the comparable nature of methane's four H-atoms.

The bonding in methane is described as sp3 hybridization, meaning that the carbon atom hybridizes its three 2p orbitals and one 2s orbital to form four sp3 hybrid orbitals. These hybrid orbitals are arranged in a tetrahedral geometry around the carbon atom, with the four hydrogen atoms occupying these orbitals.

The structure of methane is symmetrical, with all the carbon-hydrogen bonds being identical in length and strength. The molecule has a tetrahedral shape, with the bond angles between the carbon and hydrogen atoms measuring approximately 109.5 degrees.

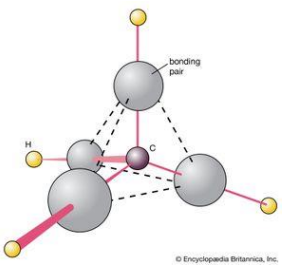

Fig. 3.1 (b) Tetrahedral shape of CH4 molecule with bond angle 109.5 ◦. [84]

Overall, the structure of methane, with its tetrahedral arrangement of atoms and symmetrical bonding, contributes to its stability and inertness, as well as its physical and chemical properties. Methane has a regular tetrahedral structure.

3.1.4 PHYSICAL PROPERTIES OF METHANE

Few properties of methane [83]-[89] are highlighted below:

a) At normal temperature, Methane gas has no color, no smell, no taste, and is not harmful.
b) It is slightly soluble in water, but it is more solubles in organic solvent like alchohol, acetone and ether.
c) On cooling, it gets converted into liquid and solid.
d) **Boiling point**: 162 °C (259.6 °F).
e) **Melting Point**: 182.5 °C (296.5 °F).
f) **Electron Affinity**: +1.2 eV.
g) **Ionization Potential**: 13.7 Volts.
h) **Bond dissociation energy/enthalpy**: 416 kJ/mol.
i) Methane is lighter than air due to its specific gravity of 0.554
j) Density of Methane: 0.657 kg/m3 (gas, 25 °C, 1 atm), 0.717 kg/m3 (gas, 0 °C, 1 atm), 422.8 g/L (liquid, −162 °C)
k) In water, it hardly dissolves at all.

3.1.5 CHEMICAL PROPERTIES OF METHANE

Methane, with its simple molecular structure, exhibits several important chemical properties:

- **Combustibility:** Methane is highly combustible and burns readily in the presence of oxygen. When ignited, it reacts with oxygen to produce carbon dioxide (CO_2) and water (H_2O) vapour [83]. This property makes methane a valuable fuel source, and it is the primary component of natural gas. The flame is fierce, drab, and barely noticeable. If the methane level is between 5 and 14 percent by volume, methane and air may react explosively. Such combination explosions, which have been common in coal mines and collieries, have contributed to a number of mining catastrophes.

$$\mathbf{CH_4 + 2\ O_2 \rightarrow CO_2 + 2\ H_2O} \qquad \mathbf{(3.1)}$$

- **Methane as a Hydrocarbon:** As a hydrocarbon, methane can undergo various chemical reactions typical of this class of compounds. These include substitution, addition, and combustion reactions.

  I. **Substitution Reactions:** Methane can undergo substitution reactions, where one or more hydrogen atoms are replaced by other atoms or groups. For example, chlorine gas (Cl_2) can react with methane to form chloromethane (CH_3Cl) by replacing one hydrogen atom. This type of reaction is often carried out under specific conditions [89], such as the presence of light or heat.

  II. **Addition Reactions**: Methane can participate in addition reactions, where atoms or groups of atoms are added to its carbon atoms. For instance, in the presence of excess oxygen, methane can undergo combustion, adding oxygen atoms to produce carbon dioxide and water.

  III. **Reaction with Halogens:** Methane can react with halogens such as chlorine or bromine to form halogenated derivatives [86]. These reactions involve the substitution of hydrogen atoms in methane with halogen atoms. For example, methane reacts with chlorine to produce chloromethane (CH_3Cl) and hydrogen chloride. [89]

$$\bullet X + CH_4 \rightarrow HX + \bullet CH_3 \quad (3.2)$$

$$\bullet CH_3 + X_2 \rightarrow CH_3X + \bullet X \quad (3.3)$$

  Here halogen X can consist of fluorine, chlorine, bromine, or iodine. The process's mechanism which is known as free radical halogenation, begins as a halogen atom is created by UV radiation or another radical initiator (such as peroxides).

- **Inertness:** Methane is relatively unreactive under normal conditions. Methane is a highly unreactive starting material because the C-H bond is exceedingly inert [87] and non-polar, with a high bond dissociation energy [89]. It does not readily undergo reactions with most common reagents or participate in typical organic reactions. This inertness is due to the strong carbon-hydrogen (C-H) bonds in methane, which require significant energy to break.

- **Greenhouse Gas**: Methane is a potent greenhouse gas, contributing to global warming [89]. It has a stronger greenhouse effect than carbon dioxide, although it occurs in lower concentrations in the atmosphere. Methane is produced by various natural and human activities, including the decay of organic matter, livestock farming, and fossil fuel extraction.

3.2 METHANE DETECTION PRINCIPLES AND SENSING MECHANISMS

Methane is the most often measured gas, with concentrations ranging from a few ppm or ppb to 100% [57]. An explosive combination formed by 4.5-15% of the quantity of methane in the air can trigger explosions in hard coal mines. Due to the time required to evacuate the afflicted region, it is critical to detect concentrations that are considerably lower than those that might trigger explosions. It is consequently critical to build methane gas leak detectors in order to give a helpful tool for detecting damaged natural gas pipes.

However, to detect low concentrations of methane, alternative methods such as electrochemical, IR-absorption. Chemiresistive diode laser. Optical fibre and cataluminescence based methane sensor due to high cost and inaccurate results while detecting molecules with similar Mass Number to Atomic Number ratio (M/Z).

Chemiresistive sensors stand out among the others due to its ease of manufacture, compatibility with current CMOS technology, and affordability. Metal oxides [72]-[82] and their derivatives are used as the sensing element in the majority of chemiresistive methane sensing systems. Unfortunately, the sensor devices created from these materials often operate at high temperatures, which increases the cost of both the manufacture of the device (since a micro heater must be included into it) and the operation of the device (because the micro heater uses more power).

Layered materials like graphene, boron nitride (BN) [71]-[77], transition metal dichalcogenides (TMDs) like WS2 and MoS2 [50,51], and MXenes like transition metal carbides, nitrides, or carbonitrides have lately replaced these conventional materials.In addition to these molecules, several different element nanostructures have also been researched for use in various electronic applications.

3.2.1 CALORIMETRIC SENSORS

Methane and other combustible gases may be found in landfills, petroleum drilling and processing areas, and coal mines via the use of calorimetric sensors in a variety of applications [57]. Catalytic gas sensors, adsorbent-based gas sensors, and thermal conductivity gas sensors are the three different categories of calorimetric gas sensors. A temperature sensor, a catalytic combustion chamber, and a heating apparatus often make up the calorimetric gas sensor.

As seen in Figure 3.2, the calorimetric sensor's operation is based on the idea that heat may be absorbed or released by chemical reactions or physical processes. The component of the calorimetric sensor that interacts with the gas is crucial. In order to lower the combustion temperature, a surface layer is often used as a catalyst for the combustion process. The three catalysts that are most often employed in calorimetric gas sensors are platinum (Pt), palladium (Pd), and rhodium (Rh). The catalyst-coated platinum or palladium coil, commonly referred to as the pellistor [90], is a common component of calorimetric sensors. When methane comes in contact with the catalyst [91], the gas oxidises in an exothermic process that generates heat. The chemical reaction causes a change in temperature of the catalytic surface, which is used by the calorimetric sensors to provide a sensing signal. The initial state, thermal equilibrium, is devoid of analyte and temperature signals. The second state occurs when the polymer absorbs the analyte, and the temperature of the polymer rises. Because of the concentration equilibrium and constant enthalpy, the signal finally decays to zero.

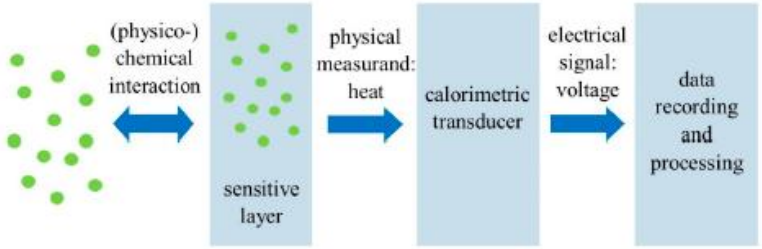

Fig. 3.2 Working principles: Calorimetric Gas Sensor.[57]

- **Solid-state sensors**: Interaction between methane and semiconducting or conductive materials [92] leading to changes in electrical properties.

3.2.1.1 CATALYTIC COMBUSTION SENSORS

Since the 1920s , catalytic sensors [93] have been the most common type of sensor used in mining to find methane in underground spaces. There are two components to the sensors: active and passive. Active element undergoes a catalytic combustion process and the passive element acts as a reference to account for fluctuations in the temperature, pressure, and humidity of the surrounding environment. The sensor is a part of the Wheatstone bridge.

Currently, there are two types of catalytic combustion sensors: pellistors and hot fiber (hot wire). Pellistors are created by heating platinum fiber and submerging it in a stream of combustible gas and air. The platinum fibre has three uses: it is a heating element, a catalyst for the combustion process, and a resistance thermometer. The circuit's electric current raises both pellistors' surface temperatures to between 400 and 500 °C, enabling the gas combination to undergo catalytic oxidation.

3.2.1.2 THERMAL CONDUCTIVITY DETECTOR

The earliest form of sensor used to analyze the composition of gas mixtures is the Thermal Conductivity Detector (TCD) [93], also known as katharometer. It works by identifying variations in thermal conductivity brought on by a shift in a carrier gas' chemical composition. A current traveling through the sensor's two or four thermistors causes them to heat up and produce an unbalanced Wheatstone measuring bridge. The sensor features a straightforward design, excellent sensitivity, and linear response across a broad measurement range. Its principal flaws are a lack of selectivity and the need to maintain constant sensor temperature, gas flow rate, and reference conditions.

3.2.2.1 SEMICONDUCTING METAL OXIDE SENSORS

Semiconducting metal oxide (SMO) sensors [68, 73] that measure electrical conductivity can distinguish between species based on the oxidation and reduction reactions that take occur between the SMO and the target gases.

Change in electrical resistance brought on by the gas of interest absorbing onto the active sensing layer may be used to determine the gas concentration [68]. SMO sensors have two main applications: air quality monitoring and safety equipment (prevention of explosion, leakage, fire, pollution, and poisoning). The two main types of SMO are n-type and p-type. Hole is a primary carrier in p-type SMO (nickel oxide m, cobalt oxide), whereas electron is the dominating carrier in n-type SMO (tin dioxide, iron (III) oxide). Because oxygen vacancies naturally create electrons, SMO methane sensors are mostly n-type [73]. An n-type SMO sensor is equipped with a little amount of electrical resistance from n-type metal oxide semiconductor crystals, such as SnO_2 or WO_3 [93].

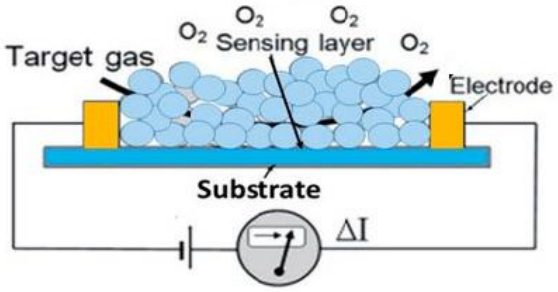

Fig. 3.3 Gas Sensing mechanism of metal oxiode. [57]

The SMO surface reacts with a reducing gas like methane when exposed to that environment, absorbs the gas molecules, lowering the potential barrier in the process to increase the surface concentration of electrons while decreasing electrical resistance. According to reports, the presence of a catalyst, which would boost the surface reactivity, has a significant impact on the conductivity response. The gas detecting system of an SMO sensor design is shown in Figure 3.3.

3.2.3 ELECTROCHEMICAL SENSORS

The International Union of Pure and Applied Chemistry (IUPAC) defines electrochemical sensors as chemical sensors that have a linked receptor and transducer.

The working electrode is where methane is oxidized in the sensor's design, together with a counter electrode that balances the current there and a reference electrode for measuring the potential of the working electrode. To maintain the system's charge neutrality, an electrolytic fluid connects the working and counter electrodes. Figure 3.4 depicts the schematic of an electrochemical sensor. The detected methane content is inversely correlated with the measured current between the working and counter electrodes. The qualities of electrochemical sensors and their applications are determined by the materials used for the electrolyte, electrodes, and catalyst.

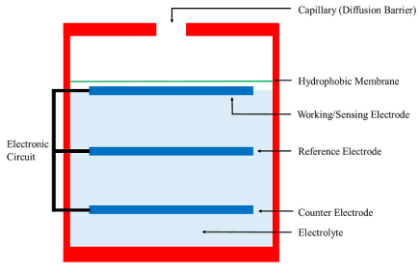

Fig. 3.4 Schematic: An electrochemical sensor [57]

Potentiometric sensors, volt-ammetric/amperometric sensors, and conductometric sensors are categorized as electrochemical sensors [80] according to the applied electrochemical transduction mode. When there is no current flowing through an electrode, potentiometric sensors evaluate its electrical potential. While amperometric sensors detect the gas concentration as a function of the current at a constant potential, voltammetric sensors determine the current as a function of the potential that swings constantly or gradually. When a target gas is present, conductometric sensors may detect changes in a material's or a film's electrical conductivity. There are two main types of electrolytes for electrochemical methane sensors: liquid electrolytes (such aqueous electrolytes and ionic liquid electrolytes), and solid electrolytes.

Aqueous electrolytes are easily available, cheap, and simple to employ. Examples of typical AEs are H_2SO_4 and NaClO. An electrochemical cell carrying pt. electrodes, aq. phosphoric acid, and an electrolyte made future AE-based methane detection applications viable in 1963.

This electrochemical cell was able to oxidize methane in the range of 60-150℃. The main issues that prevent the widespread application of AE-based sensors, however, are their volatility characteristics and broad potential window. The AE evaporates with time, requiring regular replacement, raising the sensor's cost. Methane's potential for partial oxidation reaction might result in catalyst poisoning and reduce the sensor's lifetime.

3.2.4 OPTICAL SENSORS

Catalytic (thermometric) and thermal conductivity sensors are the most often employed for detecting methane, however optical sensors are gradually replacing them [46]. Measurement of methane concentrations based on its absorption or emission properties in specific wavelength ranges. In particular challenging circumstances, hBN's high thermal conductivity and temperature stability make it an excellent material for gas detection. Numerous gas molecules (NO_2, NO, NH_3, CO, CH_4, H_2, etc.) have been adsorbed on the surface of hBN and have been the subject of both experimental and computational investigation.

The arrangement of the boron and nitrogen atoms in hBN makes it very sensitive to various gases. The electrical properties of hBN are altered when it is exposed to gas molecules, making it suitable for the development of practical gas sensors. Additionally, the sensor's sensitivity was improved and there was more surface area for the gas molecules to be adsorbed due to its ultrathin nature. The performance of hBN can work at very high temperatures without degrading, which makes it a candidate for innovative new uses as a flexible gas sensor. However, due to their inert nature, hBN-based sensors [57] have long response time, poor selectivity, and limited reversibility. As a consequence, a number of techniques have been used to improve their detecting capacities.

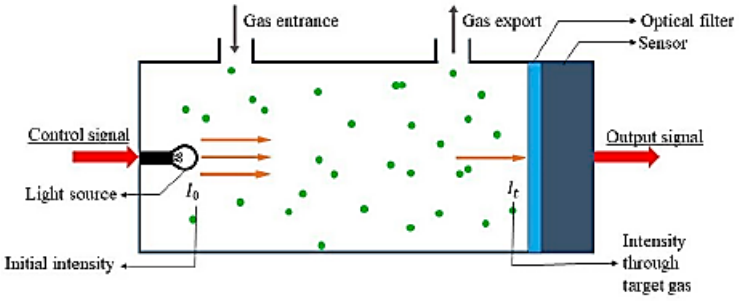

Fig. 3.5 Gas detection using Infrared absorption spectroscopy.[57]

Because of its distinct qualities, hBN is a fantastic option for applications requiring gas sensing. Here, a thorough examination of current advancements in hBN-based gas sensors is provided. It is the most used method for optical methane sensors, and it involves measuring the mid-IR light's wavelength and strength of absorption to ascertain the molecules' qualitative identification. By using mid-IR absorption sensors, it is feasible to identify the gas since individual chemical bonds have distinct absorption band wavelengths. According to this theory, the strong methane absorption lines with wavelengths of 2.3 and 3.26 μm may be used to detect methane gas using diode laser optical sensors. A functioning optical methane gas sensor is seen in Figure 3.5 and includes an optical spectrum detector, a light source to produce mid-IR light, and a tube to house the gas sample being evaluated. Mid-IR light from the light source bounces off the tube's interior walls as it travels through the gas. The IR radiation from the light would subsequently be absorbed by the gas molecules that vibrate within the IR frequency range. The optical spectrum detector determines the output intensity of the radiated light by measuring the IR light after it has passed through the gas. A value for the gas's effective absorption coefficient may be calculated using the light source's input and output intensities as well as the distance traversed. To determine if methane is present in the gas sample, utilise the effective absorption coefficient. NIR technology, TDLS, CRDS, CEAS, lidar methods, and laser photoacoustic spectroscopy are some more optical approaches for detecting methane.

Optical approaches have several benefits, including the ability to measure methane at a distance and at extremely low concentrations of ppm, ppb, and ppt. Their fundamental drawback [94,95] is that their absorption bands overlap with those of other hydrocarbons and water.

3.2.5 PYROELECTRIC SENSORS

Pyroelectric sensors employ a specific wavelength of electromagnetic radiation to detect things. They are often used as gas analyzers, thermal analyzers, laser detectors, and fire alarms. Pyroelectric sensors transform heat or electromagnetic energy into electrical energy [57]. It is a room-temperature, non-contact thermal sensor. A dielectric substrate is used in the sensor, sandwiched between two electrodes. A thermal wave is produced by an electric heater, and it passes through the substrate and the gas before arriving to the pyroelectric material across from the heater.An electrical current that can be measured and has a matching voltage is produced when the temperature of the pyroelectric material changes [96]. Due to its dependence on the

thermal conductivity and diusivity of the gas, the voltage may be utilised to determine the composition of the gas. As illustrated in Figure 3.6 a different kind of pyroelectric sensor produces heat by applying a strong infrared light source on a pyroelectric thin layer. The sensor functions similarly to an electric heater once the temperature of the pyroelectric substance changes.

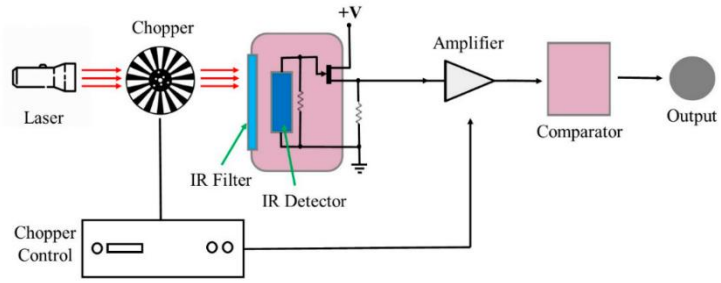

Fig. 3.6 Schematic: Pyroelectric sensor based on infrared heating. [57]

3.2.6 CHEMIRESISTIVE SENSORS

The chemiresistor makes it possible to detect gas leaks in homes, factories, and pipelines using low-power, low-cost, and distributed sensing of CH_4 in air at room temperature. According to research [58], the chemiresistor favors CH_4 over heavier hydrocarbons including n-hexane, benzene, toluene, and o-xylene. The chemiresistor was selective only for CH_4 among other heavier hydrocarbons (n-hexane, benzene, toluene, and o-xylene, as well as CO_2 and H_2, it was shown that.

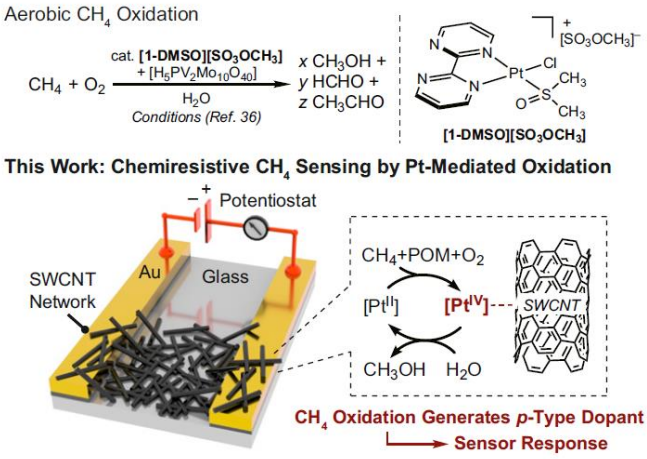

Fig. 3.7 Chemiresistive CH4 sensing mechanism: Aerobic oxidation. [58]

The purpose of Bar-Nahum et al. and Villalobos et al. was to transform the catalyst's redox cycling during CH4 oxidation into a chemiresistive response using a platinum-polyoxometalate (Pt-POM) precatalyst in a SWCNT-based chemiresistor (Fig. 3.7). The use of a POM cocatalyst (H5PV2Mo10O40) that was hypothesized to mediate the crucial Pt(II)-Pt(IV) oxidation while being regenerated by O2 led to the selection of this specific catalytic system because of its unusual reported activity in aqueous aerobic CH4 oxidation under moderate conditions. A lightweight chemiresistor was achieved for the selective detection of CH4 at room temperature in air by repurposing the durable Pt- POM precatalyst system as a selector, offering a promising solution for in-field, real-time monitoring of this problematic analyte.

3.2.7 COMPARISON OF DIFFERENT METHANE DETECTION METHOD

Table 3.1: Comparisons of different Methane Sensors. [57]

Methane Sensor Type	Working Principle	Advantage	Disadvantage
Calorimetric sensor	Calculate the heat produced by a reaction and relate it to the concentration of the reactant.	Low expense; simple design; portable; simple manufacturing Excellent methane selectivity; robustness in severe environments.	Low detecting precision; prone to catalyst toxicity, oversaturation, and cracking; high power consumption; short lifespan. High temperature is required.
Semiconducting Metal Oxide Sensor. (SMO)	A metal oxide's surface gas absorption changes its conductivity, which is subsequently measured to ascertain the gas concentration.	SMO methane sensors are typically affordable, lightweight, durable, long-lasting, and poison-resistant.	Poor selectivity, a small and high operating temperature range, a slow recovery rate, and a significant dependency on additives, temperature, and humidity are all drawbacks of SMO sensors.

Electrochemical Sensor	By oxidizing or decreasing the gas at an electrode and measuring the resultant current, you may determine the target gas concentration.	AE-based: Inexpensive. IL-based: Can detect small leaks; non-hazardous chemicals; high boiling temperatures; low volatility; and strong methane selectivity. SE-based: No leaks, secure, reliable, good methane selectivity, and it can find small leaks.	Leakage and evaporation are problems with AE-based sensors, which can raise the cost and expose the sensor to harmful substances. AE-based: prone to leakage and evaporation; hazardous chemicals; slow response time. IL-based: Prone to leakage; slow reaction time. SE-based: Requires a high temperature; is incapable of detecting low gas concentrations; is susceptible to electrolyte deterioration or loss.
Pyroelectric sensors	Calculate the heat produced by a reaction and relate it to the concentration of the reactant.	Non-destructive and oxygen-free Wide measuring range, excellent sensitivity, and operating at room temperature.	Expensive; Power consumption is high; immobile; difficult to produce.
Optical sensors	Detect variations in light waves caused by a contact between the analyte and the receptor component.	This method is non-destructive; immune to electromagnetic interference; and can operate without the need of oxygen.	Expensive; high power consumption; and a lack of relevance and distinctness of the methane optical absorption area.
Chemiresistive Sensor	The setup's resistance changes as result of the catalytic interaction between the sensing material and the target gas, producing a voltage signal.	Low-power, low-cost, and distributed sensing of CH_4 in air at room temperature	Low sensitivity (or response), poor selectivity, and instability.

3.3 PROPOSED METHANE SENSOR DESIGN AND WORKING PRINCIPLE

Design: A 1.5cm x 0.8 cm p-Si (resistivity 0.5 ohm-cm, 400 µm thick) was chosen as the substrate for growing nano BN films by thin film deposition technique. 100 µm thin BN film was deposited by the dip coating and annealing technique. Using Cu metal mask on Si electrode contacts are formed to BN.

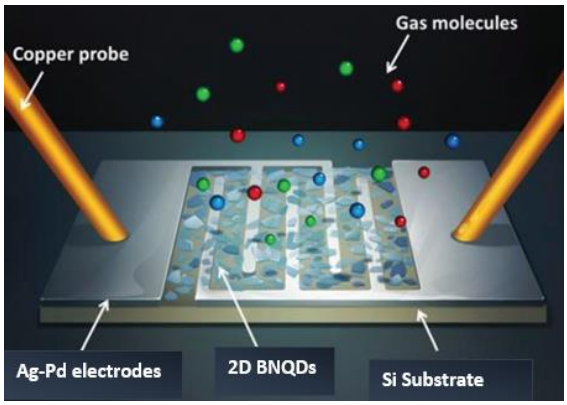

Fig. 3.8 Proposed Design of the Nanosensor

Type of Gas Detector: Among the discussed sensing mechanisms of Methane gas, the Calorimetric mechanism discussed in **section 3.2.1** has been used in present work.

Mechanism: According to the mechanism heat has been generated, and gas concentration has been measured. Methane's combustibility property (**as discussed in section 3.1, 3.1.5**) has been used in the sensor designing. It was assumed that methane comes in contact with the catalyst (3.1), the gas oxidises in an exothermic process that generates heat. The chemical reaction causes a change in temperature of the catalytic surface, hence electrical properties will change. Consequently electrical property i,e responses have been measured.

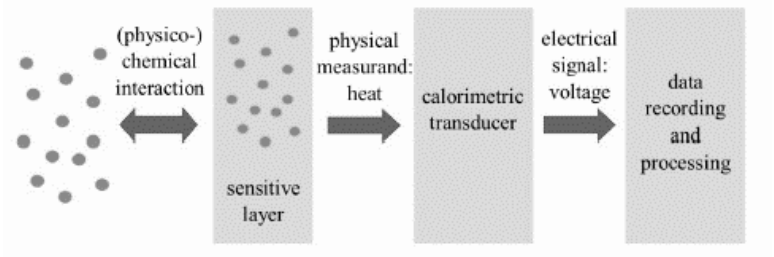

Fig. 3.9 Working principle of Designed Methane sensor. [57]

3.4 EVALUATION METRICS FOR METHANE SENSOR

When evaluating the performance of methane sensors, several key metrics are commonly used. There are two unique approaches to addressing evaluation matrices for instruments and measuring systems:

(i) Static Characteristics.
(ii) Dynamic Characteristics.

3.4.1 STATIC CHARACTERISTICS

3.4.1.1 Accuracy and Precision

Accuracy [97] measures the closeness of the sensor's output to the true methane concentration. It considers both systematic and random errors and is typically expressed as a percentage or absolute value.

Stability: Stability assesses the long-term reliability and consistency of the sensor's output over time. A stable sensor should provide consistent measurements without significant drift or degradation in performance.

Precision is used to measure the *consistency or the reproducibility* of results [97]. Low precision denotes a wide distribution of outcomes, whereas high precision suggests a compact cluster of repeated results.

3.4.1.2 Sensitivity and Resolution

Sensitivity refers to the ability of a methane sensor to detect small changes in methane concentration. It is typically measured as the change in sensor output per unit change in methane concentration. Higher sensitivity indicates better detection capabilities.

It is the ratio of the incremental output to incremental input [97] that is

$$S=\frac{\Delta y}{\Delta x} \tag{3.4}$$

Once more, the sensor response S (%) is defined as the ratio of the sensor's resistance value change in relation to its initial resistance [80] in the presence and absence of gas molecules:

$$S\ (\%) = [(Rg - Rair)/Rair] \times 100 \tag{3.5}$$

Rair is the sensor's resistance in air and Rg is device resistance in the presence of target gas.

The change in the unit of observed signal concentration is another way to describe sensitivity (S). Drift is referred to as occurring in the system whenever sensitivity or the output level fluctuates with time, temperature, or other parameters without any change in the input level, which frequently results in instability.

Resolution: The smallest incremental change in the input that would cause a discernible change in the output is referred to as resolution, and it is stated as a percentage of the measured range, or MR. The difference between the greatest input and the smallest input is used to establish the measured range.
that is,

$$\mathbf{MR = Xmax - Xmin} \quad \mathbf{(3.6)}$$

For a detectable output ~*y,* if the min change in *x* is (~) min' then the maximum resolution is

$$\boldsymbol{R_{max}}(\%) = \frac{\mathbf{100}(\Delta \mathbf{x})\boldsymbol{min}}{\boldsymbol{MR}} \quad \mathbf{(3.7)}$$

3.4.1.3 Selectivity

Selectivity measures the ability of a methane sensor to distinguish methane from other gases or potential interfering compounds. A highly selective sensor will respond primarily to methane and have minimal cross-sensitivity to other gases.[47]

Detection Limit: The detection limit of a methane sensor represents the lowest concentration of methane that can be reliably detected and distinguished from noise or background levels [46]. A lower detection limit indicates a higher sensitivity to trace levels of methane.[47]

3.4.1.4 Reproducibility and Drift

Reproducibility: The degree of similarity to which a particular value may be repeatedly evaluated is known as reproducibility [84]. The absence of drift in the instrument indicates perfect repeatability. If there is no drift, then the measured values for a particular input do not change over time.

Drift is an undesirable quality in industrial equipment that should be avoided since it is difficult to correct for and rarely noticeable. When a sensor is maintained at a certain reading for an extended length of time, drift is the divergence from that reading [84]. The change in sensor

output that occurs when the input is maintained at a level that (at first) results in a zero reading is referred to as zero drift. The full-scale drift, on the other hand, is the drift that results from keeping the input at a value that initially produces a full-scale deflection. Drift can occur for a variety of reasons, such as changes in ambient pressure, humidity, temperature, etc., or it might occur because the sensor's components vary over time owing to age, wear, and other factors.

3.4.1.5 Repeatability

Repeatability is a measure of closeness for measuring a given input over and over again.

The definition of reproducibility is expressed in terms of scale readings across a predetermined time frame. On the other hand, repeatability [97] is random in nature and is defined as the variance of scale reading. Precision, defined as the difference in output y at a certain value of the input x when acquired in two consecutive measurements, is a concept that is related to repeatability. It might be stated as % FSO. The repeatability plot is depicted in Figure 3.10.

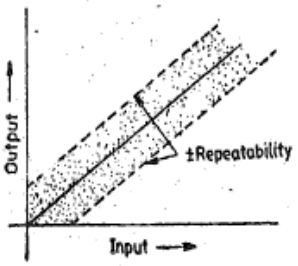

Fig. 3.10 (a). I/p- O/p relationship with ± repeatability [97]

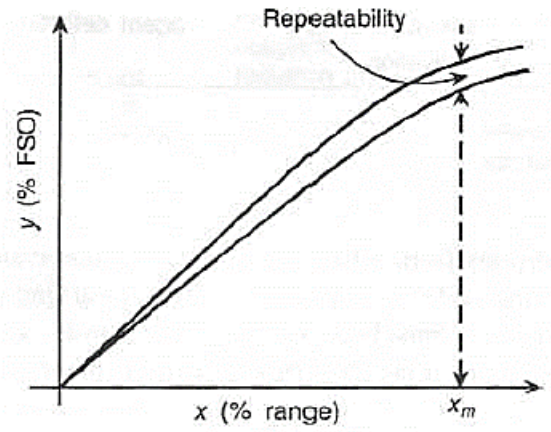

Fig. 3.10 (b) Repeatability in y-x co-ordinates [97]

3.4.1.6 Range and Span

A sensor's range is established by the lower and higher limits of its input or output. Typically, the range is defined by the necessary precision.[97]

3.4.1.7 HYSTERESIS

Difference in the output y of a sensor for a given input x (when x reaches this value in upscale and downscale directions as shown in Fig. 3.11) is called Hysteresis.

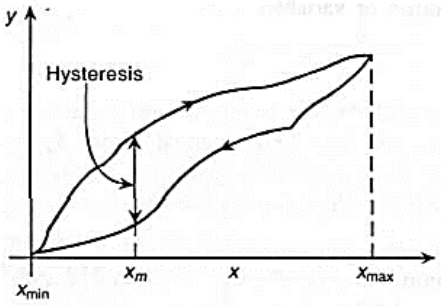

Fig. 3.11 The Hysteresis curve. [97]

The reasons vary depending on the type of sensor. In magnetic types, for example, the lag in dipole alignment that causes the effect is the hysteresis, but in semiconductor types, it is basically the injection type slow traps that cause the effect, and so on.

Output impedance is a trait that should be evaluated on an individual basis. It severely limits interaction, particularly the selection of the next stage.

3.4.1.8 LINEARITY

Linearity refers to the relationship between the sensor's output and the methane concentration. A highly linear sensor exhibits a proportional response, ensuring accurate measurements across a wide range of methane concentrations. The calibration curve determines the linearity. Under static circumstances, the static calibration curve plots the output amplitude versus the input amplitude. The linearity is the degree to which it resembles a straight line.

Nonlinearity: Deviation from linearity, which is characterized using superposition principles, is expressed as a percentage of full-scale output at a given input value. Nonlinearity, on the other hand, may be described in two ways: (i) divergence from the best suited straight line achieved using regression analysis, and (ii) variation from a straight line connecting the scale's end points. These are shown in Figs. 3.1.2(a) and (b).

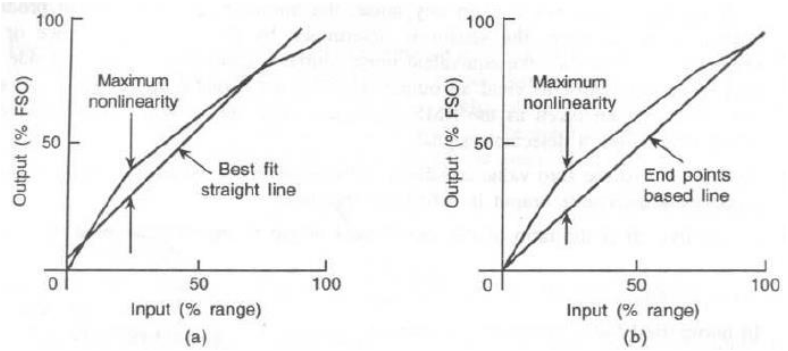

Fig. 3.12 Nonlinearity with (a) best-fit characteristics and (b) terminal-based characteristics. [97]

The first method's maximum nonlinearity is always less than the second method's maximum nonlinearity. In reality, the figure is half.

Nonlinearity causes distortion, which is defined as the divergence from the sensor's or transducer's predicted output. It can also develop as a result of the inclusion of extra input components.

3.4.2 DYNAMIC CHARACTERISTICS

The dynamic properties of a sensor describe the sensor system's temporal responsiveness. Understanding these is required to utilize a sensor effectively. Rise time, delay time, peak time, settling time % error, and steady-state error are all important frequent dynamic responses of sensors [98]. These are defined in figure 3.13, which will be used to graphically represent them.

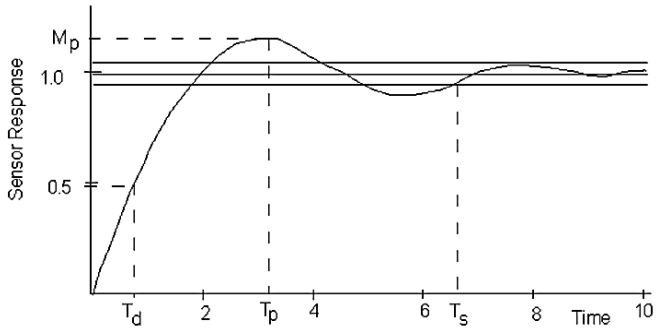

Fig. 3.13 Sensor Response: Dynamic characteristics. [98]

- The rise time of a sensor is the time taken by the sensor to pass between 10 and 90% of its steady state response.

- The delay time is the amount of time required to achieve 50% of the steady state value for the first time.
- Peak time is the amount of time it takes for a given excitement to reach its highest reading for the first time.
- The settling time is the amount of time it takes for the sensor to settle to within a specified percentage of the steady state value (say, 1%).
- The percentage overshoot is a measure of difference between the peak and the steady state value, it is expressed as a percentage.
- The variation of the actual steady-state value from the desired value is referred to as steady-state error. It is correctable by calibration. This includes determining the transfer function, frequency response, impulse response, and step response, as well as evaluating the time-dependent outputs. In this context, the two most essential criteria are (a) fidelity as defined by dynamic error and (b) reaction speed as indicated by lag. Different defined inputs are delivered to the sensor to determine the dynamic properties, and the response characteristics are investigated. The requirements for the sensor's time constant are made using step input. The sensor is often a single time constant device, and if this time constant is τ.

Table 3.2 1.5 % Response time of the sensors.[98]

% Response time	Value in terms of τ
$t_{0.1}$ or 10	0.104 τ
$t_{0.5}$ or 50	0.692 τ
$t_{0.9}$ or 90	2.303 τ

This gives $to.c_j.t_{O.5}$= 3.32 which is taken as a quick check relation. Impulse response as well as its Fourier transform are also considered for time domain as well as frequency domain studies.

Speed of Response

The response time of a methane sensor refers to the time it takes for the sensor to reach a certain percentage of its final output in response to a change in methane concentration. A faster response time is desirable in applications that require real-time monitoring.

Recovery time is the time taken by the sensor to return to its baseline output after being exposed to a specific concentration of methane. A shorter recovery time is preferred in scenarios where repeated measurements are required.

3.4.3 ERROR IN MEASUREMENTS

3.4.3.1 True Value

The average of an infinite number of measured values when the average variation owing to the various contributing variables goes to zero can be used to define the true value of a quantity that is being measured. [97]

3.4.3.2 Static Error

Static error [97] is defined as the difference between the measured value and the· true value of a quantity.

$$\boldsymbol{\delta A = A_m - A_t} \quad \textbf{(3.8)}$$

$where$

$$\delta A = error$$

$$A_m = measured\ value\ of\ quantity$$

$$A_t = true\ value\ of\ quantity$$

3.5 SIGNIFICANCE OF h-BN

3.5.1 h-BN AS A HIGH- PERFORMANCE MATERIAL

Scientific interest in this ultrathin material for a variety of applications has increased as a result of recent developments in the area of 2D hexagonal boron nitride (hBN) [75-82]. which are being utilised to realise electrical and optoelectronic devices, including wearable and portable electronics. It is one of the most promising materials for next-generation high-performance gas sensors due to its extraordinarily high thermal conductivity and temperature stability.

A potential substrate or dielectric layer for two-dimensional electrical devices is hexagonal boron nitride (h-BN). Hexagonal boron nitride Quantum dots [78] are a prospective two-dimensional material to enhance the mechanical, thermal, electrical, and optical properties of polymer nanocomposites.

X-ene (graphene, silicene, and germanene), transition-metal dichalcogenides (TMDs), hexagonal BN (h-BN), group IIIA chalcogenides (such as GaS, GaSe), group IVA dichalcogenides (such as SnS_2) [99] and other materials make up the large family of 2D materials.

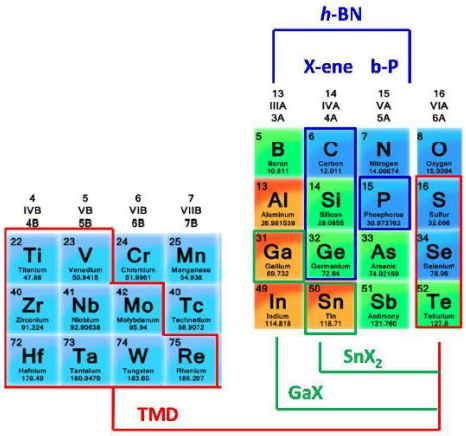

Fig. 3.14 X-ene group in Periodic table [99].

Boron Nitride, being one of the promising members of X-ene group [99], has captured the interest of researchers due to its simplicity of forming various types of nanostructures in a cost-effective manner, as well as its possible compatibility with CMOS Si technology, in which the sensor and the essential signal processing unit are merged on the same substrate.

3.5.2 STRUCTURE AND PROPERTIES OF BORON NITRIDE

The BN layers of h-BN have a partially ionic structure, which reduces covalency and electrical conductivity while enhancing interlayer contact, giving h-BN a higher degree of hardness than graphite. Additional signs of decreased electron-delocalization include the absence of colour and a significant band gap in hexagonal-BN. High anisotropy is caused by very diverse bonding, which is strong within the basal planes (planes in which boron and nitrogen atoms are covalently bonded) and weak between them.

For instance, hardness, electrical conductivity, and thermal conductivity are all much higher when seen perpendicularly than when viewed within planes. On the other hand, the properties of c-BN and w-BN are more homogeneous and isotropic. Hexagonal boron nitride (hBN), the most stable of the three crystalline forms of boron nitride (together with cubic and wurtzite BN), is the most common kind of boron nitride. There are other variants of hBN available as one-dimensional nanotubes (1D BNNT), two-dimensional nanosheets (2D BNNS), and zero-dimensional (0D fullerenes). The B and N atoms in hBN are connected by a strong covalent connection, giving the material a honeycomb structure similar to graphene [48]. A large number of BN layers are connected together by weak vdW pressures. They are set up such that layers of B and N atoms next to one another are positioned above and below one another.

Co-doping carbon and nitrogen using boron nitride is an option, as is doping beryllium p-type and boron, sulfur, or silicon n-type. Wide-gap semiconductors with a band-gap energy compatible with the UV region include hexagonal and cubic BN. When activated, H-BN or c-BN may emit UV light in the 215-250 nm range, so serving as light-emitting diodes (LEDs) or lasers.

In this part, important characteristics, such as crystal structure, physical properties, and chemical properties of h-BN are shown. Graphene and BN materials have comparable Young's modulus, fracture strengths, and crystallographic structural data. However, BN is more appropriate for electrical insulation applications than graphene because of its superior thermal stability and noticeably greater electronic bandgap. With just a 1.5% lattice mismatch in their crystal structures, graphene and h-BN are comparable.

3.5.2.1 GEOMETRY OPTIMIZATION

BN is the lightest III-IV compound and is isoelectric to carbon structures because the surrounding atoms share the same total number of electrons [20]. According to the equation of hexagonal lattice formation i,e a = b = c; $\alpha = \beta = \gamma \neq 90°$, the B and N atoms of a 2D h-BN are alternately organised to create a honeycomb structure as an analogue of graphene (Fig. 3.15 b).

Boron and nitrogen atoms are alternately linked together in hBN. Boron and nitrogen atoms are bonded together by strong covalent bonds inside a layer, similar to graphene. The B-N bond has a length of 1.45 °A and is created through sp2 hybridization. Similar to how three sp2 orbits of each B atom join with the sp2 orbit of nearby N atoms to generate a strong s bond, three sp2 orbits of each N atom also work in tandem with those of nearby B atoms to do the same. The two separate layers, on the other hand, are kept together by a weak van der Waals connection. Because of the weak van der Waals contact, the neighboring layers may be peeled off the bulk hBN crystal by exfoliation. Weak van der Waals forces unite adjacent h-BN layers, while covalent connections connect the B and N atoms in each layer. In comparison to graphite, which has an interlayer spacing of 0.335 nm, graphene has a slightly smaller interlayer spacing of 0.333 nm.

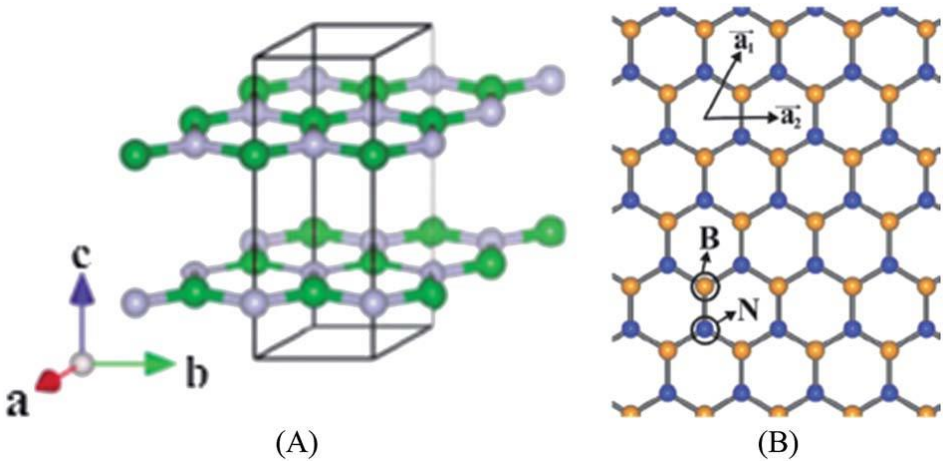

Fig. 3.15 (A) Structure of hBN, (B) Honeycomb structure of BN. [98]

BN also exists as hexagonal (h-BN), cubic (c-BN), rhombohedral (r-BN), and wurtzite (w-BN) forms. The c-BN and w-BN are sp3 hybridized, while the h-BN and r-BN contain sp2 hybridized B-N bonds. [99]

According to Figure 3.15 b, the h-BN phase, which has strong boron-nitrogen covalent intralayer bonds that provide hexagonal planar geometry and weak van der Waals interactions

between layers in the bulk state, is the most stable phase under ordinary circumstances. There is additional electrostatic interaction in the interlayer stacking due to the electronegativity mismatch between the boron and nitrogen atoms in neighbouring layers.

In contrast to how electrons are dispersed in graphene's C-C bond, electrons in the B-N bond travel towards the electronegative N atoms, vacating the boron atoms, and thus give the B-N bond a partial ionic character via polarisation. In contrast to graphite, where hexagonal nanosheets are layered in the ABAB sequence, the basal planes in h-BN are stacked in an alternate AA'AA' pattern. The tetrahedral structure of the w-BN resembles a diamond, and its AA'AA staking is similar to that of the h-BN. [100]

The interlayer slides readily in the c-axis direction of h-BN because the interlayer gap is big and the bonding force is weak. [100]

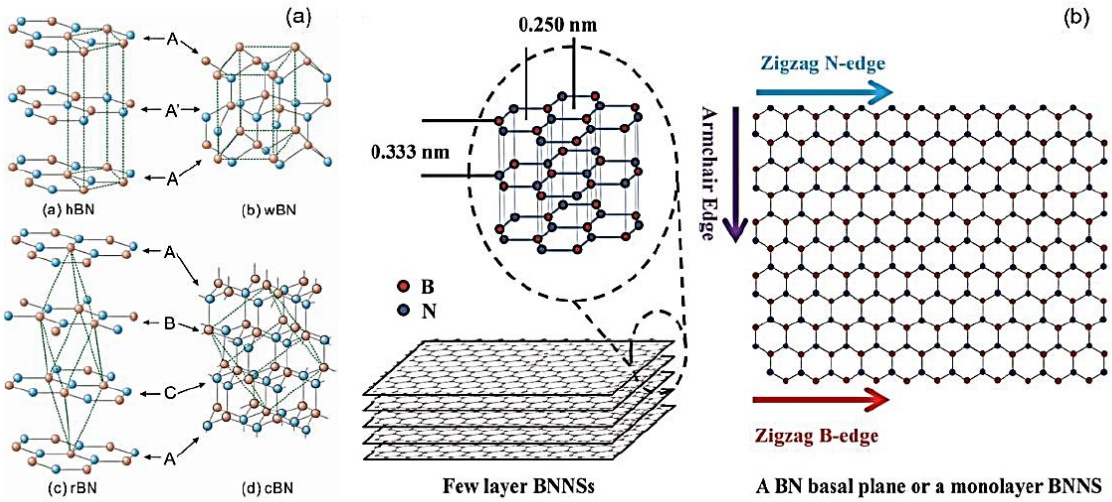

Fig. 3.16 (a) Crystal structure of h-BN, w-BN, r-BN, and c-BN (b) Structure of 2D h-BN nanostructure, with h-BN bond length of 0.145nm, the distance between two consecutive borazine rings is 0.250 nm, while the distance between their interlayers is 0.333 nm. [100]

3.5.2.2 ELECTRONIC BAND STRUCTURE

hBN is structurally equivalent to graphite. Due to its extreme transparency and status as the first known naturally occurring hyperbolic material—a substance in which in-plane bonds are more powerful than out-of-plane ones—layered hBN is often referred to as white graphene [101].

Monolayer hBN is a sp2 bonded layer material with boron (B) and nitrogen (N) atoms alternately arranged throughout its crystal structure. [102] In (bulk or multilayer) hBN, these layers are either stacked with AA' configuration (B and N atoms of one layer are translated w.r.t. another layer) as shown in Fig. 3.17 a, b, or AB configuration (B and N atoms of one layer are positioned above the N atoms of another layer) as shown in Fig. 3.17 c, d.

Weak van der Waals forces are used to pack these individual layers together. The change in the electrical band structure of monolayer and bulk hBN is illustrated in Fig. 3.17 e, f.

The inter layer interactions have an impact on the band structure of the material. The direct bandgap semiconductor property of monolayer hBN is 7.25 eV at the high symmetry K point. With several layers, it transforms into a bulk semiconductor that has an indirect bandgap of 5.79 eV, a conduction band minimum at point M, and a valence band maximum at point K.

The number of individual layers stacked and the interlayer interactions have a major role in how the bandgap of hBN and the accompanying Raman shifts vary. Larger bandgap results in enhanced electromagnetic spectrum transparency in hBN. Additionally, hBN has a relatively high refractive index. Additional electrical, optical, and crystallographic characteristics of hBN are described in Fig. 3.17 g. [103]

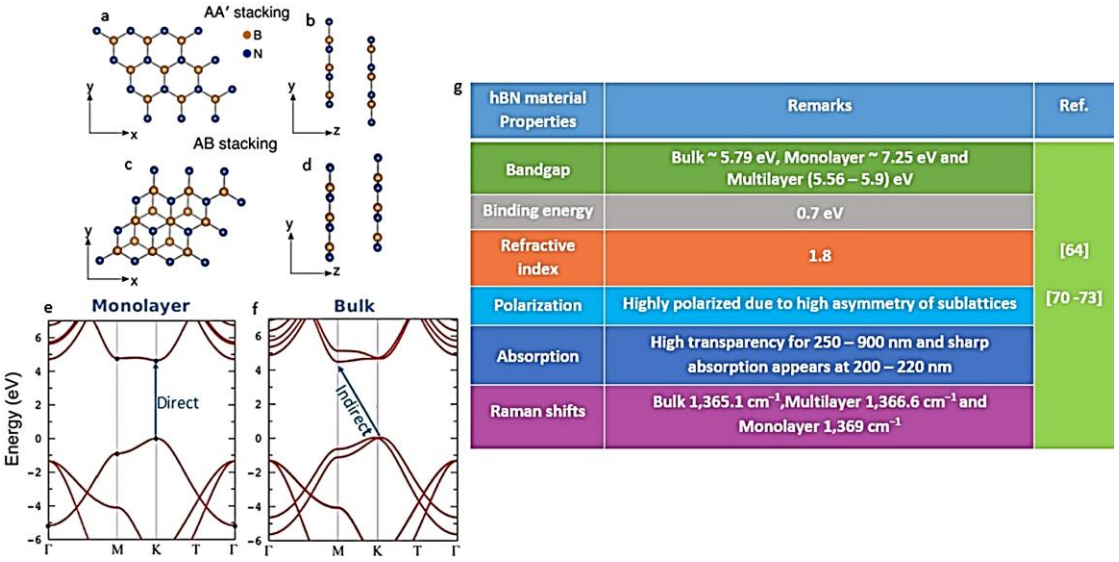

hBN material Properties	Remarks	Ref.
Bandgap	Bulk ~ 5.79 eV, Monolayer ~ 7.25 eV and Multilayer (5.56 – 5.9) eV	[64] [70 -73]
Binding energy	0.7 eV	
Refractive index	1.8	
Polarization	Highly polarized due to high asymmetry of sublattices	
Absorption	High transparency for 250 – 900 nm and sharp absorption appears at 200 – 220 nm	
Raman shifts	Bulk 1,365.1 cm^{-1},Multilayer 1,366.6 cm^{-1} and Monolayer 1,369 cm^{-1}	

Fig. 3.17 (a) The h-BN stacking diagram, the electronic band structure of monolayer and bulk Hbn, and the electrical/optical/crystal characteristics of the hBN material are all shown. (a, b) Top and side views of the AA' stacking. (c, d) AB stacking top and side views. (e, f) Monolayer and bulk hBN electronic band structures with direct and indirect bandgaps, respectively. (g) High grade crystals exhibit general hBN material features and equivalent Raman shifts (about values). [103]

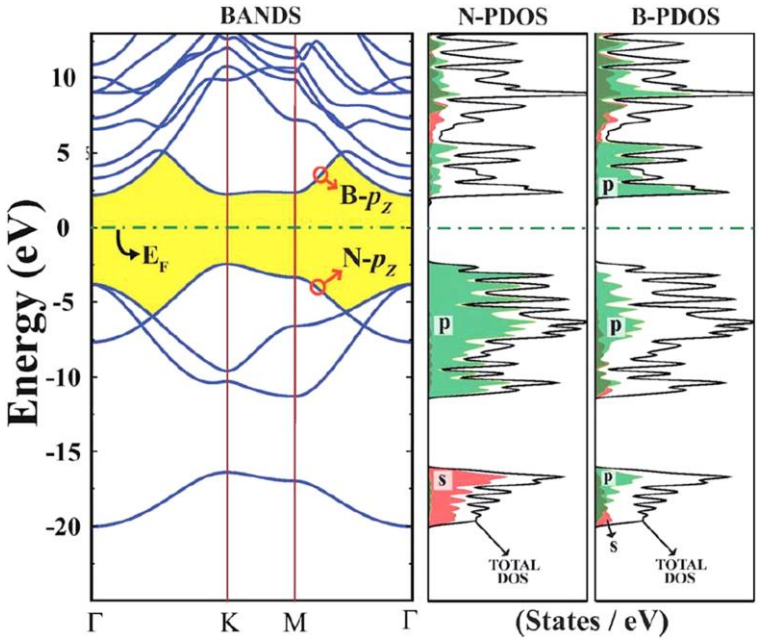

Fig. 3. 18 Orbital property and electronic band structure of h-BN. [98]

The top and bottom of the valence band of h-BN are located at the high symmetry K point, and the material has a direct band gap, as shown in Fig. 3.18. The p and p* sites on the N atom and B nucleus, respectively, control the system's HOMO and LUMO levels.

3.5.2.3 PROJECTED DENSITY OF STATE

"Density of states" refers to the distribution of available energy states for electrons within the quantum dot. It provides information about the energy levels that electrons can occupy within the system. The density of states (DOS) is typically represented as a function of energy and quantifies the number of electronic states per unit energy interval. It can be thought of as a measure of how many energy levels are available for electrons at a given energy.

By examining the density of states of an h-BN quantum dot, one can gain insights into its electronic properties [104], energy spectrum, and potential applications. The density of states profile can reveal information such as energy gaps, energy levels, and the distribution of electronic states, which are crucial for understanding the behavior of electrons within the quantum dot system. Analyzing the density of states can help researchers study phenomena such as electron transport, optical properties, and electronic interactions within the h-BN quantum dot. It also provides a basis for exploring potential applications in fields such as quantum computing, optoelectronics, and nanoscale devices.

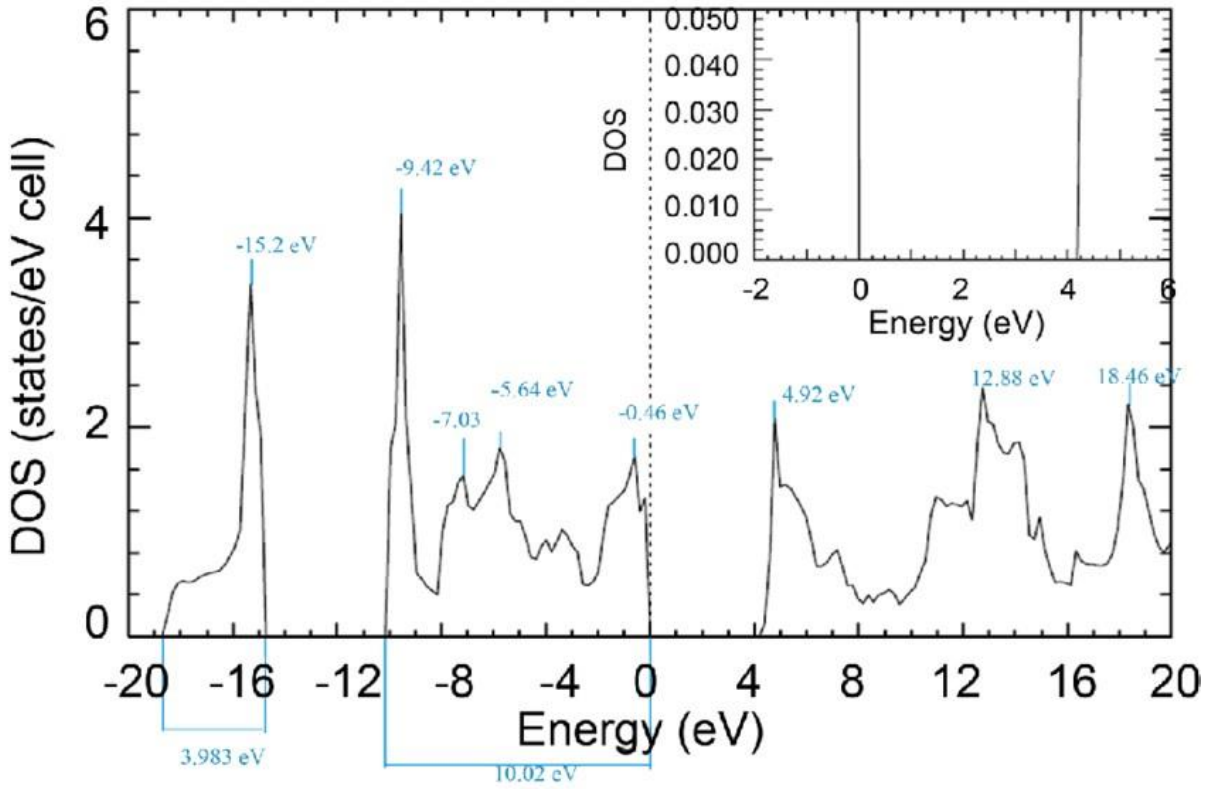

Fig. 3.19 Energy vs Density of curve of h-BN. [105]

3.5.2.4 PHYSICAL PROPERTIES

Table 3.3 Different physical properties of h-BN. [99]

Properties: h-BN	
Chemical formula	BN
Molar mass	24.82 g/mol
Appearance	Colorless crystals
Density	2.1 g/cm^3 (h-BN); 3.45 g/cm^3 (c-BN)
Melting point	2,973 °C (5,383 °F; 3,246 K)
Solubility in water	Insoluble
Electron mobility	200 cm^2/(V·s) (c-BN)

Table 3.4 Comparison of h-BN properties with Graphene and Diamond. [99]

Material	h-BN	Graphite	Diamond
Density (g/cm^3)	~2.1	~2.1	3.515
Bulk modulus (GPa)	36.5	34	440
Thermal conductivity (W/m·K)	00 30	200–2000 2–800	600–2000
Band gap (eV)	5.9–6.4	0	5.5
Refractive index	1.8		2.4
Magnetic susceptibility (μemu/g)	−0.48 −17.3	−0.2 – −2.7 −20 – −28	−1.6

Table 3.5 Comparison of physical properties between several materials and h-BN. [98]

	Al_2O_3	SiO_2		Graphite	Graphite diamond	h-BN
Lattice constant	Face-centred: 1.27	Orthogonal	$a = 1.383$ $b = 1.741$ $c = 0.504$	$a = 0.246$ nm $c = 0.667$ nm	0.3567	$a = 0.2504$ nm $c = 0.6661$ nm
		Face-centred	1.936			
Thermal conductivity (W m^{-1} K^{-1})	40	1.4		25–470	22	25.1
Dielectric constant	6.8	3.9		8.7	5.7	4

3.5.2.5 THERMAL PROPERTIES

- Thermal stability

  The chemical and thermal stabilities of hexagonal BN are astounding [77]. At temperatures of up to 1000 °C in air, 1400 °C in a vacuum, and 2800 °C in an inert atmosphere, for instance, h-BN is resistant to breakdown.

- High temperature behaviour

  h-BN has a high melting point of around 3,500°C, making it a suitable material for high-temperature applications.

- Thermal conductivity

  h-BN exhibits high thermal conductivity and temperature stability which makes it a promising gas sensing material [78]. It is helpful in heat management applications because it is a good electrical insulator and has strong thermal conductivity along the plane of the hexagonal layers. Because of its low friction, h-BN is often employed as a lubricant in high-temperature environment.

3.5.2.6 ELECTRICAL PROPERTIES

- A 2D h-BN has a smooth surface and a lattice structure that is very similar to graphene. Indications that 2D h-BN is a member of the wide band gap class of insulators include its broad optical phonon mode, wide band gap, lack of surface dangling bonds, and predicted band gaps of 6.0 eV and 4.5 eV, respectively, using the GW method and the local density approximation (LDA) method. 2D h-BN's band structure is shown in Fig. 3.18.

- This denotes that it belongs to the insulator class with a broad band gap. The direct band gap of h-BN is seen in Fig. 3.18 [98], and the high symmetry K point is where the valence band's top and rewinding bottom are located. The pi and pi* sites on the N atom and B nucleus, respectively, control the system's HOMO and LUMO levels. [20]

3.5.2.7 MECHANICAL PROPERTY

The mechanical characteristics of the 2D h-BN stand prominently. Song et al. measured the mechanical characteristics of h-BN film by embossing it with a diamond tip [78, 98]. Because of its mechanical and thermal robustness, hBN has the potential to be employed in hydrophobic coatings, UV emitters, and anti-oxidation coatings.

E2D is a post-elastic coefficient, and 2D m σ is the pretensioned stress, as illustrated in Fig. 3.7. Numerous theoretical studies and experimental findings have shown that the 2D h-BN has a substantial Young's modulus (about 270 N m^{-1}).

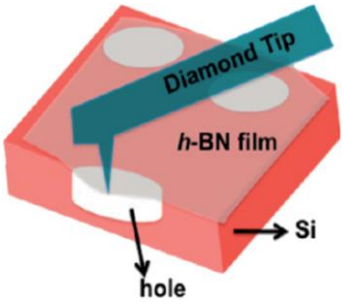

Fig. 3.20 Schematic of nanodetantion of suspended h-BN membrane. [98]

H-BN has a better thermal conductivity at room temperature than the majority of metals and ceramics, up to 400 W $m^{-1}K^{-1}$. The usual anisotropy of h-BN is shown by its 300W(m^{-1} K^{-1}) high heat conductivity in the c-axis perpendicular direction, 0-2.6*10^{-4} K^{-1} low thermal expansion coefficient, and 41 MPa high tensile strength. In a direction perpendicular to the c-axis, h-BN exhibits a decreased thermal conductivity of 20–30 W ($m^{-1}K^{-1}$) and a high compressive strength, among other properties.

3.5.2.8 OPTICAL PROPERTIES OF H-BN

Table 3.6 Photophysical properties values in hBN quantum emitters were observed. At room temperature, all of the experimental values were reached. [103]

Photophysical characteristics of hBN quantum emitters	Remarks
Emission intensity	Highest reported (To date)
Fluorescence lifetime	1.53–2.88 ns
Polarization	Linearly polarized dipole transition
Electron phonon coupling (DW factor)	0.82

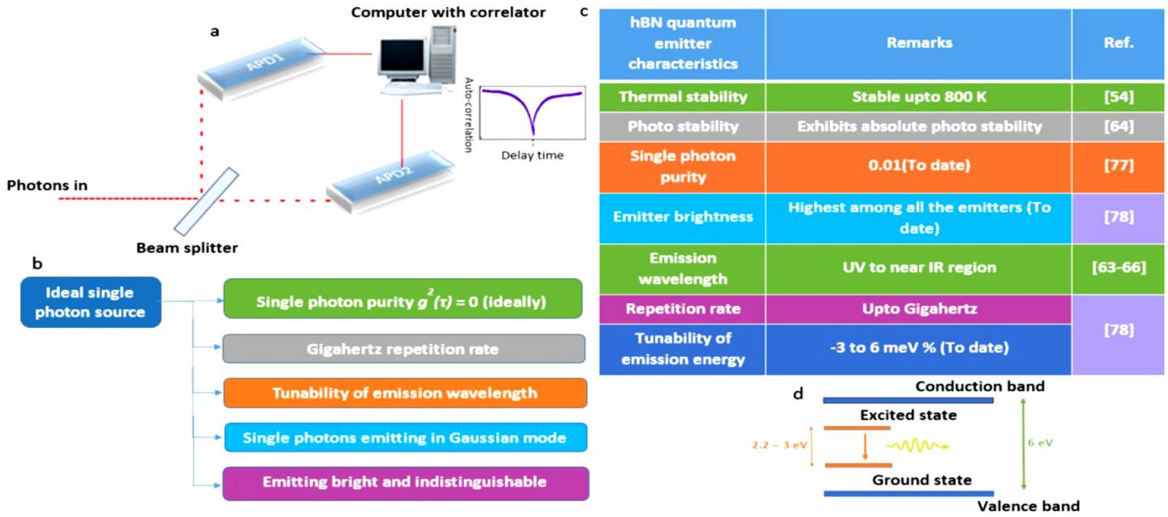

hBN quantum emitter characteristics	Remarks	Ref.
Thermal stability	Stable upto 800 K	[54]
Photo stability	Exhibits absolute photo stability	[64]
Single photon purity	0.01(To date)	[77]
Emitter brightness	Highest among all the emitters (To date)	[78]
Emission wavelength	UV to near IR region	[63-66]
Repetition rate	Upto Gigahertz	[78]
Tunability of emission energy	-3 to 6 meV % (To date)	

Fig. 3.21 HBT interferometer schematic, important properties of an ideal single photon source and empirically observed quantum emitter characteristics, pictographic representation of atomic behavior of defects inside the host bandgap. [103]

Table 3.7 Range of dipole misalignments, responsible mechanisms and their influence on light absorption. [103]

Range of dipole misalignment (Δθ)	Responsible mechanism	Influence on light absorption
$\Delta\theta \approx 0°$	If excitation light energy (ΔE) coincides with an allowed phonon energy in hBN	Direct absorption of defect
$0° \leq \Delta\theta \leq 90°$	If excitation light energy (ΔE) exceeds the maximum phonon energy in hBN	Indirect absorption through a third intermediate electronic state

When the source of light energy corresponds with the permitted phonon energy in hBN, no dipole misalignments are observed, result in direct absorption of the defect. If the excitation light surpasses the maximum phonon energy in hBN and indirect absorption of the defect occurs, the dipole misalignment value varies between 0° and 90°. [103]

3.5.2.9 MAGNETIC PROPERTIES

- A nonmagnetic semiconductor with a large band gap is 2D h-BN. Studies have shown that the spontaneous magnetization of h-BN may occur when doping or defects are introduced into 2D h-BN systems.
- Wu et al. [106] computed the scenario in which B and N atoms are swapped out for carbon atoms, causing spontaneous magnetism to develop in 2D h-BN. According to Si et al., spontaneous spin magnetization may also result from B or N vacancy defects in h-BN. These investigations imply that outstanding half-metallic magnetism may be shown by boron nitride nano-ribbons in a variety of state.
- Lai et al. investigated no passivation and passivation using zigzag boron nitride nano-ribbons and discovered that the nitrogen atom edge passivation is not magnetic and that the system exhibits semi-metallic properties. When exposed to an external electric field, passivated serrated boron nitride nano-ribbons may achieve a metal-semiconductor-semimetal transition, however V. Barone et al. discovered no spontaneous spin polarisation in these materials.
- The electronic polarization rate at the Fermi level is 100% when the B atoms are edge passivated, according to study by F. W. Zheng et al., and this material exhibits semi-metallic properties with a band gap of 0.38 eV. The conductivity of the system is controlled by metallic spin electrons.
- Additionally, when the N atoms are edge passivated, the antiferromagnetic structure is more stable than the ferromagnetic structure because the energy of the former is around 33 meV greater per (edge atom) than that of the latter.

3.5.3 CHEMICAL PROPERTIES OF HEXAGONAL BORON NITRIDE

It is insensitive to most chemicals, including acids and alkalis, and is chemically inert. According to this h-BN feature [107], it may be used to create high-performance 2D electrical and optoelectronic devices since it is the ideal dielectric material. Due to its good dielectric behavior, it is extensively used as a gate dielectric in transistors and in electrical encapsulation applications**.**

3.5.4 SYNTHESIS METHODS OF BORON NITRIDE QUANTUM DOTS

According to Fig. 3.8, "topdown" and "bottom-up" techniques are the two main methods used to construct BNQDs. The 'topdown' procedure involves physically exfoliating or chemically modifying large-size bulk h-BN into smaller-size BNQDs. [100]

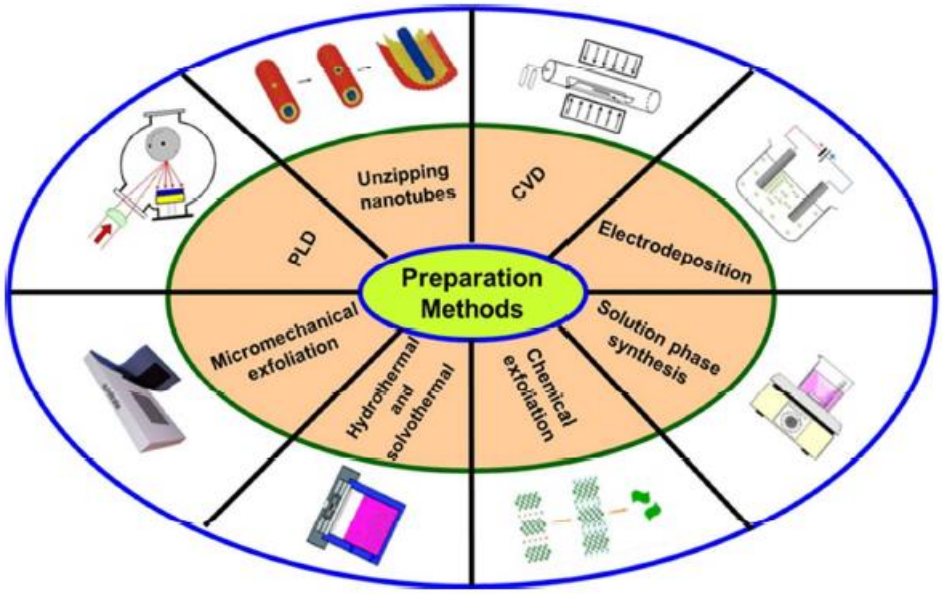

Fig. 3.22 The variety of synthetic techniques employed to create 2D layered inorganic Nanomaterials [80].

The main techniques employed in these procedures are liquid exfoliation, solvothermal/hydrothermal treatment, and the ion intercalation approach. The 'bottom-up' method entails the chemical synthesis of BNQDs using specified fundamental organic or inorganic components as precursors in particular situations. Microwave irradiation techniques and hydrothermal/solvothermal synthesis are common 'bottom-up' process methodologies. The simplicity of this technique makes doping and modification possible, but the addition of heteroatoms reduces the purity of the BNQDs that are produced to an unacceptable level. One of the numerous methods for producing BNQDs examined by researchers is the supercritical fluid (SCF) procedure, that includes layer-by-layer bulk h-BN exfoliating and then breakdown into BNQDs during SCF strategy. [100]

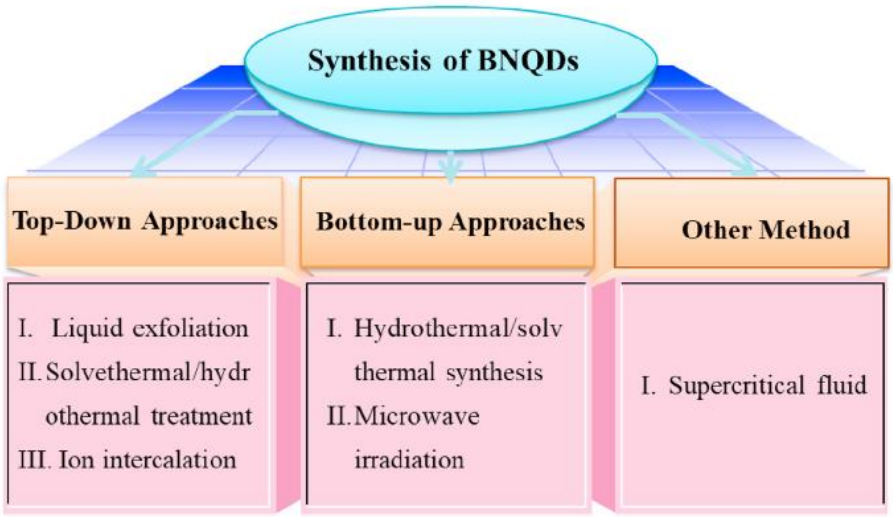

Fig. 3.23 Synthesis methods of Boron Nitride quantum dots.[99]

3.5.4.1 TOP-DOWN APPROACH

3.5.4.1.1 Liquid exfoliation method

Liquid exfoliation is a secure, environmentally friendly process that may be used to quickly manufacture BNQDs. When liquid solvents have sufficient surface energy, this method is frequently employed [108]. (Including NMP, DMF, and ethanol). BNQDs will be produced via liquid exfoliation, comminution, and separation of large-size h-BN flakes.

As an illustration, Lei et al. produced BNQDs [109] in 2015 by employing a straightforward solvothermal procedure by dispersing the bulk h-BN powder in DMF and DMSO to produce h-BN. h-BN/DMF or h-BN/DMSO suspensions were initially prepared, consecutively the resultant suspensions went through an ultrasonication procedure for minimum 8 hours [108,109]. This technique exfoliated bulk h-BN powders into high-quality h-BNNSs.

Both the mentioned solvents are highly polar solvents with the required surface energy to displace van der Waals forces [110], making it possible to exfoliate the bulk h-BN completely into thin h-BNNSs. The solution was then vigorously stirred for 24 hours at 140℃ in order to induce the high-quality h-BNNS suspension to be incised into BNQDs [109]. The discovered BNQDs with 3.3 nm average size and 2.5 nm thickness, have lattice fringes of 0.2115nm.

Additionally, BNQDs were created by cutting h-BNNSs generated from h-BN that had undergone a high-intensity ultrasonication by Stengl et al. [93]. The authors first created the bulk layered h-BN using boric acid and urea as precursors. Once they had this material, they suspended it in water and subjected it to high-intensity ultrasonication for five minutes at a pressure of six bars in a pressurized reactor for the exfoliation of the bulk h-BN into h-BNNSs. By refluxing these exfoliated h-BNNSs under atmospheric pressure in ethylene glycol for 48 hours at 198°C , BNQDs were effectively synthesized [109].

This method effectively exfoliates bulk h-BN into thin, few-layer nanosheets, which serves as an appropriate precursor for the production of high-quality BNQDs. It uses high-intensity ultrasonication. Similar to this, Kumar et al. also produced BNQDs by combining liquid-phase exfoliation with a simple, high-intensity ultrasonication technique. The scientists also looked at how the morphology, structure, and size of BNQDs were affected by different ultrasonication periods (12, 10, 9, and 6 h). BNQDs obtained from high-intensity ultrasonication for 12 h is the smallest, having more uniform particle size distribution. This could be due to the fact that h-BNNSs are simpler to exfoliate and finally transition into BNQDs due to the high intensity and prolonged ultrasonication.

It can be concluded from the aforementioned findings that the liquid exfoliation approach is one the quick and efficient way for making BNQDs with uniform particle distribution. It benefits from a cheap price and an easy preparation technique. However, its potential for development and use is limited by issues with extended ultrasonication times and poor quantum yield. Additionally, the size of the as-obtained BNQDs is significantly influenced by the solvent's polarity, which is employed to prepare BNQDs.

First and foremost, the high polarity is helpful for reducing the contact force between two nearby h-BN layers and for making it easier for the h-BN bulk to exfoliate and produce h-BNNSs. Second, because the interactions between boron and nitrogen are ionic, h-BNNSs are more likely to absorb organic substances with high amounts of polarity. During ultrasonication, B e N bonds can break to generate BNQDs as a result of reactions between the h-BNNSs and organic compounds. As a result, when using the liquid exfoliation process for producing high-quality BNQDs, selecting a suitable solvent having ideal polarity is essential.

3.5.4.1.2 Solvothermal and hydrothermal therapy

The most popular technique for creating nanomaterials is the solvothermal/hydrothermal treatment [86,67]. This approach produces QDs that are simple to process, have a high quantum yield, are homogeneous in size, and are environmentally friendly. The method also makes it simple to concurrently change and functionalize the QDs' surfaces, increasing their yield and efficiency and enabling multifield QD applications [109].

Teo's group, for example, initially ultrasonically dispersed the bulk h-BN in DMF solvent for eight hours in order to produce highly scattered nanosheets. The resulting suspension was then centrifuged for 10 minutes at 1500 rmp to remove the large particles. After that, the created nanosheets underwent a solvothermal treatment for 24 hours at 200℃ in an autoclave lined with Teflon [54]. High-speed centrifugation and filtering techniques may be employed to create high-quality BNQDs when the solvothermal treatment is complete (Fig. 3.25).

With this liquid exfoliation-solvothermal treatment method, a yield of 19.5% [72] is achievable. The researchers additionally examined at how the filling factor, synthesis temperature, and duration time affected the shape and optical characteristics of BNQDs.

A minimum lateral dimension of 2.62 nm with average thickness of roughly 3 atomic layer can be obtained when the synthesis temperature was taken as 200 °C, suspension filling factor was 66.7%. Here the duration time was 24 h [109]. It is clear that using this method will enable you to quickly create BNQDs with a high quantum yield and variable particle size. The solvothermal treatment method for the creation of BNQDs, however, has been discovered via the aforementioned investigations to be rather complete and developed. Researchers should think about changing BNQDs in the future trials to improve their performance even further.

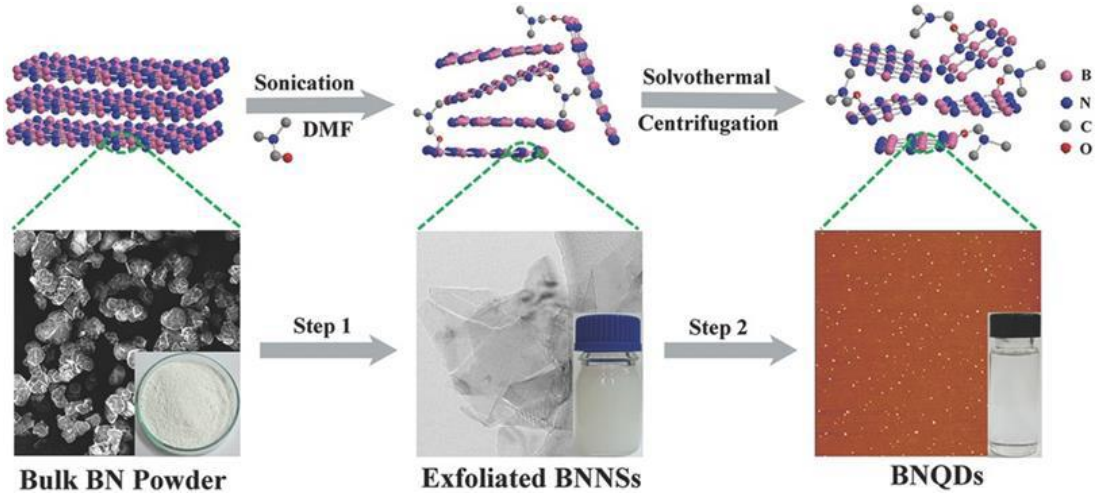

Fig. 3.24 BNQD synthesis procedure: Sonification-assisted exfoliation process of h-BN bulk powder to synthesize BN nanosheets and hydrothermal treatment to fabricate BNQDs. [100]

The size and efficiency of the produced BNQDs from hydrothermal treatment are effected by solvents' polarity. Particularly, depending on how polar the solvents are, the emission peak of the as-obtained BNQDs will have a smaller size and a larger red shift. The solvothermal/hydrothermal strategy to producing high-quality BNQDs can be as effective as the liquid exfoliation technique if a suitable solvent with the appropriate polarity is found.

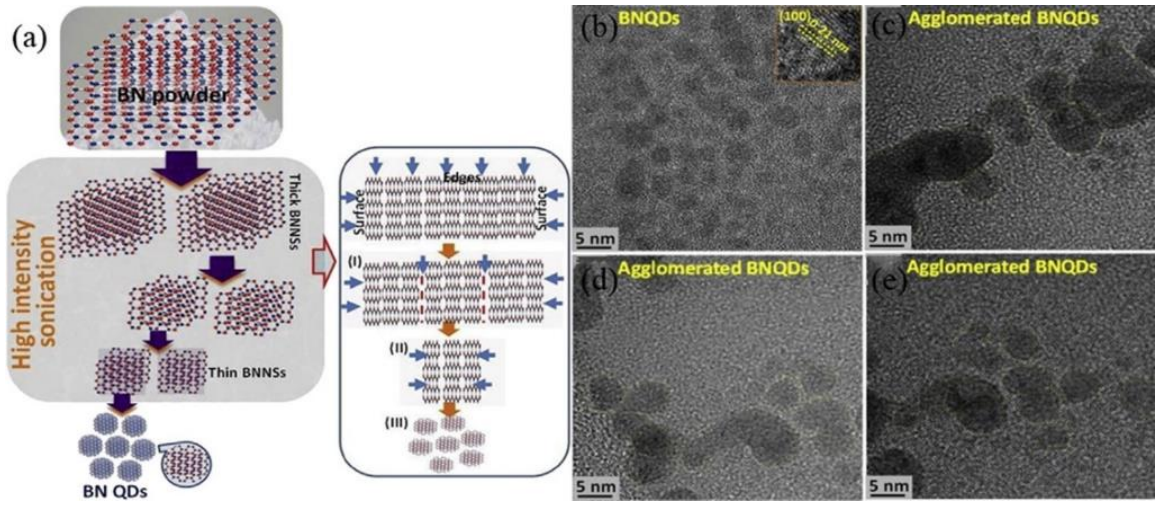

Fig. 3.25 Liquid Exfoliation: Top-down process. [111]

3.5.4.1.3 Mechanical exfoliation:

On a variety of surfaces, it is the most used method for depositing a monolayer to many layers of hBN. Due to its low cost, high-quality flakes, and simple deposition procedure, this method [76, 108] has remained popular since the separation of graphene from a graphite crystal in 2004. Exfoliated flakes have been used to study the characteristics of practically all newly found 2D layered materials. However, it is highly challenging to manufacture hBN on a big scale via mechanical exfoliation. Due of its high-temperature needs and higher expense, the CVD process is especially unpromising. Additionally, the CVD approach requires the use of precursors that include boron, which makes the process extremely risky and unstable. A proposed approach for creating high-quality hBN films is liquid exfoliation. [78]

3.5.4.2 BOTTOM-UP PROCEDURES

3.5.4.2.1 Solvothermal synthesis

The hydrothermal/solvothermal synthesis techniques [66, 67] use a tiny source molecule, water, or a synthetic solvent as a catalyst medium to synthesize Quantum Dots at high pressure and temperature.

Liu et al. [112] generated hydroxyl and amino functionalized BNQDs first in a N_2 environment. using NH_4OH and H_3BO_3 as precursors. Throughout the procedure, the effects of hydrothermal treatment time, precursor content, and reaction temperatures on the size of BNQDs were investigated [76]. When the reaction temperature was 180 °C and the reaction period was 12 hours, the findings reveal that the precursor ratio had no influence on the reaction. According to HRTEM and AFM pictures of BNQDs [112], the BNQDs as-obtained showed a favourable size (2.38 nm), an average thickness (0.91 nm), and 18.3% yield. Density functional theory was utilised to mimic the hydrothermal reaction process and the fluorescence quenching mechanism in order to better characterise the characteristics of the produced BNQDs, confirming the method's efficiency and eco-friendliness [76]. However, ammonia solution as a source of nitrogen during the material selection process is flammable and polluting, which will prevent its continued biological employment. To overcome this problem, Huo et al. in 2017 hydrothermally synthesized monolayer BNQDs at for 15 h using H_3BO_3 and $C_3H_6N_6$ as

precursors; the resultant BNQDs was of 3 nm. Melamine was chosen in this technique as the nitrogen source since it is environmentally safe and supplies new material for the creation of high-quality BNQDs.

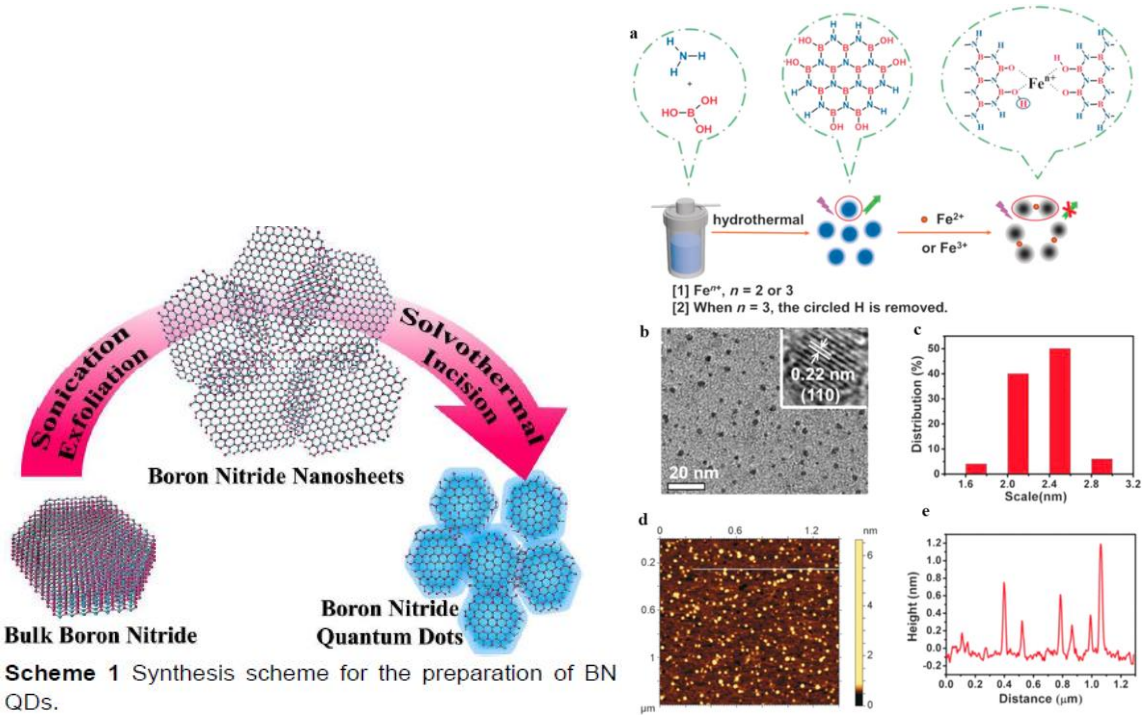

Fig. 3.26 Synthesis Scheme for the fabrication of BN QDs. [112]

In general, BNQDs with high yield and monolayer structure may be made using the hydrothermal/solvothermal synthesis. Throughout the whole process of creating BNQDs, the nitrogen source chosen is crucial. The main feature of this study is the ability to produce BNQDs with varying particle sizes and degrees of dispersion by adjusting the reaction temperature and microwave irradiation period. The corresponding sizes (at 140℃, 150℃, and 160 ℃) for microwave radiation are 4.03nm, 3.21nm, and 3.15 nm, respectively. This data shows that the BNQDs particle size (avg) steadily reduces as reaction temperature rises. Similar to this, the impact of various radiation exposure times on size was also examined. The size increased with an increase in response time (5, 10 and 25 min), and was, correspondingly, 7.05, 3.21, and 1.98 nm.

The findings of the aforementioned investigations unequivocally show that response temperature has less of an effect on lateral size and distribution than

reaction time. This could be as a result of the BNQD molecules becoming more orderedly distributed with increased microwave irradiation, which leads to a reduction in lateral size and a more orderly dispersion of the BNQD molecules. Liu et al. [109] utilized the microwave-assisted hydrothermal approach to create sulfur-regulated BNQDs (S-BNQDsT and S-BNQDsL) using melamine and boric acid as precursors and thiourea and L-cysteine as dopants.

The procedure of making BNQDs via microwave irradiation is evident from the preceding explanation since it is rapid and efficient. Additionally, the high quality and uniform dispersion of the BNQDs generated show that this method is currently the best for producing BNQDs.

3.6 PHYSICS BEHIND h-BN BASED METHANE SENSOR

Methane is a symmetrical, non-polar molecule with a high enthalpy carbon-hydrogen bond that makes it harder to identify and more stable in the gaseous phase. Understanding the chemical and textural features at the surface of the exfoliated boron nanostructure and its bulk counterpart was important to explain the gas sensing behavior, and this could be done using XPS analysis and nitrogen adsorption-desorption investigations, respectively. Chemically speaking, the surface states of bulk and exfoliated boron are the same.

The surface-to-volume ratio of hBN was higher than that of metal oxides. As a result of the wide surface's increased number of active sites for gas molecule adsorption, the sensing response value is high. h-BN is the optimal substrate for the synthesis of other materials due to its exceptionally flat surface, high stability, reduced surface roughness, and minimized Coulomb scattering [78]. The use of hBN as a sacrifice layer might lead to the creation of very effective flexible and wearable gas sensors. Since hBN is thermally stable up to 900°C, a gas sensor may function under challenging circumstances without undergoing performance degradation.

3.6.1 h-BN REACTION WITH METHANE: What happens when h-BN reacts with Methane molecules?

Hexagonal boron nitride (h-BN) quantum dots can be utilized as sensing materials to detect methane gas. The basic principle behind this type of sensor is the interaction between methane molecules and the h-BN quantum dots, which leads to changes in the optical properties of the quantum dots. Here's a general outline of the detection process. The sensor is exposed to the methane gas of interest. Methane molecules interact with the functionalized surface of the h-BN quantum dots, leading to changes in the quantum dots' electronic or optical properties. Due to its ultra-thin nature chemical, gas molecules would be absorbed in increased surface area by hBN, changing its electrical characteristics and increasing sensitivity. [110].

The changes in the optical properties of the h-BN quantum dots can be detected using various techniques, such as photoluminescence spectroscopy or electrical measurements. The sensing mechanism can involve changes in the quantum dots' emission intensity, wavelength, or

lifetime. The sensor output is analyzed to determine the concentration or presence of methane gas. This is typically done by comparing the sensor response with calibration curves or using signal processing algorithms.

Due to the significant charge (electron) transfer between the contacting surface and gas molecules, CH_4 molecules are highly reactive. Beheshtian et al. [77] determined the adsorption energy of CH4 gas molecules on the surface of BN film to be -1.06 kJ/mol. The stronger the charge transfer, the lower the adsorption energy. The interaction of the gas molecules with the surface of the nanocluster modified its electronic characteristics and enhanced its conductivity. The charge density redistribution caused by COX gas molecule exposure at the CB and CN locations. The high magnitude of the threshold voltage change indicates a considerable quantity of charge transfer following COX exposure, verifying the hBN-based gas sensor's great sensitivity. Active sensing layers may be put onto a cheap, flexible acrylic surface using the 2D hBN. This transfer method increases response time by a factor of six and sensitivity by a factor of two. As a result, a significant change in the hybrid material's electrical characteristics is detected with great sensitivity.

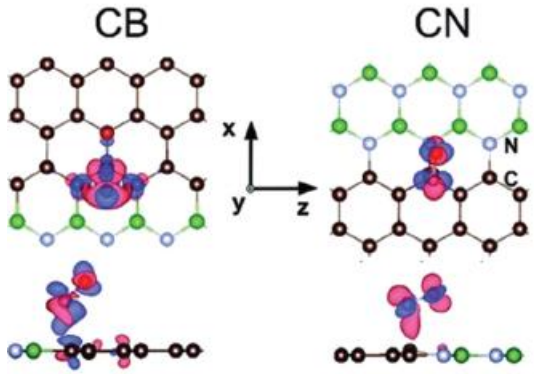

Fig. 3.27 Charge density redistribution at CB and CN. [78]

Through electrical interactions with COx and oxygen atoms, BNQDs performed as catalysts to create charge carriers. The increase in oxygen species concentration affects the composites' sensing capabilities. The conductance variation brought on by the chemisorption of oxygen molecules on the sensor surface is the basis for this resistance-based gas sensor. Ionized oxygen reacts with CH_4 gas molecules as they adsorb on the sensor surface, causing oxidative breakdown of the CH_4 molecules and electron transfer to the sensor.[79]

3.6.2 SENSING MECHANISM: How can h-BNQDs sense Methane?

The sensing process uses the chemisorption of ambient oxygen molecules on the hBN sensor layer. When the oxygen ions interacted with gas molecules, they released electrons that had been collected and returned them to the sensing layer, lowering the device resistance. As a consequence, a substantial level of sensitivity was discovered in the presence of LPG molecules. Sajjad et al. [78] measured the change in resistance brought on by exposure to oxygen and methane gas molecules in order to assess the sensitivity of a BN nanosheet-based gas sensor. A sensitivity of 7.8 was recorded in response to exposure to methane gas, indicating a potent preference for methane. Methane's polarized structure for more adsorption on the BN surface, which produces a high sensitivity.

Oxygen molecules adsorb on the sensor surface, creating oxygen ions by absorbing free electrons and enhancing device resistance. On the basis of variations in conductance brought on by oxygen adsorption as well as desorption on the hBN surface, a sensing mechanism was hypothesized.

Charge transfer between the gas molecules and the sensing element is primarily responsible for the lower operating temperature of the hBN gas sensing method. Due to electron transfer between the gas molecules and hBN, the reducing or oxidizing gas species that are electrostatically adsorbed on the surface of this material change the resistance of the sensing layer. The ability of the gaseous species to emit or trap electrons determines how much the resistivity changes. When boron nitride nanosheets are exposed to methane gas molecules, their resistance rises. The resistance reverts to its initial value when gas molecules are desorbed in an atmosphere of air or vacuum. A greater value of the sensing response is therefore acquired due to the bigger surface area's availability of more active locations for gas molecules to be adsorbed.

From the signature of the B 1s and O 1s spectra in XPS data, a significant number of surface-adsorbed oxygen species were seen in the O 1s spectra.

Measurements of electron paramagnetic resonance (EPR) in the literature revealed that this surface-adsorbed oxygen readily accept electrons from the nanomaterial's surface as

$$O_2\ (gas) \rightarrow O_2\ (adsorbed) \quad (3.9)$$

$$O_2\ (adsorbed) + e^- \rightarrow O_2^-\ (adsorbed) \quad (3.10)$$

When exposed to methane gas, the sensing device interacts with the released oxygen ion species on the Boron Quantum dots as

$$CH_4 + 2O_2^-(adsorbed) \rightarrow 2H_2O + CO_2 + 2e^- \quad (3.11)$$

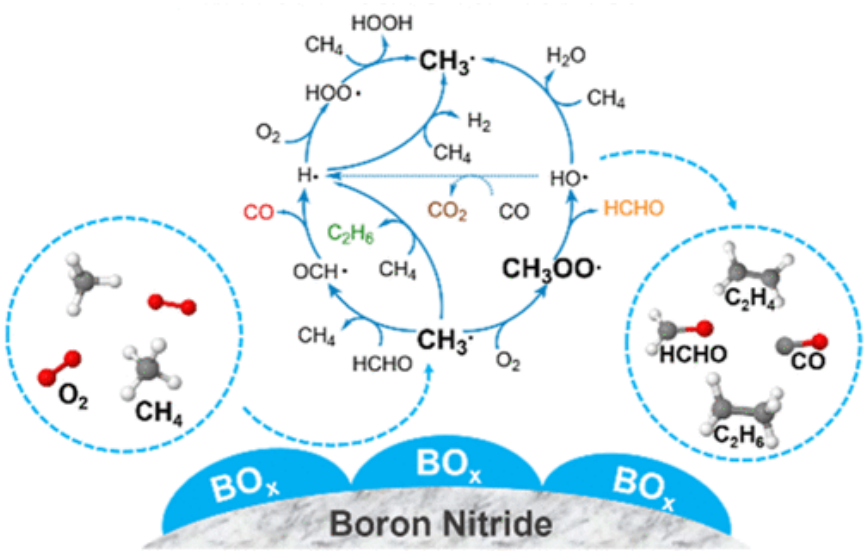

Fig. 3.28 Ion absorption Model: Boron Nitride reaction with Methane molecule. [113]

The conductivity of the boron nanostructures, where the electron is the main current carrier, is further increased by the electrons produced during this contact. This ionosorption model (fig 3.29), which is commonly employed in the sensor industry, is extremely reliant on the amount of oxygen species present on the surface, which in turn necessitates nanostructures with large specific surfaces for use as receptor films.

Chapter IV

EXPERIMENTAL SECTION

4.1 MATERIALS AND METHODS

4.1.1 MATERIALS REQUIRED

For Fabrication of hBN on Si wafer and Glass Film

a. Boron Nitride (BN) 99% pure purchased from LOBA CHEMIE PVT.LTD, amount to be taken 0.5 gm.
b. N-N Dimethylformamide purchased from EMPLURA, amount to be taken 50Ml.
c. 2- Propanol (Isopropyl Alcohol) purchased from EMPLURA
d. Acetone purchased from EMPARTA.
e. Si Wafer.

Doping Type: p type

Resistivity: 33.21MΩ

Thickness: 400μΩ

Area of substrate: 1.5cm × 0.8cm

f. Glass Film

Resistivity: 8-12 Ωcm

Thickness: 1 mm

Area of Substrate: 1.0 cm × 1.0cm

Fig. 4.1 Materials used.

4.1.2 DETAILED ANALYSIS OF USED MATERIALS

a. **BORON NITRIDE (BN)** is a chemical compound composed of boron and nitrogen atoms. It exists in several structural forms, each with unique properties.

Chemical Structure:

Boron nitride can adopt different structural arrangements, primarily hexagonal boron nitride (h-BN) and cubic boron nitride (c-BN). These structures differ in bonding and symmetry:

- Hexagonal Boron Nitride (h-BN): Also known as "white graphite" because of its layered structure, h-BN is made up of alternating boron and nitrogen atoms organized in a hexagonal lattice. The majority of the bonding in h-BN is covalent, with boron and nitrogen atoms bound together by strong sigma bonds.

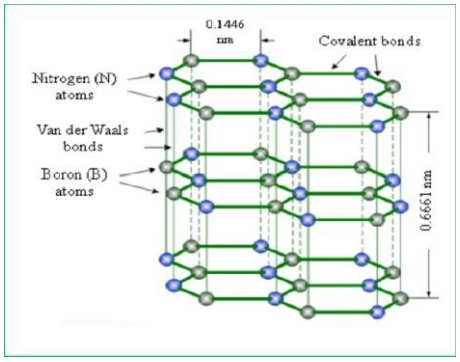

Fig. 4.2 Chemical Structure of h-BN. [114]

- Cubic Boron Nitride (c-BN): This form of boron nitride exhibits a cubic crystal structure and is analogous to diamond in terms of its hardness. c-BN is composed of a 3-D network of boron and nitrogen atoms connected by strong covalent bonds.

Physical Properties of Hexagonal Boron Nitride (h-BN):

- It appeared to be a white powder or a transparent, colourless crystal.
- h-BN with a high melting point of around 3,500°C, acts as a suitable material for high-temperature applications.

Fig. 4.3 Boron Nitride Powder form

- It is an excellent electrical insulator and possesses high thermal conductivity along the plane of the hexagonal layers, making it useful in heat management applications.
- h-BN has low friction and is often used as a lubricant in high-temperature environments.
- It is chemically inert and resistant to most chemicals, including acids and alkalis.

Applications:

Boron nitride's unique properties make it valuable in various applications:

- Hexagonal Boron Nitride (h-BN):
- High-temperature applications: Due to its exceptional thermal stability, h-BN is used as a refractory material in crucibles, nozzles, and furnace linings.
- Lubricants: The low friction properties of h-BN find applications as solid lubricants, mold release agents, and coatings for reducing friction and wear.
- Electrical insulation: h-BN act as an insulating material in high-temperature environments, such as in electronic components, insulating substrates, and high-voltage insulators.
- Nanomaterials: Nanostructured h-BN is used in composite materials, nanotubes, and thin films for several applications, including electronics, optics, and energy storage.

b. N-N DIMETHYLFORMAMIDE

Dimethylformamide is an organic compound with the formula $(CH_3)_2NC(O)H$. Commonly abbreviated as DMF. DMF is a common solvent for chemical reactions.

Structure and properties:

- As with most amides, spectroscopic data shows that the C-N and C-O bonds are partially double bonds. As a result, the infrared spectrum displays a C=O stretching frequency of only 1675 cm^{-1}, whereas a ketone absorbs approximately 1700 cm^{-1}.

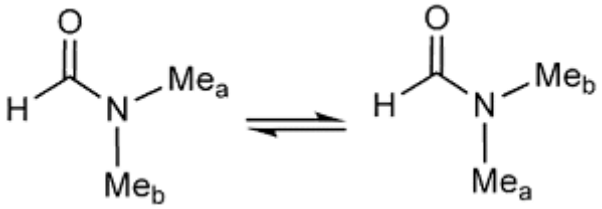

Fig. 4.4 Chemical structure of DMF. [115]

- DMF is a well-known example of a fluxional molecule.
- The ambient temperature H NMR spectrum contains two methyl signals, indicating that rotation about the (O) C-N bond is impeded.
- The 500 MHz NMR spectra of this chemical exhibits only one signal for the methyl groups at temperatures close to 100 °C.

- DMF is miscible with water.
- At 20 °C, the vapour pressure is 3.5 hPa.
- An experimentally calculated equilibrium constant at 25 °C yields a Henry's law constant of 7.47 105 hPa m3 mol1.
- The partition coefficient log P_{OW} is calculated to be -0.85.[11] Because the density of DMF (0.95 g cm^{-3} at 20 °C) is similar to that of water, considerable floating or stratification in surface waters cannot be anticipated in the event of unintentional losses.

Fig. 4.5 DMF

c. 2- PROPANOL (ISOPROPYL ALCOHOL)

Isopropyl alcohol is a colorless, flammable chemical compound with a strong alcoholic odor. It is also known as 2-propanol or isopropanol. Propan-2-ol is its IUPAC name.

An isopropyl group connected to a hydroxyl group (chemical formula (CH3)2CHOH), in which the alcohol's carbon atom is attached to two additional carbon atoms, is the most basic type of secondary alcohol.

Structure and Properties:

It is an ethyl methyl ether structural isomer and propan-1-ol.

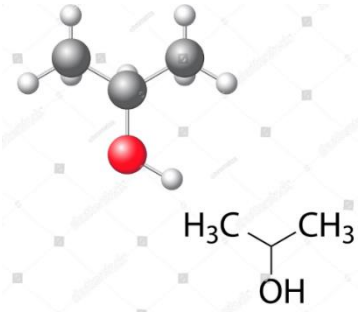

Fig. 4.6 Chemical Structure of 2- Propanol. [118]

- As isopropyl is an organic polar molecule, it is miscible in water, ethanol, and chloroform.
- It dissolves ethyl cellulose, polyvinyl butyral, as well as a wide range of oils, alkaloids, and natural resins. Isopropyl alcohol, unlike ethanol or methanol, is not miscible with salt solutions. Salting out refers to the process of separating concentrated isopropyl alcohol into a distinct layer.
- Isopropyl alcohol reacts with water to produce an azeotrope, resulting in a boiling point of 80.37 °C (176.67 °F) and a composition of 87.7% by mass (91% by volume) isopropyl alcohol. Melting points of alcohol mixtures are low. It has a somewhat harsh flavor and is not suitable for drinking**.**
- It gets extremely viscous as temperature decreases and freezes at -89 °C (-128 °F).
- In the ultraviolet-visible spectrum, isopropyl alcohol has the highest absorption at 205 nm.

Fig. 4.7 2- Propanol

Application:

It is a major constituent in antiseptics, disinfectants, hand sanitizers, and detergents, as well as a variety of industrial and household compounds. Every year, more over a million tonnes are produced globally.

d. ACETONE:

Structure and Properties:

- Acetone (also known as 2-propanone or dimethyl ketone) is an organic compound having the formula (CH3)2CO. It is the most basic and smallest ketone (>C=O).
- It is a colorless, extremely volatile, combustible liquid with a distinct pungent odor. Acetone is a miscible organic solvent with water that is widely used in industry, the household, and laboratories.

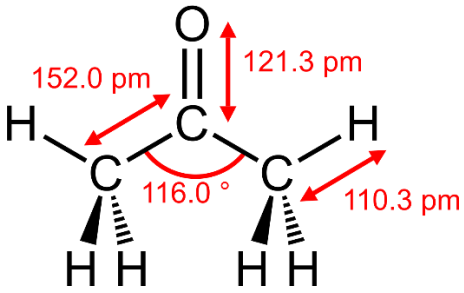

Fig. 4.8 Chemical structure of Acetone. [116]

Applications:

- Mainly used as a solvent and in the manufacturing of methyl methacrylate and bisphenol A, both of which are precursors to commonly-used plastics.
- It is used as a solvent in variety of household products including nail polish remover and paint thinner.
- Acetone is synthesized and disposed of in the human body as a part of regular metabolic processes. It is generally found in the blood and urine. It is produced in greater quantities in diabetic ketoacidosis patients. Ketogenic diets that raise ketone bodies in the blood (acetone, -hydroxybutyric acid, and acetoacetic acid) are used to treat epileptic episodes in children with refractory epilepsy.

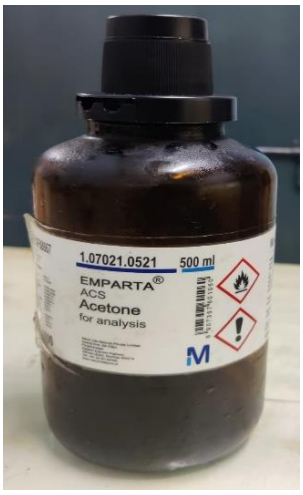

Fig. 4.9 Acetone

- Acetone is a volatile organic compound (VOC)-free substance in the United States.

4.2 NANOSENSOR DESIGN STEPS

4.2.1 FLOWCHART: h-BN Q-DOTS SYSTHESIS

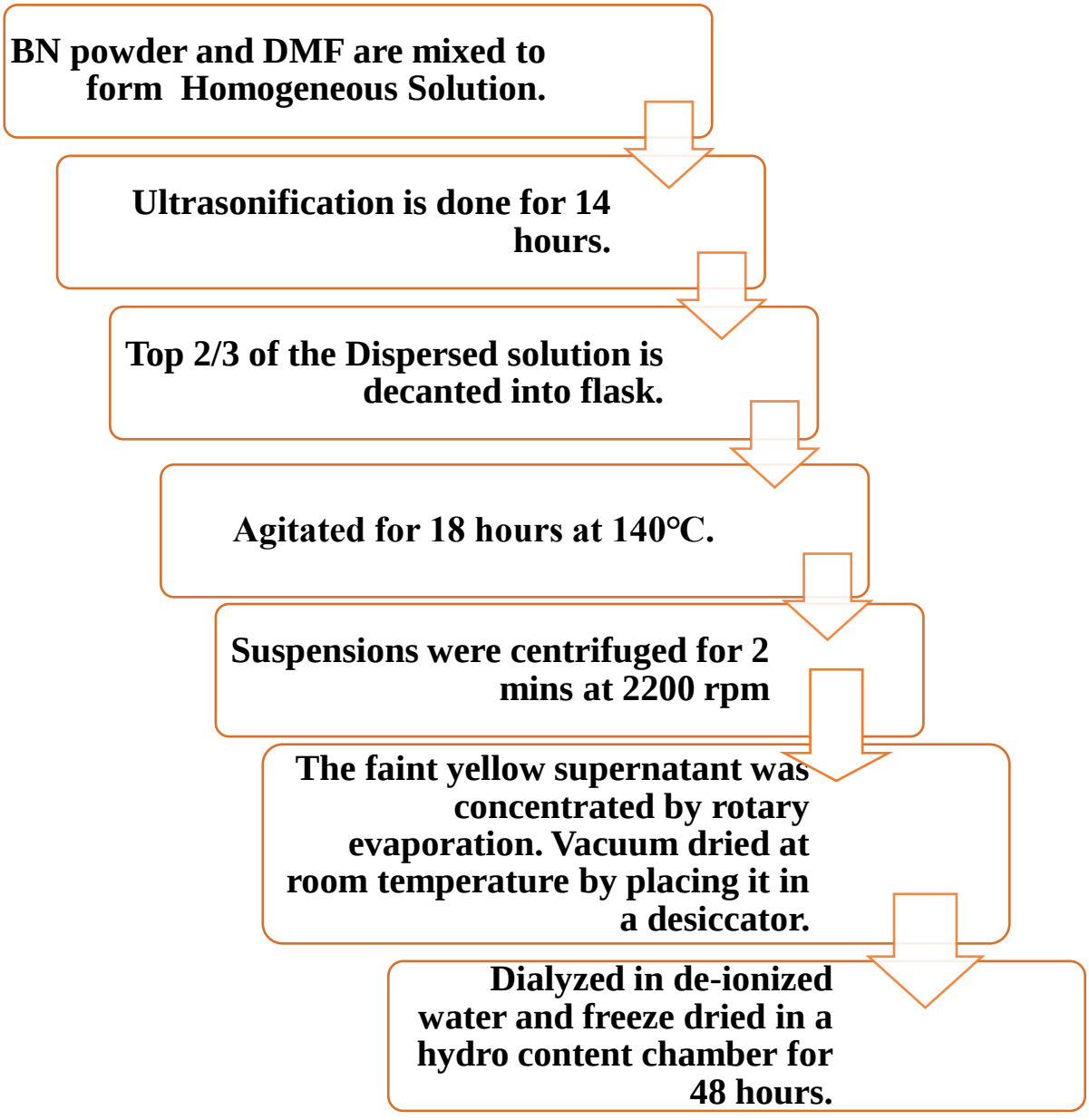

4.2.2 PROCESS FLOW

I. STEP I

0.5 gm of Boron Nitride powder was combined with a 50 mL solution of Dimethylformamide $(CH_3)_2NC(O)H$ in a 100 mL beaker while being continuously sonicated using ULTRASONIC CLEANERS (SA INSTRUMENTS AND SYSTEMS, CAPACITY- 5 LTR, POWER O/P- 100W, POWER I/P; 230 V, FREQUENCY – 30±3KHz, TIMER- 0-99 min) for at least 14 hours.

Fig. 4.10 Ultrasonification Process in Ultrasonic Cleaner

II. STEP II

Then, the exfoliated Boron Nitride nanosheet-containing top 2/3 of the dispersion was decanted into a flask and vigorously stirred on a hot plate (COLE-PATRMER) for 18 hours at 140-degree C.

Fig. 4.11 Magnetic stirring process on a Hot-Plate.

III. STEP III

The resultant suspensions were centrifuged for 2 minutes at 2200 rpm to separate the centrifugate and supernatant. The faint yellow supernatant was BN QDs dispersion.

IV. STEP IV

The faint yellow supernatant was later concentrated by rotary evaporation and Vacuum dried at room temperature by placing it in a desiccator.

Fig. 4.12 The Precipitate being vacuum dried in a Desiccator.

V. STEP V

They were then dialyzed in de-ionized water and freeze dried in a hydro content chamber for 48 hours to *remove the remaining solvent.*

Fig. 4.13 The resulting BN QDots (powder form) stored in a centrifuge tube.

4.2.3. FABRICATION ON GLASS SUBSTRATE

a) A 1 mm thick, 8-12 ohm-cm resistivity glass material approximately 1 cm x 1 cm was used as the substrate for generating nano BN layers using thin film deposition method.
b) Approximately 1000 nm thin BN film was deposited by the drop casting and annealing technique.
c) Using Cu metal mask on Si electrode contacts are formed to BN.
d) 0.03 gm 0.4 M hexagonal Boron Nitride powder (98 %) was dispersed in a suitable solvent or dispersing agent. Here the solvent used for this purpose is
e) 30 mL of 2- propanol and was stirred at room temperature.
f) The Disperse is been stirred for 2 hours to ensure proper dispersion and deagglomeration of the powdered particle.
g) The dispersed BN nanoparticles coating on the p type Si sample can be done using drop casting method.
h) The sample is kept on a hot-plate and drop casted the material on it using a Syringe.
i) The sample is heated to a high temperature during fabrication to encourage the reaction with the reducing gas and to eliminate the water generated during this reaction. Electrical connections have been established using silver paste and small copper wire.
j) The sample was then heated at 110°C for 3-4 hours to evaporate the solvent and eliminate the organic residue by creating very small crystals on the wafer surface. To achieve 900nm thickness, the drop casting method was carried out seven times.
k) A constant 10 V supply (Scanning Potentiostat-362) was used during anodization and the increase of I with the formation of CH_3OH was monitored till the saturation of I indicated the termination of the oxide formation.
l) The thickness of the BN/Si after thin film grown is 401 μm.
m) The contact region's diameter was kept constant at 2 mm.

Fig. 4.14 Magnetic Stirring on Hot plate

Fig. 4.15 Drop casting the solution

Fig. 4.16 The sample is heated to settle down the nanoparticles.

Fig. 4.17 The prepared sample

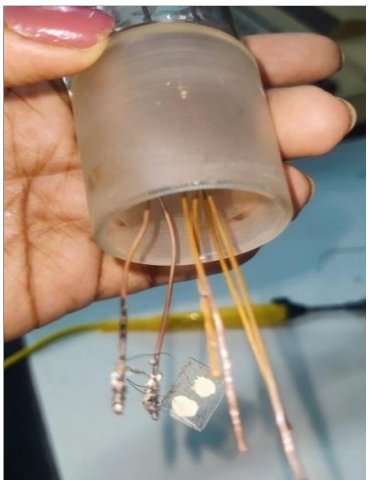

Fig. 4.18 Final sensor configuration.

4.2.4 FABRICATION ON Si SUBSTRATE

a) A 1.5cm x 0.8 cm p-Si (resistivity 0.5 ohm-cm, 400 μm thick) was chosen as the substrate for growing nano BN films by thin film deposition technique. 100 μm thin BN film was deposited by the dip coating and annealing technique. Using Cu metal mask on Si electrode contacts are formed to BN.

b) 0.3 gm 4.03M hexagonal Boron Nitride powder (98 %) was dispersed in a suitable solvent or dispersing agent. Here the solvent used for this purpose is 30mL of 2- propanol and was stirred at room temperature. The Disperse is been sonicated for 2 hours to ensure proper dispersion and deagglomeration of the powdered particle.

c) The dispersed BN nanoparticles coating on the p type Si sample can be done using dip-coating. Dip coating technique is preferred for uniform layer on the surface of sample. The coating is done using a dip coating machine along with the software interface (PromptDipCoatingControl) for controlling parameters like Dipping Counts (6), Dipping Delay (9 sec) and Drying Delay (9 sec).

d) The sample is heated to a high temperature during fabrication in order to speed up the reaction with the reducing gas and eliminate water that is produced during this reaction. Electrical connections have been established using tiny pieces of copper wire and silver paste.

e) In order to evaporate the solvent and eliminate the organic residue, the sample was next heated at 110°C for 10 min, producing tiny crystals on the wafer surface. To obtain a 100 μm thickness, the dipping procedure was performed three times.

f) Finally, the samples were then heated to 600 °C for annealing.

g) A constant 10 V supply (Scanning Potentiostat-362) was used during anodization and the increase of current with the formation of CH3OH was recorded till the saturation of the current indicated the termination of the oxide formation. The thickness of the BN thin film grown is 500 μm respectively.

h) The X-ray diffraction (XRD) and the FESEM were employed to study the polycrystalline nature, the grain size, the surface morphology and the porosity of the deposited hBN thin film.

i) The diameter of the contact area was kept 2 mm.

Fig. 4.19 Sample (wafer) Cleaning Process

Fig. 4.20 Magnetic Stirring Process of the solution.

Fig. 4.21 Ultrasonification of Dispersed Solution.

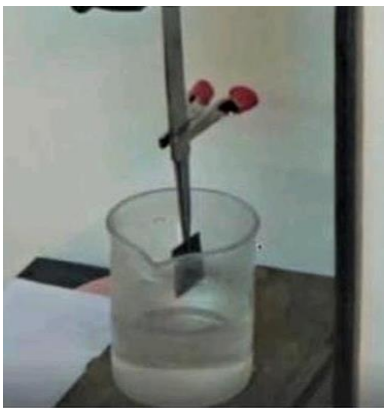

Fig. 4.22 Dipping Process.

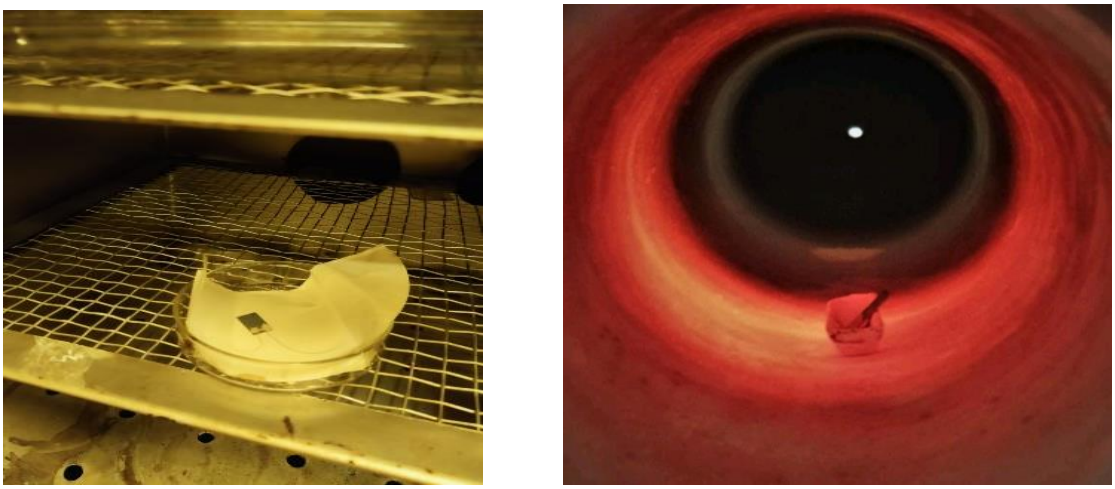

Fig. 4.23 Annealing Process at 120 °C and 600 °C

The Final sensor configuration is shown in below Fig. 4.24.

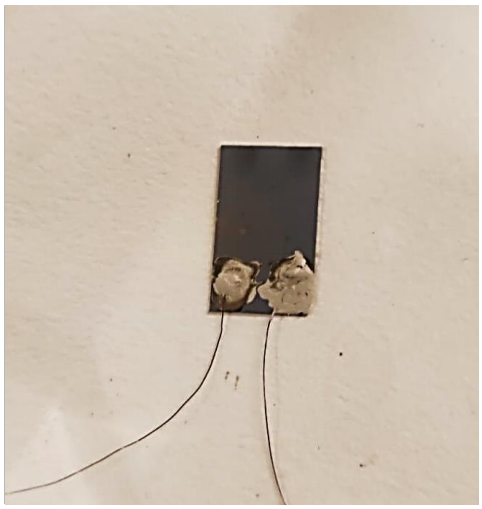

Fig. 4.24 Methane sensor

4.2.5 CHARACTERISTICS OF hBN/Si and h-BN/Glass FILM

FILM THICKNESS MEASUREMENT

hBN/Si Film and hBN/Glass thicknesses were measured by Screw Gauge. After fabrication on the Si film, it was discovered to be around 500 m thick.

4.2.6 ELECTRICAL CONDUCTIVITY MEASUREMENT

In order to study the sensor's features, a test chamber connecting to gas flow chamber (Fig 4.25) is used where a closed glass tube measuring 10 cm long by 4 cm wide and equipped with gas inlet and outflow provisions, positioned coaxially within a resistively heated furnace with a 4 cm zone of constant temperature. A heating element was used to regulate the temperature of the sensor. Probes were used to make electrical contact, voltages were applied across the contact pads, and currents were monitored. Using a copper constantan thermocouple that was inbuilt in a precision temperature controller, the temperature was kept within 1◦C.

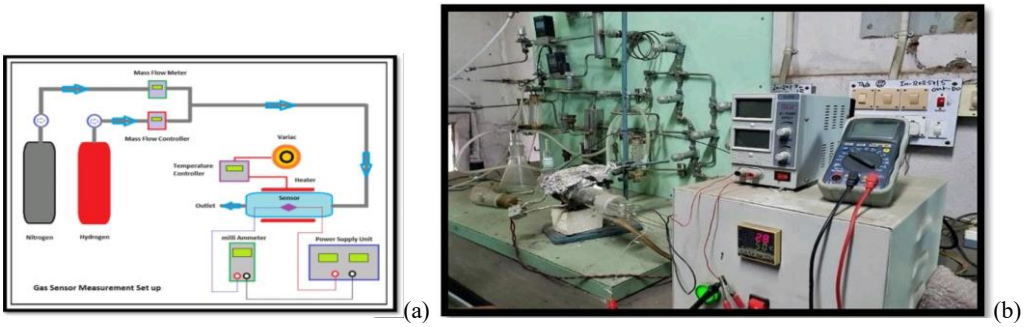

(a) (b)

Fig. 4.25 (a) Gas Flow Process, (b) Electrical measurement Set-up

Using a mass flow controller and mass flow meter from Alicat Scientific, high purity (100%) CH_4 and N_2 were combined and allowed to pass through the gas-sensing chamber for the sensor analysis. As a result, the mass flow rate and the concentration of the methane gas managed to be stable throughout the entire experiment. The gas pressure above the sensor device was maintained constant at one atmosphere throughout the course of the experiments. The test chamber was flushed with N_2 gas for 15 minutes after the achievement of the operating temperature and before beginning the sensor studies. This was done for every set of trials conducted at various temperatures.

4.2.7 OBSERVATION OF MORPHOLOGY

With the exposure to Methane Gas in the presence of N2 gas, the conductivity of sensor increases (discussed in **chapter 3 section 3.5).** As discussed in **Section 3.5.2** from C**hapter 3,** the resistance of the sensing layer is impacted by the reducing or oxidizing gas species that are electrostatically adsorbed on the surface of hBN and cause an electron transfer between the gas molecules and hBN. With different operating temperature the sensor shows different characteristics. The result and characteristic curves are given in the next segment. Oxygen molecules attach on the sensor surface in ambient environments, creating oxygen ions by absorbing free electrons and enhancing device resistance. On the basis of variations in conductance brought on by oxygen adsorption and desorption on the hBN surface, a sensing mechanism was hypothesized. Here hBN also acts as catalyst to increase the rate of reaction or we can say due to the hBN quantum dots the response time is quick.

4.3 RESULT

The Methane sensors were investigated at various temperature for methane concentrations with nitrogen serving as the carrier gas between 50 °C and 200 °C. The bias voltage was adjusted between 0.1 and 27.6 volts. At various operating temperatures like 50°C 100°C, 150°C and 200 °C, the response magnitude for CH_4 concentration were observed.

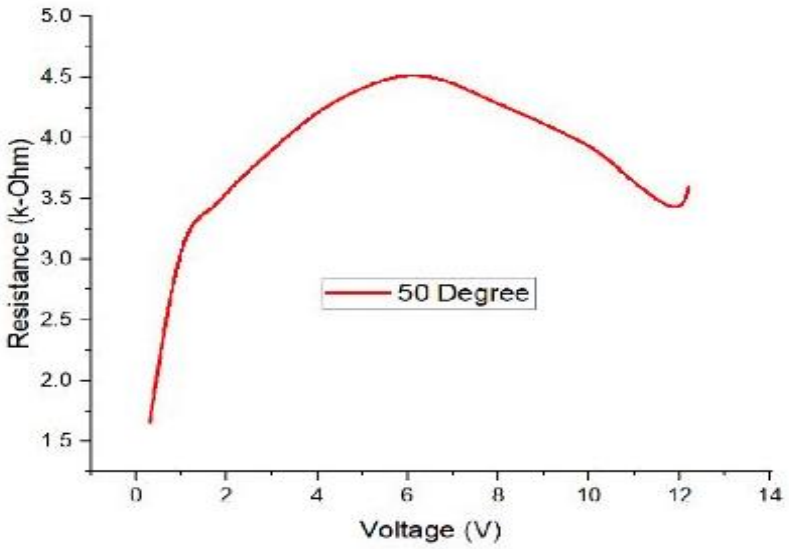

(a)

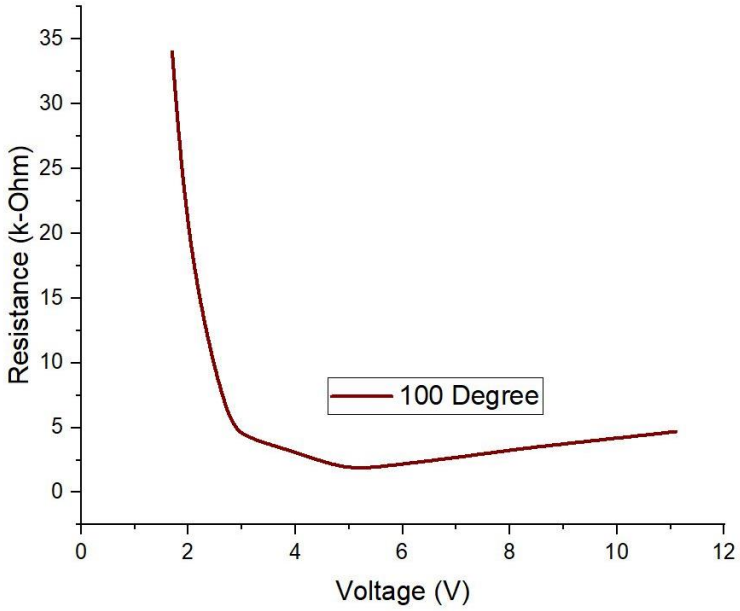

(b)

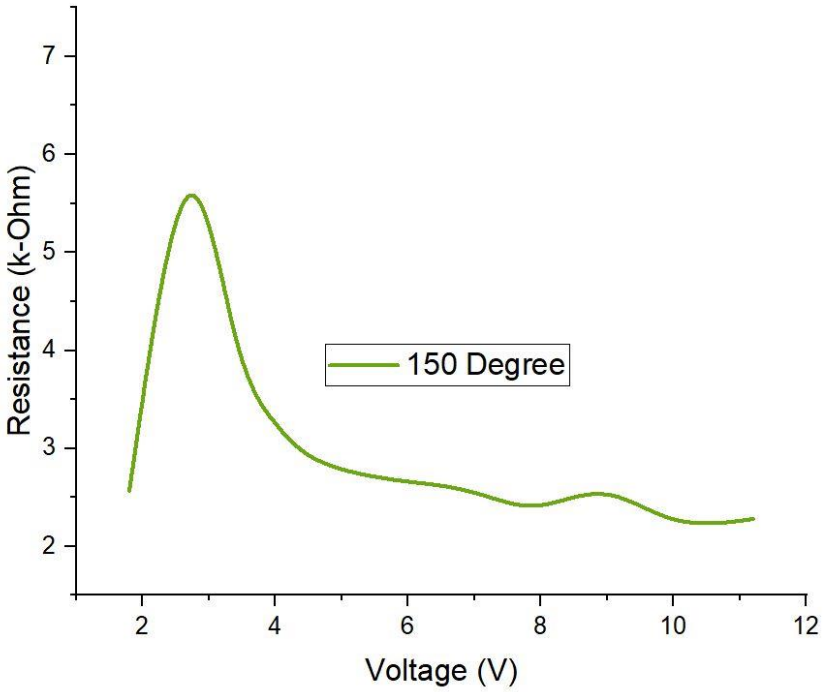

(c)

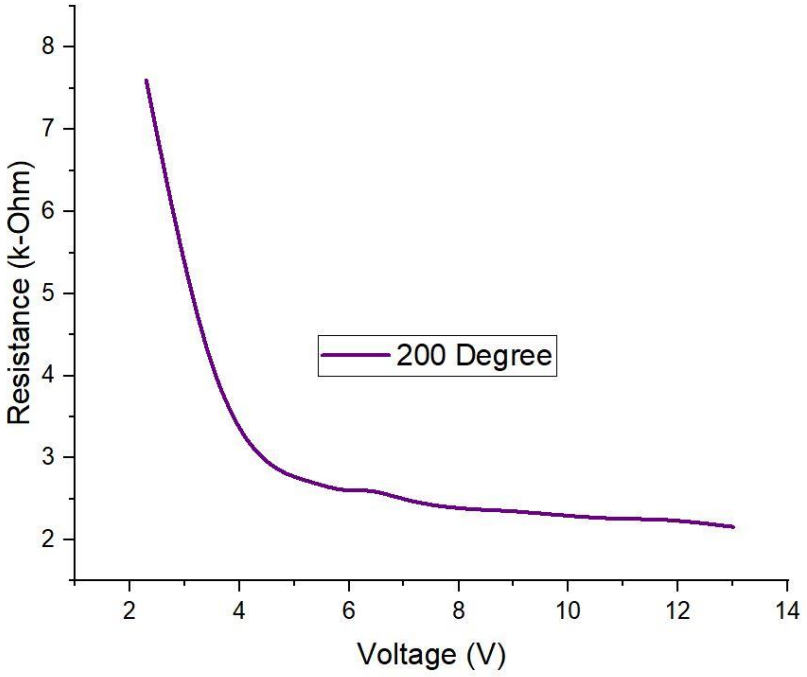

(d)

Fig 4.26 Operating voltage vs Resistance characteristics at various Operating Temperature: (a) 50 °C (b) 100 °C (c) 150 °C and (d) 200 °C

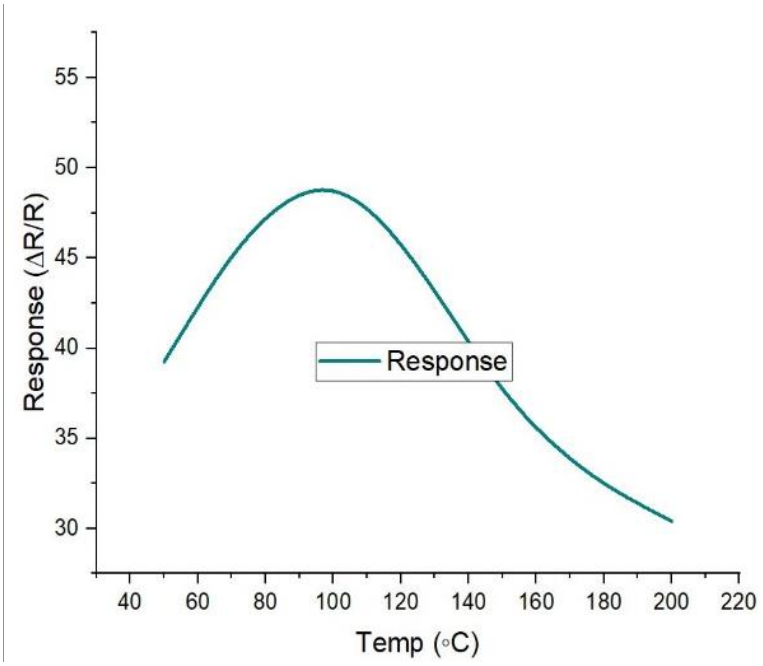

Fig. 4.27 Variation of Sensor response as a function of operating temperature.

The above figure reveals the response variation as function of operating temperature. From the observation, it can be concluded that the highest response time of the designed gas sensor is obtained at 150 °C.

4.3.1 CHARACTERIZATION

4.3.1.1 FE SEM CHARACTERIZATION OF BORON NITRIDE QUANTUM DOTS

FESEM picture reveal clearly from the film grown using top-down method that the quantum dots have much smaller grain size and larger pore size compared to that in this process.

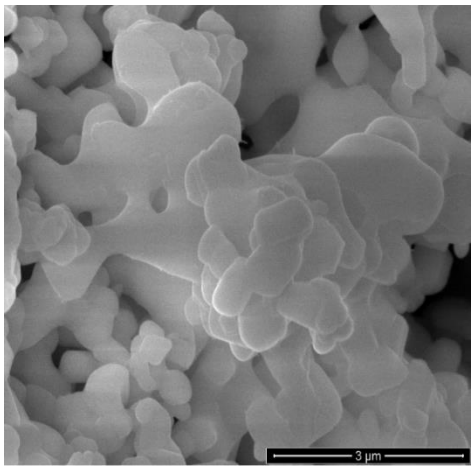

Fig. 4.28 Particle size distribution of hBN Quantum dots.

4.3.1.2 XRD STUDY OF BORON NITRIDE QUANTUM DOTS

Hexagonal Boron Nitride quantum dots were produced from raw boron nitride crystals (in powder form) using special synthesis method. Phase identification of the prepared BN quamtum dots was examined using the X-ray diffraction (XRD) of Rigaku diffractometer using CuKα line radiation (λ= 1.54 Å). The nano hexagonal boron nitride powder had a high density, a specific surface area, and mean particle size of 3.70nm.

The x-ray difractogram of the nano hBN powder is presented here (See in Figure 4.29). Few sharp and well-defined peaks can be observed in the x-ray diffraction pattern correspond to hexagonal boron nitride. Then nano hBN particles exhibited thin plate-like morphologies with rounded surfaces. The major peak is produced at roughly 27°, which corresponds to the (002) plane of Boron Nitride.

It is noted that other peaks are formed at about 46° and 56° that are indicative of different materials. Those are regarded as hump. The intensity of the main face and other peaks quickly reduces when the BN powder is exfoliated into the hBN QDs, suggesting the creation of a highly exfoliated material. According to prior research, the 3.70 nm d spacing for the hBN QDs corresponds to a BN crystal with a (002) face. The crystal size was calculated from the Scherer formula. The average crystal size is 0.75 nm

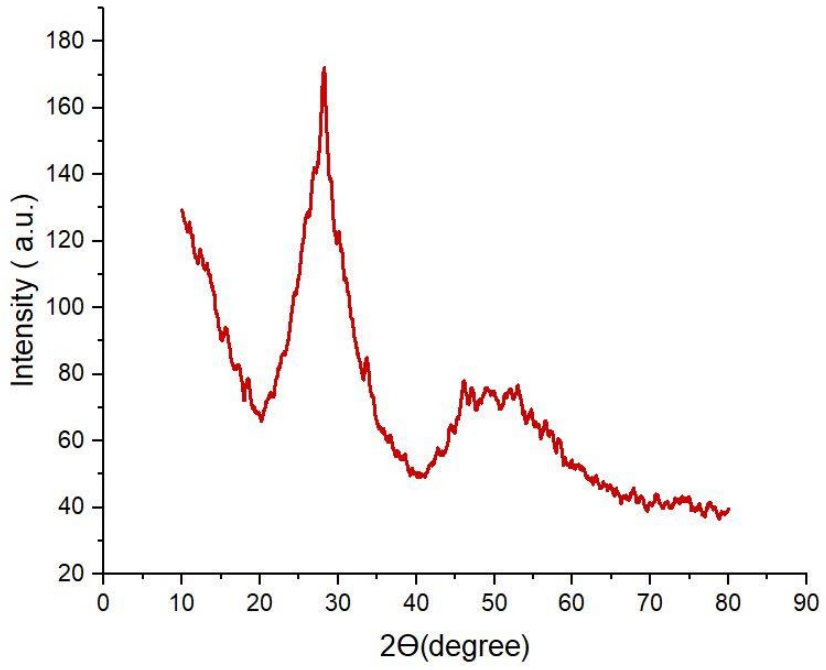

Fig. 4.29 X-ray Diffraction (XRD) Patterns of the prepared Composite 2Θ= 10◦-80◦

4.3.2 NANOSENSOR PERFORMANCE EVALUATION

The reaction time was computed as the amount of time needed to attain a saturation sensitivity. **(From eq. no. 3.5**) The recovery time was determined at 54.4%. This is the time to drop the sensor response from the saturation sensitivity to the baseline value when the gas pulse was switched off.

Figure 4.27 depicts the variation of response with operating temperature under exposure to Methane gas. Since the optimal operating voltage for both types sensors is fairly low, hence it is ideal for low power applications. However, it's noteworthy to note that when exposed to methane in nitrogen, the response of the electrochemically created sensor is considerably larger at 150 °C.

4.4 DISCUSSION

The aim of this research work was to design a 2D material based nanosensor to sense methane gas. For the development of 2D material-based nanostructure, two composite structures of h-BN/SiO2 and h-BN/Si were designed. For fabricating the composite structure, Liquid exfoliation technique has been used for synthesizing BN Quantum Dots. The synthesizing of Quantum Dots had been a success. The XRD result of the h-BN quantum dots confirmed the success of the synthesization. The SEM morphology also indicated that the particles of h-BN have been dispersed into nanoscale.

The second part was to fabricate the sensor. Glass film and Si sample have been chosen as the substrates. The deposition processes in the both cases were smooth. The contacts were made for measurement of electrical properties.

The final part of the experiment was to measure response while it is exposed to Methane gas. BN based Si film gave some amusing performances, in terms of Sensitivity, Selectivity, Resistivity and Response time. While the glass substrate failed to show required response. Though hBN/SiO_2 reacted to the target gas in very few seconds, but it failed to continue to give the required data, after a delay the sensor fabricated on a glass substrate stopped giving any data, in response to increase in voltage value.

It was assumed that since the concentration of the BN molecules was very less. The molecules could not be deposited on the substrate. With the increase in concentration of h-BN molecules in the depositing solution, the gas sensor might work as required.

On the other hand, gas sensor made on Si substrate is considered as success. Hence the key findings of the work.

I. The designed Methane sensor (fabricated on Si substrate) meets the intended purpose and demonstrated the desired functionality. The sensor can successfully detect the target analyte or parameter accurately and reliably. Hence it is feasible.
II. The sensor gives a sensitivity of 54.6% at 150 ◦C, also the response time is few seconds only.
III. Since the layered 2D nanomaterial h-BN exhibits the required properties, such as enhanced surface area, high reactivity, or unique optical or electronic characteristics, it was a great choice for sensing methane molecule.
IV. The fabrication process was feasible and cost effective too, but the mass production of the material is quite a difficult since new researches have been produced day by day. Also, the fabrication procedure was done manually, hence the thought of the mass production is quite fascinating.
V. Compared to existing technology for designing nanosensor, the proposed method was simple, cost effective with great sensitivity as a pioneer in the methane sensing world.
VI. The proposed gas-sensor design has a great potential area for improvement and further development of the nanosensor. For example, graphene can be used as the substrate for depositing BN thin film, this heterostructure would have more sensitivity durability due to the mechanical property and electrical property of Graphene.

Chapter V

CONCLUSION AND FUTURE SCOPE

5.1 CONCLUSION

It can be concluded in this thesis work that the design of a nanosensor is a complex and multidisciplinary process that requires careful consideration of various factors. Furthermore, because of their unique features and high sensitivity, 2D material-based nano gas sensors show some tremendous potential for gas detection and monitoring applications, which aids in the integration of 2D materials with revolutionary device designs and manufacturing processes.

This will lead to the creation of extremely sensitive, selective, and portable gas sensors for a variety of industrial, environmental, and healthcare applications. The current research effort has been a success in many ways, but it still has to be improved for commercial and industrial applications. More research and development is needed to overcome the current obstacles and transform these advances into practical and commercially viable gas sensing systems.

Despite significant progress, plenty of challenges remain in the development of 2D material-based nano gas sensors. Some of the key limitations in designing nano gas sensors include:

- Fabrication complexity: The fabrication process for nano gas sensors can be complex and challenging. Creating nanostructures with precise dimensions and properties often requires specialized equipment and expertise, making the production process more demanding compared to conventional sensors.
- Cost: The fabrication of nano gas sensors can be expensive due to the need for specialized materials and equipment. This cost factor may limit their widespread adoption, especially in applications with tight budget constraints.
- Sensitivity to environmental conditions: Nanosensors may be sensitive to environmental conditions such as temperature, humidity, and other gases. These factors can affect the sensor's performance and introduce noise or interference in the readings.
- Selectivity: Methane is a colourless and odourless gas, making its detection challenging, especially at low concentrations. Achieving high sensitivity to detect low levels of methane accurately without false positives or negatives is a significant design challenge. Some

nanostructures may respond to multiple gases, making it difficult to distinguish the target gas from interfering gases in complex environments.

- Long-Term Stability: Over time, the sensor's performance may degrade due to material aging, contamination, or other factors. Ensuring long-term stability is essential for reliable and consistent monitoring. Hence repeatability can be disturbed very easily.
- Power consumption: Nano sensors may require advanced electronics and power sources for signal amplification and processing, leading to increased power consumption in certain cases.
- Reproducibility: Consistency in sensor performance can be a concern in nano gas sensor production. Variations in fabrication processes and material properties can lead to differences in sensor response among different units.
- Packaging and integration: Integrating gas sensors into practical devices and systems can be challenging. Proper packaging is necessary to protect the sensitive nanostructures while allowing gas interaction, and ensuring reliable electrical connections.
- Safety and Robustness: Methane gas sensors may be used in hazardous environments, and they must be designed to withstand harsh conditions while ensuring safe operation.
- Toxicity and environmental impact: Some nanomaterials used in gas sensors may raise concerns about their toxicity and potential environmental impact, requiring careful handling and disposal methods.

Despite these limitations, ongoing research and advancements in nanotechnology continue to address many of these challenges. As a result, nano gas sensors hold significant promise for various applications, including environmental monitoring, industrial safety, healthcare, and more. Overcoming these limitations will pave the way for more efficient and reliable nano gas sensors in the future.

5.2 FUTURE SCOPES

Boron nitride quantum dots (BNQDs) are an emerging area of research with promising potential in various applications, including gas sensing due to the ease of formation of various kinds of nanostructures in cost effective way. With advancements in nanotechnology and microfabrication techniques, BNQD-based sensors may become more compact, lightweight, and suitable for integration into portable devices, Internet of Things (IoT) applications, and wearable devices. These miniaturized sensors can find applications in personal safety monitoring, environmental monitoring, and industrial settings. The current research effort has been a success in many ways, but it still has to be improved for commercial and industrial applications. More research and development is needed to overcome the current obstacles and transform these advances into practical and commercially viable gas sensing systems. Based on the trends and developments in gas sensing technologies up to that point some insights into the potential future scope of BNQD-based methane sensors can be highlighted :

I. Alumina (Al_2O_3) as the Substrate material:

Due to its excellent electrical insulation, high mechanical strength, hardness, high resistance to corrosion, and especially its high thermal conductivity for a ceramic material features, alumina will function as an ideal substrate instead of glass.

II. Graphene as the Substrate material:

Graphene has a few excellent mechanical properties, making it the thinnest and strongest semiconducting material. This feature of graphene makes it an excellent substrate material for gas sensing purpose. Furthermore, both h-BN and Graphene have the same electronic structure (hexagonal rings with strong covalent sp2 bonds) and almost the same lattice constant, making it simple to compose an h-BN/Graphene heterostructure by direct stacking of individual h-BN and Graphene monolayers.

Heterostructures have a wide range of potential applications. Furthermore, due to their exceptional electrical properties, wide surface-to-volume ratio, and ease of application, 2D materials can be easily integrated into a variety of nanoelectronic devices.

III. Use of different compositions as Sensing material:

Other 2D materials, in addition to the h-BN material for sensing, can be fabricated on the separate sides of the same substrate. On two extreme ends of the same substrate or target

material, various compositions with varying molar concentrations can be deposited. Since the Xene group is very compatible with CMOS Si technology, the sensor and signal processing unit can be integrated on the same platform.

IV. Improve in material synthesization techniques:

Along with the Liquid exfoliation method employed in this experiment, it is expected that the Chemical Vapour deposition technique for the direct growth of the heterostructure will result in significantly more uniform deposition.

V. Improved Characterization technique:

A wide range of properties, including mechanical strength, thermal stability, electrical conductivity, and corrosion resistance, can be analyzed using advanced material characterization techniques like AFM, XPS, FTIR, and TEM. To analyze the shape, dispersion, and quantify and assess particle size, transmission electron microscopy produces (TEM) two-dimensional pictures of the perceived nanoparticles. Fourier Transform Infrared Spectroscopy (FTIR) creates an infrared absorption spectrum to identify chemical bonds in a molecule.The smoothness or homogeneity of the material on the device's surface can be determined using atomic force microscopy (AFM), that can produce three-dimensional pictures of surfaces at high magnification.For surface chemical analysis, X-ray photoelectron spectroscopy (XPS) is the most popular analytical method.By identifying the material characteristics of different components in a system, these techniques help to optimize designs for the improved reliability and efficiency.

By continuing the refining process of synthesis and characterization of BNQDs, their sensitivity and selectivity towards methane detection will be improved. This might pave the way for the creation of very sensitive and particular methane sensors capable of detecting low levels of the gas in a variety of situations.

VI. Measurement techniques Advancement:

The thermocouple utilized in this experiment has a maximum temperature range of 0°C-200°C. Since h-BN has an insulating property at low temperatures, it will be preferable to employ high temperature ambience for future gas detection analysis.

REFERENCES

[1] A. P. Nikalje, "Nanotechnology and its applications in medicine," *Med chem,* vol. 5.2, pp. 081-089, 2015.

[2] A. Nayyar, V. Puri and D. N. Le, "Internet of Nano Things (IoNT): Next Evolutionary Step in Nanotechnology," *Nanoscience and Nanotechnology,* vol. 7.1, pp. 4-8, 2017.

[3] M. D. Wang, D. M. Shin, J. W. Simons and N. Shuming, "Nanotechnology in Targeted Cancer Therapy," *Expert review of anticancer therapy,* vol. 7.6, pp. 833-837, 2007.

[4] "Applications of sensors," 30 June 2020. [Online]. Available: https://www.variohm.com/news-media/technical-blog-archive/applications-of-sensors-.

[5] "Applications of nanotechnology," [Online]. Available: https://en.wikipedia.org/wiki/Applications_of_nanotechnology.

[6] "Selecting the Right Sensors for Industrial Applications," electronicsforu.com, 12 July 2018. [Online]. Available: https://www.electronicsforu.com/buyers-guides/right-sensors-industrial-applications.

[7] J. Lozano, C. Apetrei, M. G.-. Varnamkhasti, D. Matatagui and J. P. Santos, "Sensors and Systems for Environmental Monitoring and Control," *Journal of Sensors 2017,* 2017.

[8] S. L. Ullo and G. R. Sinha, "Advances in smart environment monitoring systems using IoT and sensors," *Sensors,* vol. 20.11, p. 3113, 2020.

[9] O. Alkhoori, A. Hassan, O. Almansoori, M. Debe, K. Salah, R. Jayaraman, J. Arshad and M. H. U. Rehman, "Design and implementation of CryptoCargo: A blockchain-powered smart shipping container for vaccine distribution.," *IEEE Access,* vol. 9, pp. 53786-53803, 2021.

[10] "Things you need to know about car sensors," StudentLesson, [Online]. Available: https://studentlesson.com/car-sensors-definition-functions-diagram-types-working/.

[11] N. Promphet, S. Ummartyotin, W. Ngeontae, P. Puthongkham and N. Rodthongkum, "Non-invasive wearable chemical sensors in real-life applications," *Analytica Chimica Acta,* vol. 1179, p. 338643, 2021.

[12] H. Haick and N. Tang, "Artificial Intelligence in Medical Sensors for Clinical Decisions," *ACS Nano ,* vol. 15.3, p. 3557–3567, 2021.

[13] J. Ariza, K. Garcés, N. Cardozo, J. Pablo, R. Sánchez and F. J. Vargas, “IoT architecture for adaptation to transient devices,” *Journal of Parallel and Distributed Computing,* vol. 148, pp. 14-30, 2021.

[14] A. Tsitsigkos, F. Entezami, R. A. Tipu , C. Politis and E. A. Panaousis, “A Case Study of Internet of Things Using Wireless Sensor Networks and Smartphones,” *In Proceedings of the Wireless World Research Forum (WWRF) Meeting: Technologies and Visions for a Sustainable Wireless Internet, Athens, Greece,,* vol. 2325, p. 4, 2012.

[15] A. Khanna, . R. Goyal, M. Verma and D. Joshi, “Intelligent traffic management system for smart cities,” *In Futuristic Trends in Network and Communication Technologies: First International Conference, FTNCT 2018, Solan, India,,* no. Springer Singapore, pp. 152-164, 2018.

[16] “50 Sensor Applications for a Smarter World,” 2020, September 9.

[17] J. Zhang, L. Xianghong, G. Neri and N. Pinna, “Nanostructured materials for room-temperature gas sensors,” *Advanced materials,* vol. 28.5, pp. 795-831, 2016.

[18] C. C. Bueno, P. S. Garcia and F. d. L. Leite, “Nanosensors,” in Nanoscience and its Applications., 2017, pp. 121-122.

[19] A. Nayyar, V. Puri and D. N. Le, “Internet of nano things (IoNT): Next evolutionary step in nanotechnology,” Nanoscience and Nanotechnology, vol. 7(1), pp. 4-8, 2017.

[20] R. Patel, P Bobde, V Singh, D Panchal, S Pal, “Synthesis and applications of carbon nanomaterials-based sensors,” in *Advanced Nanomaterials for Point of Care Diagnosis and Therapy*, Elsevier, 2022, pp. 451-476.

[21] [Online]. Available: https://en.wikipedia.org/wiki/Nanosensor.

[22] A. G. Alemu, A. T. Alemu "Recent advances of nanomaterial sensor for point-of care diagnostics applications and research.," *Advanced Nanomaterials for Point of Care Diagnosis and Therapy,* pp. 181-202, 2022.

[23] R. Abdel-Karim, Y. Reda, and A. Abdel-Fattah “Nanostructured materials-based nanosensors,” J*ournal of The Electrochemical Society,* vol. 167.3, p. 037554, 2020.

[24] D. H. Vance, A. W. Czarnik, "Functional group convergency in a binuclear dephosphorylation reagent.," *Journal of the American Chemical Society ,* vol. 115.25, pp. 12165-12166, 1993.

[25] S. Agrawal, R. Prajapati, " Nanosensors and their pharmaceutical applications: a review.," *Int J Pharm Sci Technol ,* vol. 4, pp. 1528-1535, 2012.

[26] A. M. e. Grumezescu, New pesticides and soil sensors., Academic Press, 2017.

[27] T.C. Lim, S. Ramakrishna " A conceptual review of nanosensors," Zeitschrift für Naturforschung A , Vols. 61.7-8, pp. 402-412, 2006.

[28] Y. Zhang, M. Li, X. Gao, Y. Chen, and T. Liu. "Nanotechnology in cancer diagnosis: progress, challenges and opportunities," J*ournal of hematology & oncology,* vol. 12.1, pp. 1-13, 2019.

[29] A. Rizwan, A. Zoha, R. Zhang, W. Ahmad, K. Arshad, N. A. Ali, A. Alomainy, Md A. Imran, and Q. H. Abbasi., "A review on the role of nano-communication in future healthcare systems: A big data analytics perspective," no. IEEE Access 6, pp. 41903-41920, 2018.

[30] M. Javaid, A. Haleem, R. P. Singh, S. Rab and R. Suman, "Exploring the potential of nanosensors: A brief overview.," *Sensors International ,* vol. 2, p. 100130, 2021.

[31] F. J. Iftikhar, A. Shah, M. S. Akhter, S. Kurbanoglu and S. A. Ozkan, "Introduction to nanosensors," in *In New Developments in Nanosensors for Pharmaceutical Analysis*, Academic Press , pp. 1-46, 2019.

[32] M. T. Rahman and E. V. Rebrov, "Microreactors for gold nanoparticles synthesis: From faraday to flow," *Processes,* vol. 2.2, pp. 466-493, 2014.

[33] DV Shtansky, AT Matveev, ES Permyakova, DV Leybo, A. S. Konopatsky, and P. B. Sorokin. "Recent progress in fabrication and application of BN nanostructures and BN-based nanohybrids." *Nanomaterials* vol. 12.16, pp-2810, 2022.

[34] "Different types of nanomaterials". [Online]. Available: https://wiki.anton-paar.com/in-en/different-types-of-nanomaterials/

[35] "Nanoparticles, nanotubes and nanocomposites" [Online]. Available: https://www.compositesworld.com/articles/nanoparticles-nanotubes-and-nanocomposites.

[36] "Nanomanufacturing". [Online]. Available: https://en.wikipedia.org/wiki/Nanomanufacturing#:~:text=Nanomanufacturing%20is%20both%20the%20production,laser%20ablation%2C%20etching%20and%20others

[37] Y. Choi and S. Lee, "Biosynthesis of inorganic nanomaterials using microbial cells and bacteriophages," *Nature Reviews Chemistry,* vol. 4.12, pp. 638-656, 2020.

[38] T. Zhang, S. Mubeen, N. V. Myung and M. A. Deshusses, "Recent progress in carbon nanotube-based gas sensors," *Nanotechnology,* vol. 19.33, p. 332001, 2008.

[39] V. A. Spirescu, C. Chircov, A. M. Grumezescu, B. Ș. Vasile and E. Andronescu., "Inorganic Nanoparticles and Composite Films for Antimicrobial Therapies," *International Journal of Molecular Sciences 22,* vol. 22.9, p. 4595, 2021.

[40] S. N. Shtykov, and T. Yu Rusanova. "Nanomaterials and nanotechnologies in chemical and biochemical sensors: Capabilities and applications." *Russian Journal of General Chemistry* vol. 78, pp-2521-2531, 2008.

[41] G. Ahmad, A. Nawaz, S. Nawaz, N. A. Shad, M. M. Sajid and Y. Javed, "Nanomaterial-based gas sensor for environmental science and technology," in *Nanofabrication for Smart Nanosensor Applications Micro and Nano Technologies*, ELSEVIER, 2020, pp. 229-252.

[42] [Online]. Available: https://www.britannica.com/science/fullerene.

[43] T Dai, W He, C Yao, X Ma, W Ren, Y Mai, A Wu , "Applications of inorganic nanoparticles in the diagnosis and therapy of atherosclerosis." *Biomaterials science*, vol 8.14, p.3784-3799,2020.

[44] S. Sagadevan. "Semiconductor nanomaterials, methods and applications: a review." *Nanoscience and Nanotechnology,* vol. 3. 3 pp. 62-74, 2013.

[45] H. Roshan, M. Sheikhi, M. Haghighi and P. Padidar, "High-Performance Room Temperature Methane Gas Sensor Based on Lead Sulfide / Reduced Graphene Oxide Nanocomposite," *EEE Sensors Journal ,* vol. 20.5, pp. 2526-2532, 2019.

[46] P. Bhattacharyya, P. Basu and S. Basu, "Methane detection by nano ZnO based MIM sensor devices," *Sensors & Transducers,* vol. 10, p. 121, 2011.

[47] A.Biaggi-Labiosa, F. Sola, M. Lebrón-Colón, L. J. Evans, J. C. Xu, G. W. Hunter, G. M. Berger and J. M. Gonzalez, "A novel methane sensor based on porous SnO2 nanorods: room temperature to high temperature detection," *Nanotechnology,* vol. 23.45, p. 455501, 2012.

[48] T. Naseem, and T. Durrani. "The role of some important metal oxide nanoparticles for wastewater and antibacterial applications: A review." *Environmental Chemistry and Ecotoxicology,* vol.3, pp. 59-75,2021.

[49] H. Cheng-Zhong, L. Feng and L. Xiang-Dong, "Theoretical study on gas sensing properties of boron nitride nanotubes," *Acta Chimica Sinica ,* vol. 66.14, pp. 1641-1646, 2008

[50] F. Ji, X. Ren, X. Zheng, Y. Liu, L. Pang, J. Jiang and S. F. Liu, "2D-MoO3 nanosheets for superior gas sensors," *Nanoscale,* vol. 8.16, pp. 8696-8703, 2016.

[51] S. J. Ray, "First-principles study of MoS2, phosphorene and graphene based single electron transistor for gas sensing applications." *Sensors and Actuators B: Chemical* 222, pp.492-498,2016

[52] C. C. Bueno, P.S Garcia, C. Steffens, D.K. Deda, F. de Lima Leite, "Nanosensors-an Overview.", *Nanoscience and its Applications,* pp. 121-122, 2017.

[53] Y Li, H Wang, Y Chen, M Yang. "A multi-walled carbon nanotube/palladium nanocomposite prepared by a facile method for the detection of methane at room temperature." *Sensors and actuators B: Chemical*, vol. 132.1, pp. 155-158.2008.

[54] T. Zhang, S. Mubeen, NV Myung and M.A. Deshusses. "Recent progress in carbon nanotube-based gas sensors." *Nanotechnology*, vol.19.33 33 p.332001, 2008

[55] N. M. Shaalan, D. Hamad, A. Aljaafari, A. Y. Abdel-Latief, and M. A. Abdel-Rahim. "Preparation and characterization of developed CuxSn1− xO2 nanocomposite and its promising methane gas sensing properties." *Sensors*, vol.19.10 , p. 2257, 2019

[56] V Krivetskiy, M Andree and A Efitorov "Selective detection of hydrocarbons in real atmospheric conditions by single MOX sensor in temperature modulation mode." *Multidisciplinary Digital Publishing Institute Proceedings*, vol 14.1 p.47. 2019.

[57] T Aldhafeeri, MK Tran, R Vrolyk, M Pope, M Fowler. "A review of methane gas detection sensors: Recent developments and future perspectives." *Inventions*, vol 5.3, p.28. 2020.

[58] M. J. Bezdek, S. X. L. Luo, K. H. Ku, and T. M. Swager. "A chemiresistive methane sensor." *Proceedings of the National Academy of Sciences*, vol 118.2, p. e2022515118,2021.

[59] H. R. Moshayedi, M. Rabiee and N Rabiee. "Graphene oxide/polyaniline-based multi nano sensor for simultaneous detection of carbon dioxide, methane, ethanol and ammonia gases." *Iranian Journal of Chemistry and Chemical Engineering (IJCCE),* vol. 39.3, pp. 93-105.2020

[60] L. Furst, M. Feliciano, L. Frare, and G. Igrejas. "A Portable Device for Methane Measurement Using a Low-Cost Semiconductor Sensor: Development, Calibration and Environmental Applications." *Sensors.* Vol 21.22, p.7456,2021.

[61] I. S. P. Nagahage, E. A. A. D. Nagahage, and T. Fujino. "Assessment of the applicability of a low-cost sensor–based methane monitoring system for continuous multi-channel sampling." *Environmental Monitoring and Assessment*, vol 193,pp. 1-14,2021

[62] M Kwaśny and A Bombalska . Kwaśny, Mirosław, and Aneta Bombalska. "Optical methods of methane detection." *Sensors*, vol 23.5, p.2834,2023.

[63] K. G. Ong, K. Zeng, and C.A. Grimes. "A wireless, passive carbon nanotube-based gas sensor." *IEEE Sensors Journal*, vol 2.2, pp. 82-8. 2002.

[64] M. Safari, M. Gholizadeh, and A. Salehi."Modeling and simulation of a MOSFET gas sensor with platinum gate for hydrogen gas detection." *Sensors and Actuators B: Chemical*, vol. 141.1, pp. 1-6. 2009

[65] A. J. Moshayedi, A. Toudeshki, and D. C. Gharpure. "Mathematical modeling for SnO 2 gas sensor based on second-order response." In 2013 *IEEE Symposium on Industrial Electronics & Applications*, pp. 33-38. IEEE, 2013.

[66] A. Inaba, K. Yoo, Y. Takei, K. Matsumoto, and I. Shimoyama. "Ammonia gas sensing using a graphene field–effect transistor gated by ionic liquid." *Sensors and Actuators B: Chemical*, vol.195, pp. 15-21. 2014.

[67] F. Sarf. "Metal oxide gas sensors by nanostructures." Gas Sensors, vol. 1. 2020.

[68] A. Lahlalia, O. Le. Neel, R. Shankar, S. Selberherr and L. Filipovic. "Improved sensing capability of integrated semiconducting metal oxide gas sensor devices." *Sensors*, vol 19.2 p. 374. 2019.

[69] Y. Nishiue. "Ultra-Low Power MEMS Gas Sensor Technology and Application." *Gas Sensors Based on Semiconducting Metal Oxides: Basic Understanding & Application Fields*. p. 29. 2019.

[70] P. Sun,"Gas Sensors Based on Oxide Semiconductors with Porous Nanostructures." Multidisciplinary Digital Publishing Institute Proceedings, vol 14.1, p. 13, 2019.

[71] Bh.Sharma,A. Sharma, M. Joshi, and J-H. Myung, J-H. "Sputtered SnO2/ZnO Heterostructures for Improved NO2 Gas Sensing Properties." *Chemosensors*, vol 8.3, p. 67, 2020.

[72] I. S. Fahim, A. M. Hassanein, L. A. Said, and A. H. Madian. "Design and fabrication of CNT/graphene-based polymer nanocomposite applications in nanosensors." In *Nanofabrication for Smart Nanosensor Applications*, pp. 281-294. Elsevier, 2020.

[73] B. Saruhan, R. L. Fomekong and S. Nahirniak. "Review: influences of semiconductor metal oxide properties on gas sensing characteristics. Front Sens. 2021; 2." p. 657931, 2021.

[74] P. V. Shinde. "Magnetic gas sensing: Working principles and recent developments." *Nanoscale Advances*, vol 3.6, pp. 1551-1568, 2021.

[75] N. Sharma, V. Pandey, A. Gupta, S.T. Tan, S. Tripathy and M. Kumar. "Recent progress on Group III-nitride nanostructures-based Gas Sensors." *Journal of Materials Chemistry* C. 2022.

[76] H. Cheng-Zhong, L Feng, and L Xiang-Dong. "Theoretical study on gas sensing properties of boron nitride nanotubes." *Acta Chimica Sinica* vol 66. 14, pp. 1641-1646. 2008.

[77] K. K. Kim, A. Hsu, X. Jia, S. M. Kim, Y. Shi, M. Dresselhaus, T. Palacios, and J. Kong. "Synthesis and characterization of hexagonal boron nitride film as a dielectric layer for graphene devices." *ACS nano*. vol 6. 10, pp. 8583-8590. 2012

[78] N. Goel, and M. Kumar."Recent advances in ultrathin 2D hexagonal boron nitride-based gas sensors." *Journal of Materials Chemistry*, vol 9.5, pp. 1537-1549. 2021.

[79] A. Acharya, S. Sharma, X. Liu, D. Zhang, and Y. K. Yap. "A Review on van der Waals Boron Nitride Quantum Dots." vol C 7.2, p. 35, 2021.

[80] P. K. Kannan, D. J. Late, H. Morgan and C.S. Rout. "Recent developments in 2D layered inorganic nanomaterials for sensing." Nanoscale, vol 7.32, pp. 13293-13312. 2015.

[81] H. Morgan, C. S. Rout, and D. J. Late. "Future prospects of 2D materials for sensing applications." Fundamentals and Sensing Applications of 2D Materials. pp. 481-482.2019.

[82] N Nayir, Q Mao, T Wang, M Kowalik, Y Zhang, M. Wang, S. Dwivedi, GU. Jeong, Y. K. Shin, and A. CT v. Duin. "Modeling and simulations for 2D materials: a ReaxFF perspective." 2D Materials, 2023.

[83] R. Maiti, D. Chakravarty, N. Tewari and S. Roy, in *Chemistry Textbook*, Chaya Prakashani, 2014, pp. 906-908. “Methane,” 9 August 2023.

[84] [Online]. Available: https://www.britannica.com/science/paraffin-hydrocarbon

[85] Ramírez-Solís, A. (2014). On the Accuracy of the Complete Basis Set Extrapolation for Anionic Systems: A Case Study of the Electron Affinity of Methane. Computational chemistry,2,31-41.

[86] [Online]. Available: https://pubs.acs.org/doi/pdf/10.1021/ja01419a002#:~:text=potential%20of%20methane%20is%2013.7%20volts.

[87] [Online]. Available: https://en.wikipedia.org/wiki/Methane_functionalization

[88] [Online].Available:https://chem.libretexts.org/Bookshelves/Physical_and_Theoretical_Chemistry_Textbook_Maps/Supplemental_Modules_(Physical_and_Theoretical_Chemistry)/Thermodynamics/Energies_and_Potentials/Enthalpy/Bond_Enthalpies.

[89] "Methane" [Online]. Available: https://en.wikipedia.org/wiki/Methane

[90] C. Dücso, M. Ádám, P. Fürjes, M. Hirschfelder,S. Kulinyi, I. Bársony."Explosion-proof monitoring of hydrocarbons by mechanically stabilised, integrable calorimetric microsensors." *Sensors and Actuators B: Chemica*l, vol. 95,pp. 189–194,2003.

[91] F Bíró, C Dücső, GZ Radnóczi, Z Baji, M Takács and I.Bársony. "ALD nano-catalyst for micro-calorimetric detection of hydrocarbons." *Sens. Actuators B Chem.*Vol.247, pp.617-625,2017.

[92] A. M. Azad, S. A. Akbar, S. G. Mhaisalkar, L. D. Birkefeld, and K. S. Goto. "Solid-state gas sensors: A review." *Journal of the Electrochemical Society* vol 139, no. 12,p. 3690. 1992.

[93] N. H. Park, T. Akamatsu, T. Itoh, N. Izu, and W. Shin "Calorimetric thermoelectric gas sensor for the detection of hydrogen, methane and mixed gases." *Sensors,* vol. 14, no. 5, pp. 8350-8362,2014.

[94] M Kwaśny and A Bombalska . Kwaśny, Mirosław, and Aneta Bombalska. "Optical methods of methane detection." *Sensors*, vol 23.5, p.2834,2023.

[95] A. B. D. Shaik and P. Palla. "Optical quantum technologies with hexagonal boron nitride single photon sources." *Scientific reports*, vol 11.1, pp.12285. 2021

[96] B. Alexander, "Mathematical Processing of a Pyroelectric Detector"; Ivanchenko: Volodymyr Dahl, East Ukrainian, 2019.

[97] AK Sawhney, P Sawhney, "*A course in mechanical measurements and instrumentation*." Vol. 3. Dhanpat Rai, New Delhi, 1995.

[98] "Lecture 2: Sensors." [Online]. Available: https://ieda.ust.hk/dfaculty/ajay/courses/alp/ieem110/lecs/sensors/sensors.html

[99] LM Xie. "Two-dimensional transition metal dichalcogenide alloys: preparation, characterization and applications." *Nanoscale* 7, no. 44 , pp. 18392-18401,2015.

[100] J. Wang, F. Ma, and M. Sun. "Graphene, hexagonal boron nitride, and their heterostructures: properties and applications." *RSC advances*, vol 7.27. pp. 16801-16822. 2017

[101] [Online]. Available: https://en.wikipedia.org/wiki/Boron_nitride

[102] A. Acharya, S. Sharma, X. Liu, D. Zhang, and Y. K. Yap. "A Review on van der Waals Boron Nitride Quantum Dots." vol C 7.2, p. 35, 2021.

[103] Garg, M. Garg, R. Rani, A. L. Sharma, and S. Singh. "White graphene quantum dots as electrochemical sensing platform for ferritin." Faraday Discussions, vol 227, pp. 204-212. 2021

[104] S. Madakbaş, E. Çakmakçı, and M. V. Kahraman. "Preparation and thermal properties of polyacrylonitrile/hexagonal boron nitride composites." Thermochimica Acta, vol 552, pp. 1-4. 2013.

[105] A. B. D. Shaik and P. Palla. "Optical quantum technologies with hexagonal boron nitride single photon sources." Scientific reports, vol 11.1, pp.12285. 2021

[106] R Beiranvand, and S Valedbagi. "Electronic and optical properties of h-BN nanosheet: A first principles calculation." *Diamond and Related Materials*, vol 58. pp. 190-195. 2015

[107] Y. Malozovsky, C. Bamba, A. Stewart, L. Franklin, and D. Bagayoko. "Accurate Ground State Electronic and Related Properties of Hexagonal Boron Nitride (h-BN)." *arXiv preprint arXiv:2001.11596*. 2020.

[108] L. Ci, L. Song, C. Jin, D. Jariwala, D. Wu, Y. Li, and A. Srivastava. "Atomic layers of hybridized boron nitride and graphene domains." Nature materials, vol 9.5, pp. 430-435. 2010.

[109] GR Bhimanapati, Z Lin, V Meunier, Y Jung, J. Cha.,S. Das, and Di Xiao "Recent advances in two-dimensional materials beyond graphene." *ACS nano*, vol. 9, no. 12, pp. 11509-11539.2015

[110] M. K. L. Marsh, M. Souliman, and R. B. Kaner "Co-solvent exfoliation and suspension of hexagonal boron nitride." Chemical communications. vol 51.1, pp. 187-190. 2015

[111] Z. Lei, S. Xu, J. Wan, and P. Wu. "Facile preparation and multifunctional applications of boron nitride quantum dots." *Nanoscale*. vol 7, no. 45, pp. 18902-18907.2015

[112] KS Novoselov, A Mishchenko, A Carvalho. Novoselov, K. S., Artem Mishchenko, Alexandra Carvalho, and A. H. Castro Neto. "2D materials and van der Waals heterostructures." *Science* 353, no. 6298. pp. aac9439. 2016

[113] X. Zhang, L. An, C. Bai, L. Chen, and Y. Yu. "Hexagonal boron nitride quantum dots: Properties, preparation and applications." *Materials Today Chemistry* vol. 20, pp. 100425. 2021

[114] Z. Lei, S. Xu, J. Wan, and P. Wu. “Facile preparation and multifunctional applications of boron nitride quantum dots." *Nanoscale*. vol 7, no. 45, pp. 18902-18907.2015

[115] P. Han, R. Yan, Y. Wei, L. Li, J. Luo, Y. Pan, and B. Wang et al. "Mechanistic Insights into Radical-Induced Selective Oxidation of Methane over Nonmetallic Boron Nitride Catalysts." *Journal of the American Chemical Society,* vol. 145, no. 19, pp. 10564-10575, 2023

[116] S. Majety, X. K. Cao, R. Dahal, B. N. Pantha, J. Li, J.Y. Lin, H.X. Jiang. "Semiconducting hexagonal boron nitride for deep ultraviolet photonics." In *Quantum Sensing and Nanophotonic Devices IX*, vol. 8268, pp. 607-614. SPIE, 2012.

[117] S. Nayak, S. Bhattacharjee and B. P. Singh. "A systematic study on the effect of acidic, basic and neutral additives on dispersion of multiwalled carbon nanotubes using a dimethylformamide solution." *Advances in Natural Sciences: Nanoscience and Nanotechnology*, vol 5, no. 4, p. 045005. 2014

[118] “Propanol structure” [Online]. Available: https://www.shutterstock.com/image-vector/propanol-structural-chemical-formula-model-isopropanol-302722490

[119] “Acetone”. [Online]. Available: https://en.wikipedia.org/wiki/Acetone